2012-09

CROSSLAYER OPTIMIZATION IN AN LTE NETWORK TO REDUCE THE EFFECT OF CO-CHANNEL INTERFERENCE

Tan, Kim Hong

Monterey, California. Naval Postgraduate School

http://hdl.handle.net/10945/70932

NAVAL POSTGRADUATE SCHOOL

MONTEREY, CALIFORNIA

THESIS

CROSSLAYER OPTIMIZATION IN AN LTE NETWORK TO REDUCE THE EFFECT OF CO-CHANNEL INTERFERENCE

by

Kim Hong Tan

September 2012

Thesis Advisor:	Tri T. Ha
Thesis Co-Advisors:	Weilian Su
	Ric Romero

Approved for public release; distribution is unlimited

THIS PAGE INTENTIONALLY LEFT BLANK

REPORT DOCUMENTATION PAGE			*Form Approved OMB No. 0704–0188*
Public reporting burden for this collection of information is estimated to average 1 hour per response, including the time for reviewing instruction, searching existing data sources, gathering and maintaining the data needed, and completing and reviewing the collection of information. Send comments regarding this burden estimate or any other aspect of this collection of information, including suggestions for reducing this burden, to Washington headquarters Services, Directorate for Information Operations and Reports, 1215 Jefferson Davis Highway, Suite 1204, Arlington, VA 22202–4302, and to the Office of Management and Budget, Paperwork Reduction Project (0704–0188) Washington DC 20503.			
1. AGENCY USE ONLY *(Leave blank)*	**2. REPORT DATE** September 2012	**3. REPORT TYPE AND DATES COVERED** Master's Thesis	
4. TITLE AND SUBTITLE Crosslayer Optimization in LTE Network to Reduce the Effect of Co-Channel Interference			**5. FUNDING NUMBERS**
6. AUTHOR(S) Kim Hong Tan			
7. PERFORMING ORGANIZATION NAME(S) AND ADDRESS(ES) Naval Postgraduate School Monterey, CA 93943–5000			**8. PERFORMING ORGANIZATION REPORT NUMBER**
9. SPONSORING /MONITORING AGENCY NAME(S) AND ADDRESS(ES) N/A			**10. SPONSORING/MONITORING AGENCY REPORT NUMBER**
11. SUPPLEMENTARY NOTES The views expressed in this thesis are those of the author and do not reflect the official policy or position of the Department of Defense or the U.S. Government. IRB Protocol number ______N/A______.			
12a. DISTRIBUTION / AVAILABILITY STATEMENT Approved for public release; distribution is unlimited			**12b. DISTRIBUTION CODE**

13. ABSTRACT (maximum 200 words)

In this thesis, synergy between the physical layer and the Medium Access Control (MAC) layer of a Long Term Evolution (LTE) network is exploited to reduce the co-channel interference in both the forward and reverse channels. By doing such cross-layer optimization analysis, physical and MAC layer control decisions reach their full potential when they are designed in an integrated manner.

The proposed solution focuses on the integration of the concepts of orthogonal frequency-division multiple access (OFDMA), sectorization, and Latin Square to improve the signal-to-interference ratio (SIR) with the most effective resource utilization. Sectorization in the physical layer alone is able to improve the SIR, however, by also implementing OFDMA and Latin Square techniques to reduce the effect of co-channel interference, better SIR can be achieved. There is some impact on resource utilization, however. The solution seeks to achieve an optimum point of tradeoff between improvement in the SIR and the acceptable amount of the unutilized resources.

14. SUBJECT TERMS Long Term Evolution, Orthogonal Frequency-Division Multiple Access, Medium Access Control, Co-Channel Interference, Sectorization, Latin Square			**15. NUMBER OF PAGES** 133
			16. PRICE CODE
17. SECURITY CLASSIFICATION OF REPORT Unclassified	**18. SECURITY CLASSIFICATION OF THIS PAGE** Unclassified	**19. SECURITY CLASSIFICATION OF ABSTRACT** Unclassified	**20. LIMITATION OF ABSTRACT** UU

NSN 7540–01–280–5500 | Standard Form 298 (Rev. 2–89) Prescribed by ANSI Std. 239–18

THIS PAGE INTENTIONALLY LEFT BLANK

Approved for public release; distribution is unlimited

CROSSLAYER OPTIMIZATION IN AN LTE NETWORK TO REDUCE THE EFFECT OF CO-CHANNEL INTERFERENCE

Kim Hong Tan
Civilian, Defence Science and Technology Agency, Singapore
B.Eng (Electrical & Electronic Engineering), Nanyang Technological University, 2005

Submitted in partial fulfillment of the
requirements for the degree of

MASTER OF SCIENCE IN ELECTRICAL ENGINEERING

from the

NAVAL POSTGRADUATE SCHOOL
September 2012

Author: Kim Hong Tan

Approved by: Tri T. Ha
Thesis Advisor

Weilian Su
Ric Romero
Thesis Co-Advisors

R. Clark Robertson
Chair, Department of Electrical and Computer Engineering

THIS PAGE INTENTIONALLY LEFT BLANK

ABSTRACT

In this thesis, synergy between the physical layer and the Medium Access Control (MAC) layer of a Long Term Evolution (LTE) network is exploited to reduce the co-channel interference in both the forward and reverse channels. By doing such cross-layer optimization analysis, physical and MAC layer control decisions reach their full potential when they are designed in an integrated manner.

The proposed solution focuses on the integration of the concepts of orthogonal frequency-division multiple access (OFDMA), sectorization, and Latin Square to improve the signal-to-interference ratio (SIR) with the most effective resource utilization. Sectorization in the physical layer alone is able to improve the SIR, however, by also implementing OFDMA and Latin Square techniques to reduce the effect of co-channel interference, better SIR can be achieved. There is some impact on resource utilization, however. The solution seeks to achieve an optimum point of tradeoff between improvement in the SIR and the acceptable amount of the unutilized resources.

THIS PAGE INTENTIONALLY LEFT BLANK

TABLE OF CONTENTS

THIS PAGE INTENTIONALLY LEFT BLANK

LIST OF FIGURES

THIS PAGE INTENTIONALLY LEFT BLANK

LIST OF TABLES

THIS PAGE INTENTIONALLY LEFT BLANK

LIST OF ACRONYMS AND ABBREVIATIONS

2G	Second Generation
3G	Third Generation
4G	Fourth Generation
16QAM	Sixteen-Quadrature Amplitude Modulation
64QAM	64-Quadrature Amplitude Modulation
CCU	Cell Center User
CEU	Cell Edge User
CCI	Co-Channel Interference
CCPCH	Common Control Physical Channel
CDD	Cyclic Delay Diversity
CIR	Channel Impulse Response
CP	Cyclic Prefix
CQI	Channel Quality Indication
EFFR	Enhanced Fractional Frequency Reuse
eNB	Enhanced Node B (Enhanced Base Station)
E-UTRAN	Evolved Universal Terrestrial Radio Access Network
FFT	Fast Fourier Transform
FRF	Frequency Reuse Factor
IFFT	Inverse Fast Fourier Transformation
IFR	Incremental Frequency Reuse
LS	Latin Square
LTE	Long-Term Evolution
MAC	Medium Access Control
MIMO	Multiple-Input and Multiple-Output
OFDM	Orthogonal Frequency-Division Multiplexing
OFDMA	Orthogonal Frequency-Division Multiple-Access
PAPR	Peak-Average-Power Ratio
PDCCH	Physical Downlink Control Channel
PDCP	Packet Data Convergence Protocol
PDSCH	Physical Downlink Shared Channel

PUCCH	Physical Uplink Control Channel
PUSCH	Physical Uplink Shared Channel
QoS	Quality of Service
QPSK	Quadrature Phase-Shift Keying
RB	Resource Block
RLC	Radio Link Control
SAP	Service Access Point
SFR	Soft Frequency Reuse (SFR)
SIR	Signal-to-Interference Ratio
TDMA	Time Division Multiple Access
UE	User Equipment

EXECUTIVE SUMMARY

A Long Term Evolution (LTE) network is a fourth generation (4G) wireless network that is able to offer high speed Internet access through the use of mobile phones. With a large increase in the number of mobile subscribers on wireless networks and a growing demand for higher data speed access and efficiency for applications such as video on the go, much emphasis has been placed on the quality of service in terms of minimal co-channel interference.

Current co-channel interference mitigation techniques include frequency reuse with 120°-sectorization. In addition, as the cell edge users (CEUs) are often the ones who suffer the worst co-channel interference, the users in each cell are grouped into two types for co-channel interference analysis, i.e., cell center users (CCU) and CEUs. Although this technique improves the experience of the users, especially the CEUs, the synergy between the physical layer and the Medium Access Control (MAC) layer can be exploited to reduce the effect of co-channel interference in both the forward and reverse channels.

The proposed solution first involves improving the cell structure of LTE in the physical layer by using 60°-sectorization as shown in Figure 1, with the users grouped into two types: cell center and cell edge. While the performance of the signal-to-interference ratio (SIR) for the CCU in 60°-sectorization remains as good as in 120°-sectorization, the SIR performance for the CEU with 60°-sectorization improves by 6% and 48% in the forward channel and in the reverse channel, respectively. This happens because the distance of some of the interfering sources are now farther away, and signal loss is proportional to the *nth* power of the distance, where *n* is the path loss exponent.

To further enhance the SIR performance, the concepts of orthogonal frequency-division multiple access (OFDMA), sectorization and Latin Square are integrated to improve the SIR with the least number of unutilized resources. First, by using the concept of OFDMA and Latin Square, the resources for each user per Enhanced Node B (eNB) are allocated in a staggered manner as shown in Figure 2. Each user sends its data using the allocated frequency channel in the particular time slot.

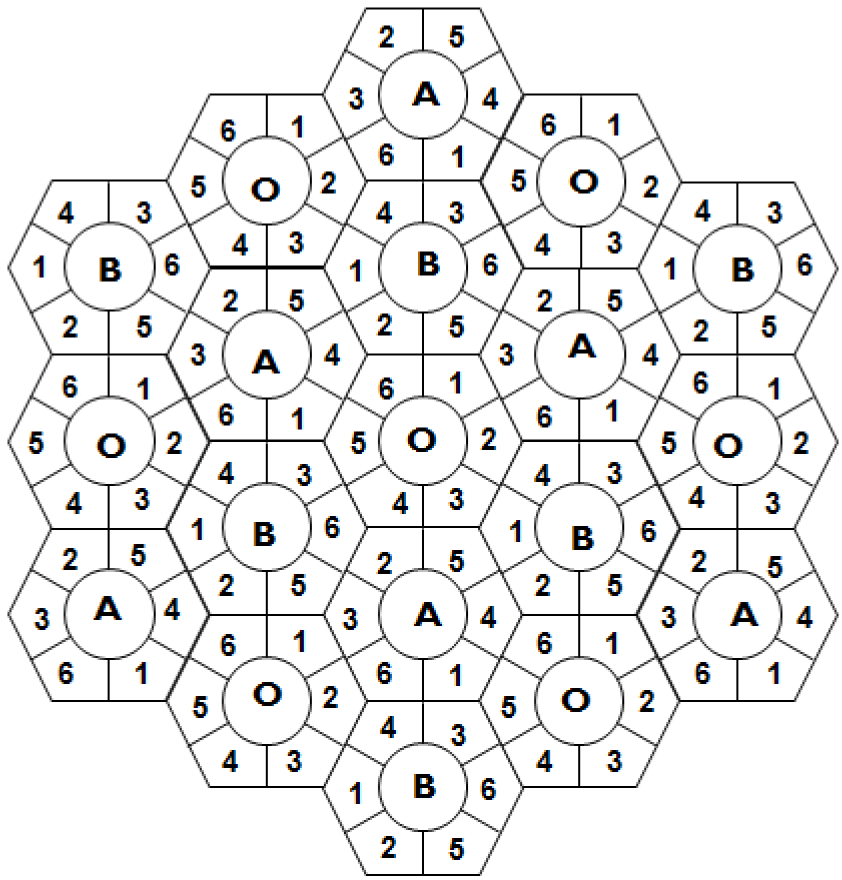

Figure 1. Frequency Reuse Scheme for 60°-sectoring.

In Figure 2, the assigned frequency channel for user A1 and user B1 changes each time frame to allow for frequency diversity. For example, the data sent out by user A1 in eNB in cell A (eNB_A), colored in solid grey, is first done in F1 in time slot 1, then F2 in time slot 2, F3 in time slot 3, F4 in time slot 4, and F5 in time slot 5. Similarly, for user B1 in eNB in cell B (eNB_B), shaded with stripes in Figure 2, the assigned frequency channel also changes each time frame to allow for frequency diversity. The data sent out by user B1 in eNB_B is first placed in F5 in time slot 1, then F1 in time slot 2, F2 in time slot 3, F3 in time slot 4, and F4 in time slot 5.

By hopping over the entire band, frequency diversity can be achieved, and the probability of overlapping channels is reduced. In addition, the interference seen due to inter-cell transmissions comes from different virtual channels, lowering the effect of co-channel interference.

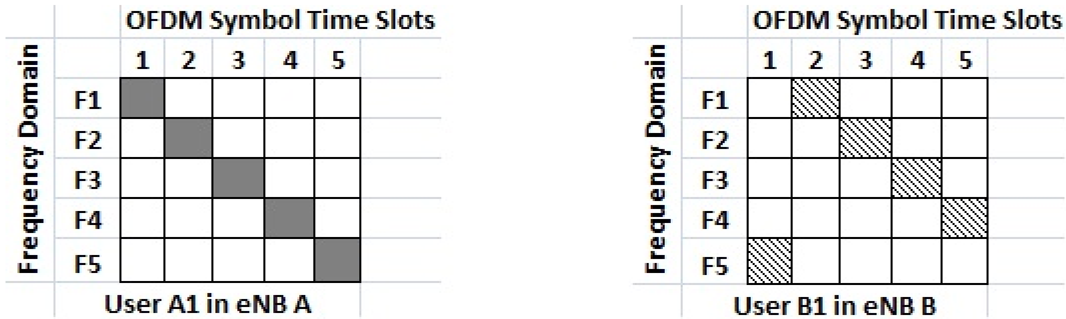

Figure 2. Resource allocation for one user per eNB.

With the probability p_i of a neighboring eNB interfering with the eNB of interest to be determined, the SIR for both forward and reverse channels was calculated based on the following generic equation, where $P_{desired}$ is the desired power received, and I_i is the interference received:

$$SIR = \frac{P_{desired}}{(p_1 I_1) + (p_2 I_2) + (p_3 I_3) + (p_4 I_4) + \cdots}.$$

THIS PAGE INTENTIONALLY LEFT BLANK

ACKNOWLEDGMENTS

I would like to thank my thesis advisors, Professor Tri Ha, Professor Weilian Su, and Professor Ric Romero, for their guidance, encouragement and patience. Without their assistance, this thesis would not have been completed with such great fulfillment. It has been an interesting learning journey.

I would also like to thank my wonderful husband, Huseh Tien, my family, and friends for their encouragement and support during my course of study.

THIS PAGE INTENTIONALLY LEFT BLANK

I. INTRODUCTION

A. BACKGROUND

From as early as the 19th century, through the vast contributions from the commercial, government, and military on technological developments and advancements, data communications have evolved from simple wired connections to modern robust wireless systems. The second decade of this century is seeing an increasing number of subscribers on wireless networks and a growing demand for higher data speed access and efficiency for web, streaming, and interactive video applications on the go. A Long Term Evolution (LTE) network is a fourth generation (4G) wireless network that is able to offer high-speed Internet access through the use of mobile phones. It is also able to handle large memory capacity that allows video phone calls and other multiple concurrent streaming systems to be accessed.

B. OBJECTIVE

LTE is the next generation wireless data communications standard poised to dominate mobile data connectivity in both commercial and military domains, but just like second generation (2G) and third generation (3G) network systems, it is interference-limited. To improve system throughput, the Medium Access Control (MAC) sub-layer must be redesigned to minimize co-channel interference on both forward and reverse channels. Contrary to popular belief, it is the forward channel and not the reverse channel that limits throughput. In this thesis, we investigate cross-layer optimization in LTE and the integration of orthogonal frequency-division multiple access (OFDMA) with co-channel interference mitigation algorithms to minimize the effect of co-channel interference on both forward and reverse channels so as to attain wide area and seamless coverage.

C. THESIS OUTLINE

This thesis is organized into eight chapters as follows. The various existing cell structures and the frequency reuse techniques to achieve better coverage and high spectral efficiency in LTE, while at the same time attempting to mitigate co-channel interference

(CCI) are covered in Chapter II. The existing scheduling approach in the Medium Access Control (MAC) sub-layer for CCI management is also covered.

The technical architecture and design of an LTE network with aspects on forward and reverse channels access schemes are described in Chapter III, with emphasis on the technical specifications on layers 1 and 2 only since the cross-layer optimization study would be done based on these two layers. The role of interference mitigation in OFDMA is also discussed.

A detailed link analysis in terms of interference mitigation for both forward and reverse channels for an LTE network, using 120°-sectoring and 60°-sectoring are discussed in Chapter IV and Chapter V, respectively.

The MAC sub-layer for analysis on interference mitigation is considered in Chapter VI.

The analysis and simulations conducted based on the cross-layer analysis made in Chapters IV, V, and VI, and the results and summary of the finding are presented in Chapter VII.

The conclusion and recommendations for further potential signal-to-interference ratio (SIR) improvement are presented in Chapter VIII.

D. POTENTIAL APPLICATIONS/BENEFITS

The benefit of the proposed study will help improve the performance of an LTE network by exploiting the synergy between the physical and the MAC layers.

II. LITERATURE REVIEW

A. CO-CHANNEL INTERFERENCE MITIGATIONS

Future wireless data networks aim to offer high data rate coverage over large areas. With the OFDMA technique adopted, interferences such as inter-symbol interference and intra-cell interference are minimized. This leaves co-channel interference (CCI) as the main problem that adversely affects the quality of service (QoS) of the data network.

Three main proposals to combat CCI as listed in 3GPP TR 25.814 [11] are CCI cancellation, CCI coordination, and CCI randomization. CCI cancellation only suppresses the dominating interference with the use of multiple antennas but requires extremely high complexity, while CCI randomization scrambles and interleaves the signal but does not reduce the interference. Finally, CCI coordination applies restrictions on both the downlink and uplink resource manager and on the transmitted power among the cells, making it the method with the most potential to reduce CCI. For instance, with an effective coordination and reuse of resources in a cellular system, the system capacity can be enhanced significantly. As such, with a lower rate at which the same frequency can be used again in the network, known as frequency reuse factor (FRF), more available bandwidth can be obtained for each cell. While this means that the FRF of 1 is desirable, most users would be seriously affected by strong CCI, especially users on the cell edge. One of the CCI mitigation schemes is to increase the cluster-order. This would lead to a decrease of the available bandwidth for each cell, resulting in restricted data transmissions and lower system spectrum efficiency among cells. Therefore, there is a need for careful resource planning and scheduling in the MAC sub-layer to reduce CCI optimally.

In this paper, an investigation of the cross-layer optimization in an LTE network is done to reduce the effect of CCI on both forward and reverse channels. With proper resource management in a coordinated scheduling between cells, such as restrictions on the time/power allocation to the cell and adopting the frequency reuse scheme [1], it is hypothesized that co-channel interference can be mitigated. The following literature review illustrates and supports this hypothesis.

1. Soft Frequency Reuse Scheme

In articles [2] through [6], the authors presented techniques aiming to improve cell-edge performance while retaining a system spectrum efficiency of FRF of 1, known as the Soft Frequency Reuse (SFR) scheme. The users are grouped into two types: cell-centered users (CCU) with a frequency reuse factor (FRF) of 1, and cell-edge users (CEU) with a frequency reuse factor (FRF) of 3. Such an arrangement is shown in Figure 1 from [3].

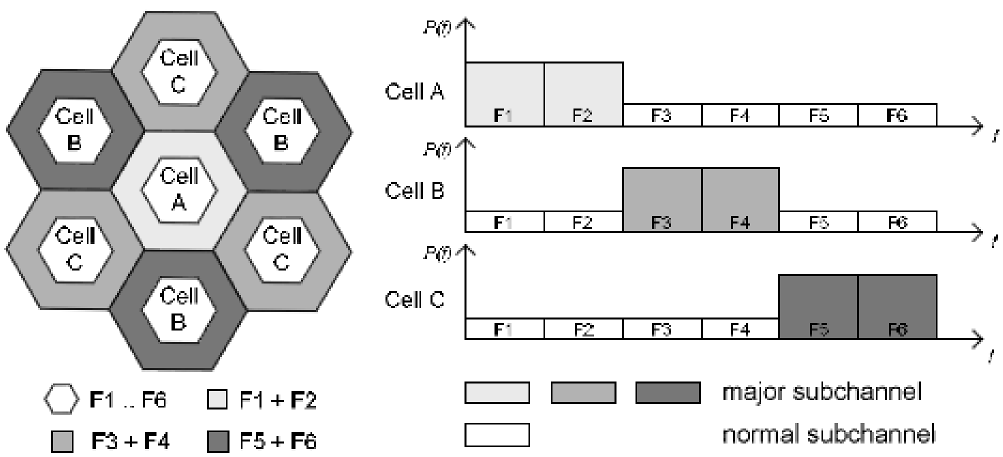

Figure 1. Concept of the SFR scheme in a cellular system based on FRF=3 for CEUs and FRF=1 for CCUs. From [3].

One third of the whole available bandwidth is assigned to each CEU segment with higher power, and directly adjacent cells are orthogonal. The CCUs can access all frequency resources but with a lower transmission power to avoid causing CCI to the neighboring cells.

This scheme is considered relatively simple; however, the CEUs have a maximum of one third of the entire bandwidth to utilize, which leads to a lower spectrum efficiency. Secondly, in a low traffic load situation, there are sub-channels left idle and underutilized in the system, which is undesirable.

2. Incremental Frequency Reuse Scheme

In [3], another technique called the Incremental Frequency Reuse (IFR) scheme was presented to reduce the CCI in a low traffic load situation. As seen in Figure 2 from [3], there is no demarcation of user types. The main concept here is that bandwidth resources are dispensed to contiguous cells, such that there is a better utilization of resources in a low traffic load situation. This is done by allocating the first one third of the frequency to Cell A, the second third of the frequency to Cell B, and the final one third of the frequency to Cell C. The subchannels are allocated successively along with increasing traffic load until the entire frequency is used up. This technique is inferior to the SFR scheme in a full load condition, however.

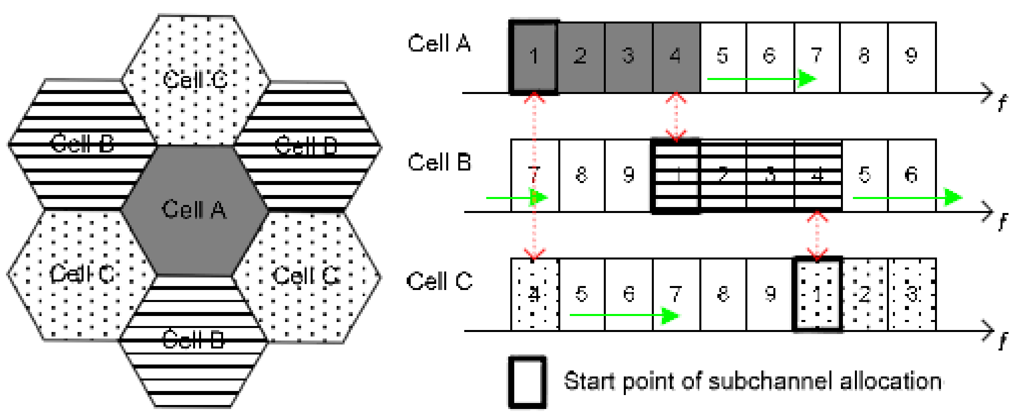

Figure 2. Operation policy of the IFR scheme in a cellular system with 3 various types of neighboring cells. From [3].

3. Enhanced Fractional Frequency Reuse Scheme

In [3], based on the FRF and IFR schemes, the authors evaluated a proposed scheme called Enhanced Fractional Frequency Reuse (EFFR), as shown in Figure 3. In this scheme, three cell types for directly contiguous cells are defined, and a frequency band is reserved for each cell as indicated with the thick border and defined as the cell's primary segment. The first subchannel of the primary segment is allocated to the cell edge area, and the remaining subchannels are assigned to the cell center area. The remaining subchannels not in this primary segment are grouped as the secondary segment, which can be used by the cell in an interference-aware manner. This scheme concentrates on power allocation and an interference-aware reuse mechanism and was found to have improvements in cell capacity gains and wider cell coverage. It seems to rely heavily on self-awareness and adjustment of the system, however, which may be too idealistic.

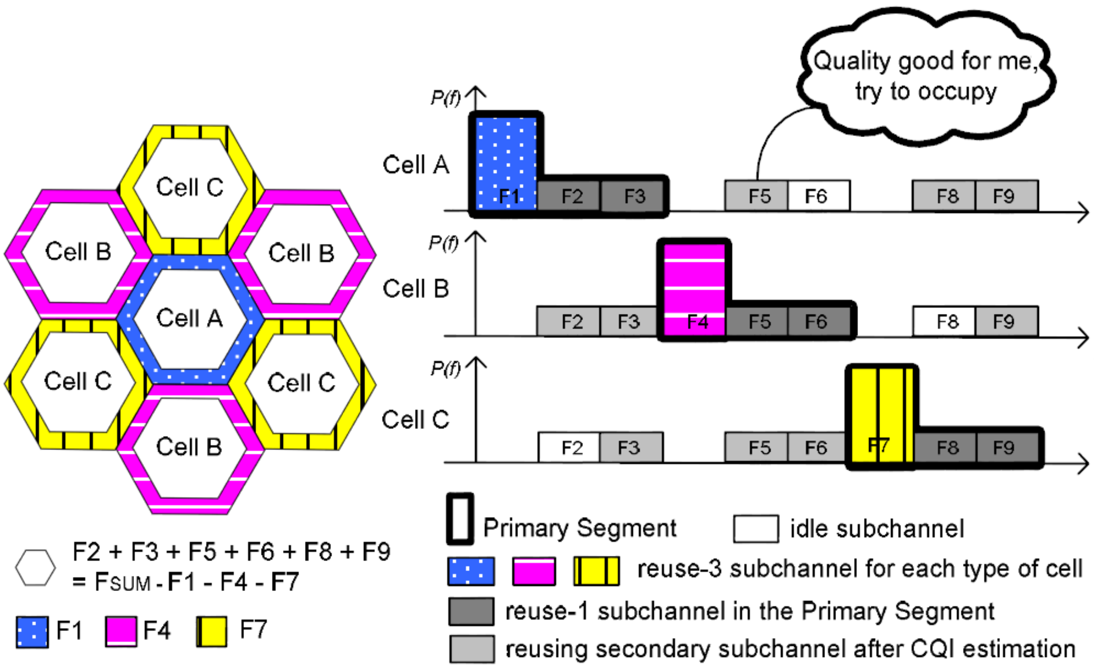

Figure 3. Concept of the EFFR scheme in a cellular system based on partition of exclusively reuse-3 subchannels and reuse-1 subchannels in the Primary Segment, as well as interference aware reuse on the Secondary Segment. From [3].

4. X Scheme for Interference Coordination

In [2], the authors had a coordination technique based on users' ratio and frequency allocation called "X" derived and evaluated. An example of the X scheme is shown in Figure 4, with cell-edge user traffic heavy in cell 1; moderate in cells 2, 4, and 6; and light in cells 3,5,and 7. In such a scenario, frequency resource is borrowed from cells 3, 5 and 7 to allocate to cell 1, with the cell-center users using a reduced power so that cell 1 can use the same frequency resource allocated to the cell-edge users in the neighboring cells without interference. As this scheme takes into account the change of traffic load between the two different groups of users, and among the neighboring cells, the authors are able to simulate and show that the whole network performance is improved in terms of throughput, delay, delay jitter, and signal-to-interference-and-noiseratio (SINR). However, it seems to require too much coordination for practical application because of the additional system complexity introduced.

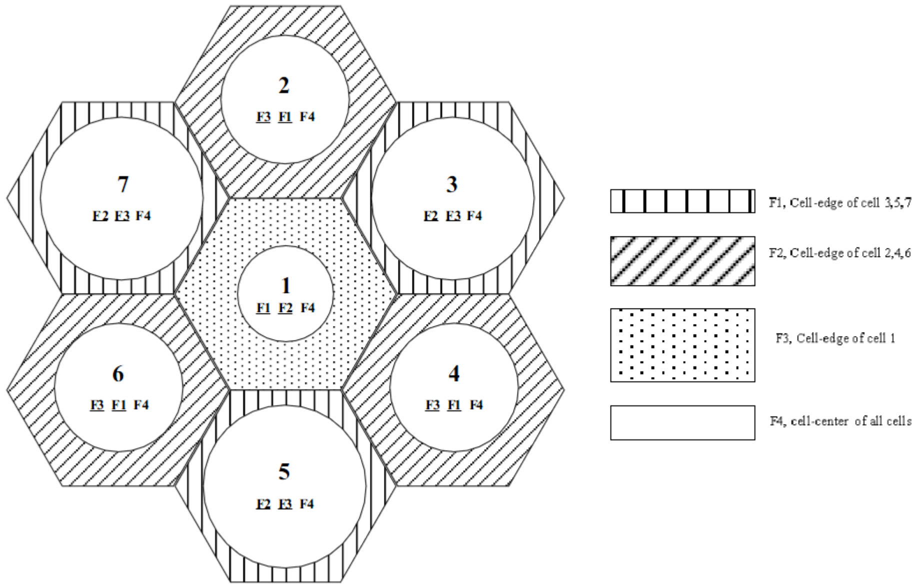

Figure 4. Frequency reuse scheme of X scheme. From [2].

5. Network Power Planning Scheme

In [2], the authors also presented a frequency reuse scheme of Alcatel named Network Power Planning. The entire frequency band is divided into seven subsets with corresponding power, as shown in Figure 5 from [2]. F1, F2, and F6 are allocated, respectively, for cell-edge users in cell 1 with full power according to the sector in which the users transmit or receive. A reduced power is used for the center area of the cell. Here, the FRF for the center cell is 1, and for the edge cell it is 3/7 rather than 1/3.

6. Scheduling Strategy at the MAC Sub-layer

The frequency reuse techniques described in Sections 1 to 5 of this chapter require a good scheduling strategy. This refers to the need to take the situation in the neighboring cells into account, including the exchange of interference indicators between the eNB in the MAC sub-layer [19]. For instance, an eNB in Figure 6 may signal to its neighboring eNBs the intention to transmit with a lower transmission power in the downlink on a set of resource blocks. The neighboring eNBs then exploit this information by recognizing it as a zone of low interference where it is advantageous to schedule communication with the cell edge users who otherwise cannot attain high data rates due to the interference level.

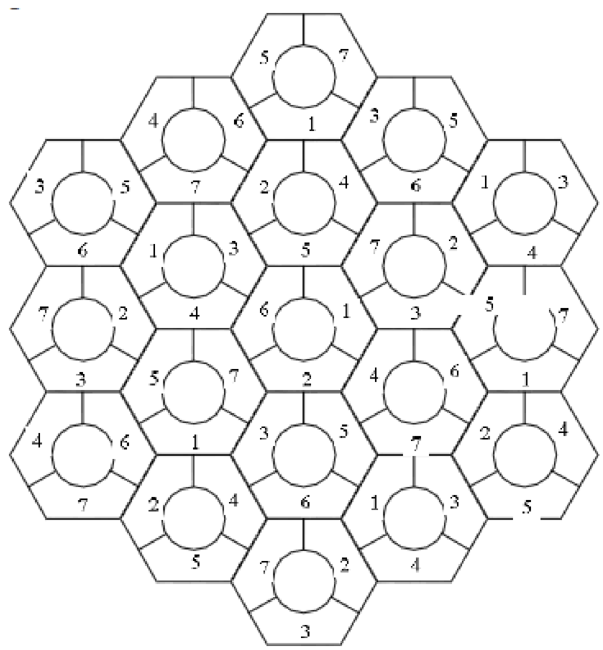

Figure 5. Frequency reuse scheme of Network Power Planning scheme. From [2].

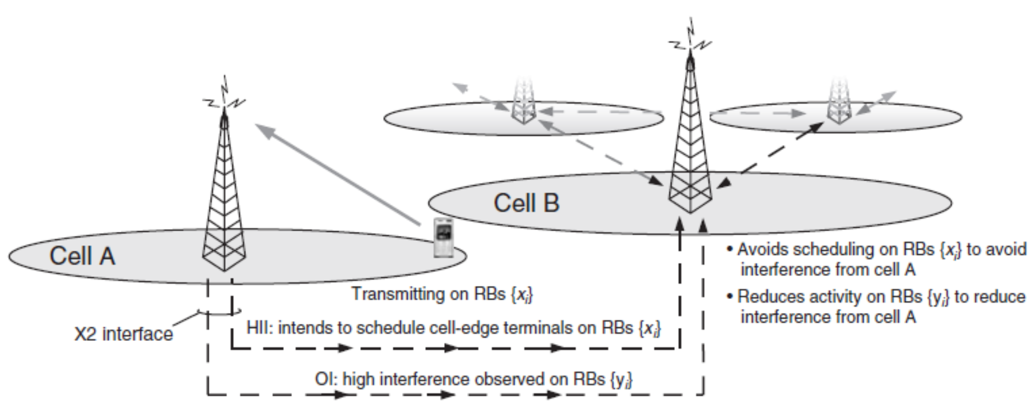

Figure 6. Example of uplink co-channel interference coordination. From [19].

The two interference indicators that are exchanged between neighboring eNBs on the X2 interface are the high-interference indicator (HII) and the overload indicator (OI). Referring to Figure 6 again, we see that Cell A sends a HII, which is a proactive operation that gives information to other eNBs, including Cell B, about the resource blocks on which Cell A intends to schedule the CEUs. This activity is deemed as interference for Cell B; hence, Cell B wants to avoid scheduling transmission to the CEU if possible.

The OI is a reactive operation that controls the interference in an appropriate range after it occurs. When the CCI reaches a certain threshold, the OI is triggered to inform the interference level to its neighbors. The neighbors then determine whether they are the main interference sources before taking the necessary action to reduce their transmission power or do nothing at all.

In summary, the OI can effectively improve spectrum efficiency by having the CCI under control and operating in an appropriate range in an ideal situation at the expense of complexity and heavy overhead. HII can effectively reduce CCI and provide a higher QoS with poor spectral efficiency. [20]

B. THESIS WORK

In summary, the results from the literature show that proper planning and coordination of the resources play a vital role in CCI management. To enhance the mean system capacity while restraining the CCI at the cell edge, a thorough analysis on the frequency reuse scheme of Alcatel’s proposal [2] is chosen for evaluation, mainly because it adopts a sectoring technique. This is a technique proven to aid in mitigating co-channel interference in 3G cellular networks [8]-[9] and is easy to understand and implement. After that, an expansion on this proposal to 60°-sectoring is also investigated.

To complement the sectoring techniques that are proposed, resource scheduling with the use of Latin Square in the MAC sub-layer among the neighboring eNBs is evaluated. With cross-layer optimization analysis, physical and MAC layer control decisions are able to reach their full potential when they are cooperatively designed with each other.

THIS PAGE INTENTIONALLY LEFT BLANK

III. LTE ARCHITECTURE AND DESIGN

A. MOTIVATION FOR LTE

Other than LTE's promising high performance and spectral efficiency improvement to the cellular network, another benefit of LTE is its ability to build on existing 2G and 3G cellular infrastructures, thereby aiding in seamless handoff and connectivity between previous standards and LTE and reducing infrastructure costs. As LTE is able to support IP-only network with rates up to 150 Mbps, new applications and services such as voice over IP, streaming multimedia, and videoconferencing can be supported.

B. OVERVIEW

A high-level view of the LTE architecture [7] is shown in Figure 7, where the eNB (another name for base station used in LTE) interfaces with other eNB and User Equipment (UE). The E-UTRAN refers to the entire network and is the official standard name for LTE.

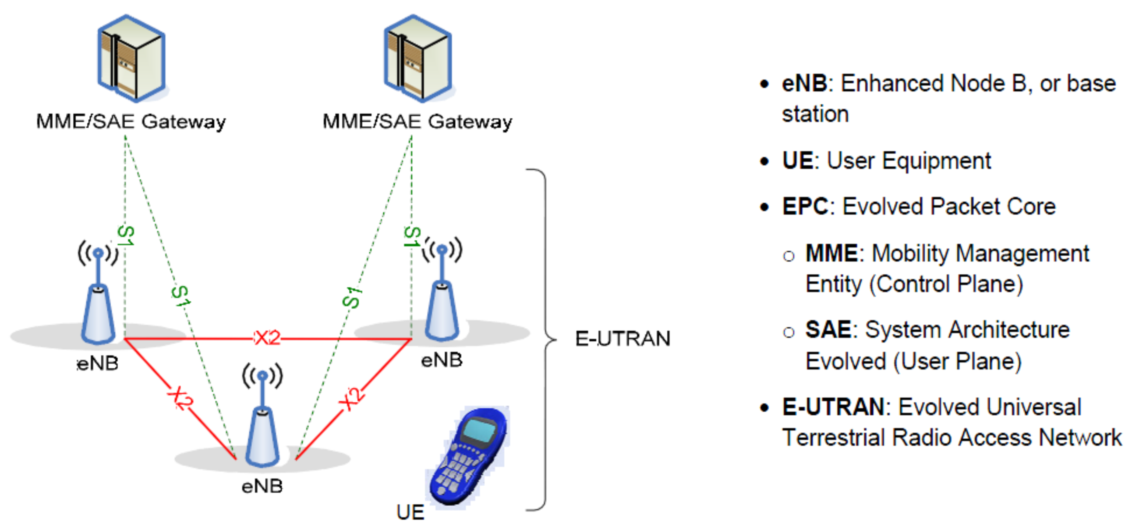

Figure 7. LTE architecture overview. From [4].

C. RADIO PARAMETERS FOR LTE

1. Key Parameters

The key parameters in terms of the duplexing technique, the frequency range, and the channel bandwidth that LTE operates on, the modulation schemes and multiple access techniques used by LTE, and the Multiple-Input and Multiple-Output (MIMO) technology as well as its peak data rate are summarized in Table 1. [12]

Table 1. Key parameters for LTE. From [12].

Frequency Range	**UMTS FDD bands and UMTS TDD bands**					
Channel bandwidth, 1 Resource Block=180 kHz	**1.4 MHz**	**3 MHz**	**5 MHz**	**10 MHz**	**15 MHz**	**20 MHz**
	6 Resource Blocks	15 Resource Blocks	25 Resource Blocks	50 Resource Blocks	75 Resource Blocks	100 Resource Blocks
Modulation Schemes	**Downlink:** QPSK, 16QAM, 64QAM **Uplink:** QPSK, 16QAM, 64QAM (optional for handset)					
Multiple Access	**Downlink:** OFDMA (Orthogonal Frequency Division Multiple Access) **Uplink:** SC-FDMA (Single Carrier Frequency Division Multiple Access)					
MIMO technology	**Downlink:** Wide choice of MIMO configuration options for transmit diversity, spatial multiplexing, and cyclic delay diversity (max. 4 antennas at base station and handset) **Uplink:** Multi user collaborative MIMO					
Peak Data Rate	**Downlink:** 150 Mbps (UE category 4, 2x2 MIMO, 20 MHz) 300 Mbps (UE category 5, 4x4 MIMO, 20 MHz) **Uplink:** 75 Mbps (20 MHz)					

2. Frequency Bands

LTE is designed to operate in the frequency bands listed in Table 2 [10, 12]

Table 2. Frequency bands for LTE. From [10, 12]

E-UTRA Operating Band	Uplink (UL) operating band BS receive UE transmit	Downlink (DL) operating band BS transmit UE receive	Duplex Mode
	F_{UL_low} – F_{UL_high}	F_{DL_low} – F_{DL_high}	
1	1920 MHz – 1980 MHz	2110 MHz – 2170 MHz	FDD
2	1850 MHz – 1910 MHz	1930 MHz – 1990 MHz	FDD
3	1710 MHz – 1785 MHz	1805 MHz – 1880 MHz	FDD
4	1710 MHz – 1755 MHz	2110 MHz – 2155 MHz	FDD
5	824 MHz – 849 MHz	869 MHz – 894MHz	FDD
6[1]	830 MHz – 840 MHz	875 MHz – 885 MHz	FDD
7	2500 MHz – 2570 MHz	2620 MHz – 2690 MHz	FDD
8	880 MHz – 915 MHz	925 MHz – 960 MHz	FDD
9	1749.9 MHz – 1784.9 MHz	1844.9 MHz – 1879.9 MHz	FDD
10	1710 MHz – 1770 MHz	2110 MHz – 2170 MHz	FDD
11	1427.9 MHz – 1447.9 MHz	1475.9 MHz – 1495.9 MHz	FDD
12	699 MHz – 716 MHz	729 MHz – 746 MHz	FDD
13	777 MHz – 787 MHz	746 MHz – 756 MHz	FDD
14	788 MHz – 798 MHz	758 MHz – 768 MHz	FDD
15	Reserved	Reserved	FDD
16	Reserved	Reserved	FDD
17	704 MHz – 716 MHz	734 MHz – 746 MHz	FDD
18	815 MHz – 830 MHz	860 MHz – 875 MHz	FDD
19	830 MHz – 845 MHz	875 MHz – 890 MHz	FDD
20	832 MHz – 862 MHz	791 MHz – 821 MHz	FDD
21	1447.9 MHz – 1462.9 MHz	1495.9 MHz – 1510.9 MHz	FDD
22	3410 MHz – 3490 MHz	3510 MHz – 3590 MHz	FDD
23	2000 MHz – 2020 MHz	2180 MHz – 2200 MHz	FDD
24	1626.5 MHz – 1660.5 MHz	1525 MHz – 1559 MHz	FDD
25	1850 MHz – 1915 MHz	1930 MHz – 1995 MHz	FDD
...			
33	1900 MHz – 1920 MHz	1900 MHz – 1920 MHz	TDD
34	2010 MHz – 2025 MHz	2010 MHz – 2025 MHz	TDD
35	1850 MHz – 1910 MHz	1850 MHz – 1910 MHz	TDD
36	1930 MHz – 1990 MHz	1930 MHz – 1990 MHz	TDD
37	1910 MHz – 1930 MHz	1910 MHz – 1930 MHz	TDD
38	2570 MHz – 2620 MHz	2570 MHz – 2620 MHz	TDD
39	1880 MHz – 1920 MHz	1880 MHz – 1920 MHz	TDD
40	2300 MHz – 2400 MHz	2300 MHz – 2400 MHz	TDD
41	2496 MHz 2690 MHz	2496 MHz 2690 MHz	TDD
42	3400 MHz – 3600 MHz	3400 MHz – 3600 MHz	TDD
43	3600 MHz – 3800 MHz	3600 MHz – 3800 MHz	TDD
NOTE 1: Band 6 is not applicable			

D. MULTIPLE ACCESS TECHNIQUES

Orthogonal frequency-division multiplexing access (OFDMA) allows simultaneous data access from several users by allocating resources for these users in both time and frequency domains. This is possible because the OFDM symbols are allocated by time-division multiple access (TDMA), while the sub-carriers within an OFDM symbol are allocated by OFDMA [12, 13]. In this manner, multiple users can use the same sub-channel at different times while minimizing the chance of causing inter-carrier interference. This is illustrated in Figure 8.

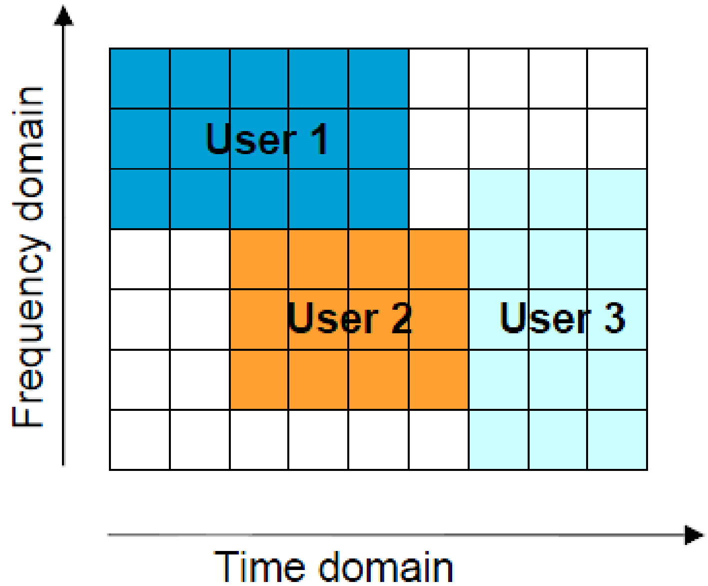

Figure 8. Orthogonal frequency-division multiplexing access. From [12].

1. OFDMA for Downlink

The subcarrier spacing used in LTE is 15 kHz, which can also be found from the equation *B/L*, where *B* is the channel bandwidth and *L* is the number of subcarriers. The purpose of subcarrier spacing is to avoid inter-symbol interference (ISI). However, due to multipath delay spread, ISI still exists. To eliminate ISI, a cyclic prefix is used as a guard interval, with two types of possible configurations available. The first is termed as normal cyclic prefix, with 5.2 µs for the first symbol and 4.7 µs for other symbols. The second configuration is called an extended cyclic prefix, with 16.7 µs. The frequency-time representation of OFDMA is illustrated in Figures 9 and 10. [12]

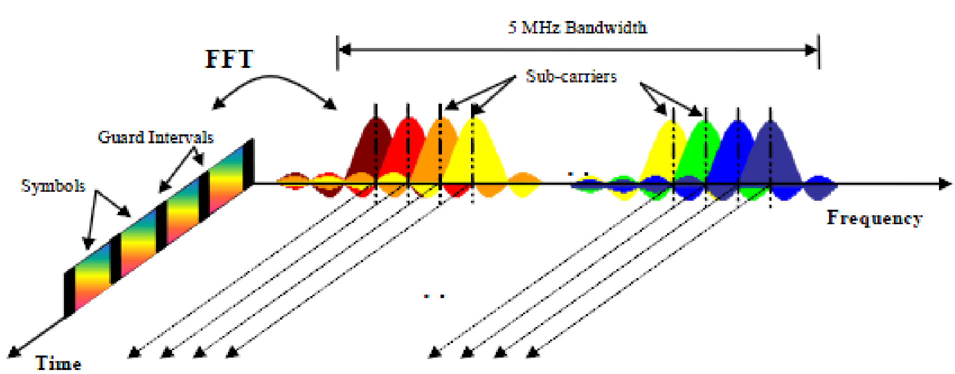

Figure 9. Frequency-time representation of an OFDM signal. From [12].

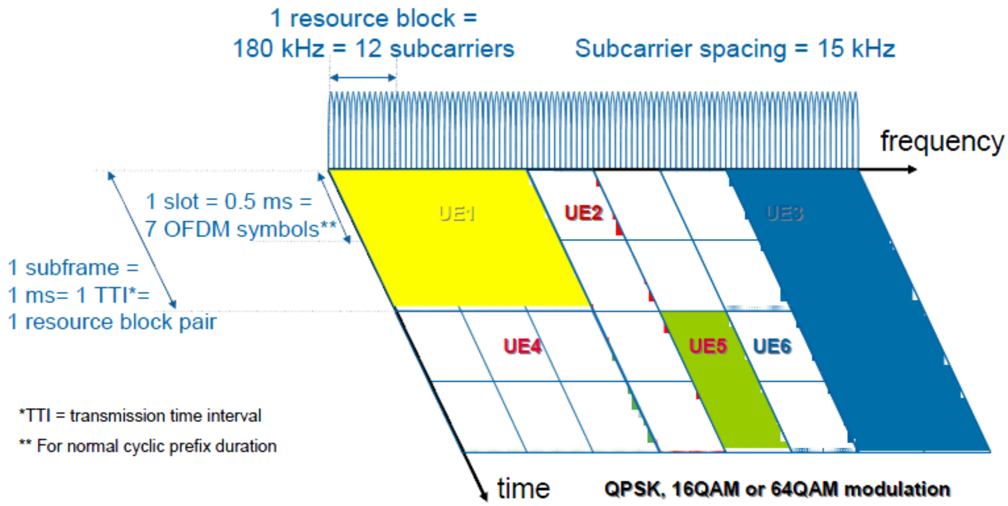

Figure 10. OFDMA time-frequency multiplexing. From [12].

2. SC-FDMA for Uplink

Single carrier-frequency-division multiple access (SC-FDMA) is a multiple access technique that utilizes single carrier modulation, discrete fourier transform (DFT)-spread orthogonal frequency multiplexing, and frequency domain equalization. As each subcarrier carries a portion of superimposed DFT-spread data symbols, it is also known as DFT-spread-OFDM (DFT-s-OFDM) [12, 14]. The transmitter and receiver block diagram is shown in Figure 11.

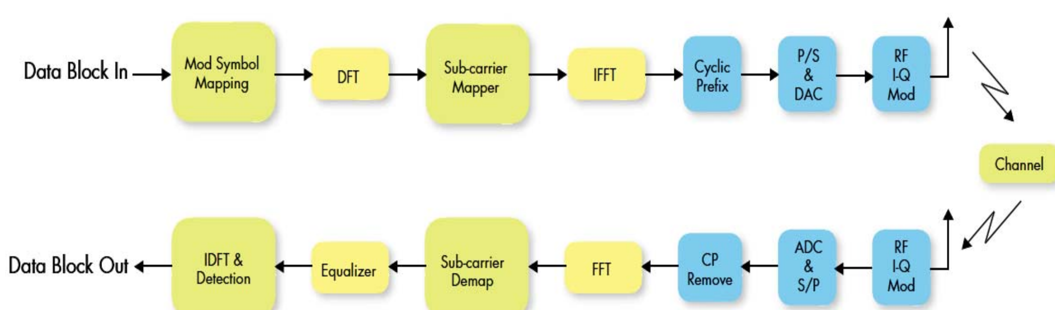

Figure 11. SC-FDMA transmitter and receiver. From [14].

The SC-FDMA transmitter carries data symbols over a group of subcarriers transmitted simultaneously; the group of subcarriers that carries each data symbol can be viewed as one frequency band carrying data sequentially in a standard FDMA.

Despite the similar performance and complexity between SC-FDMA and OFDMA, the main advantage of SC-FDMA is the low peak-average-power ratio (PAPR) of the transmitted signal. The PAPR is defined as the ratio of the peak power to the average power of the transmitted signal. As most UEs are battery operated, power conservation is of utmost concern to them, making SC-FDMA the preferred access technique for the uplink transmission.

E. PHYSICAL LAYER

1. Generic Frame Structure

As shown in Table 1, the LTE physical layer supports any bandwidth from 1.4 MHz to 20 MHz in steps of 180 kHz known as a resource block (RB). A RB is defined as consisting of 12 consecutive subcarriers for one time slot, 0.5 ms, or 7 OFDM symbols for normal cyclic prefix duration. It is the smallest element of resource allocation assigned by the base station scheduler [12, 15]. The LTE transmissions are segmented into frames of 10 ms in duration, and each frame consists of 20 time slots of 0.5 ms. Sub-frames contain two slot periods and are 1.0 ms in duration. This generic frame structure is shown in Figure 12.

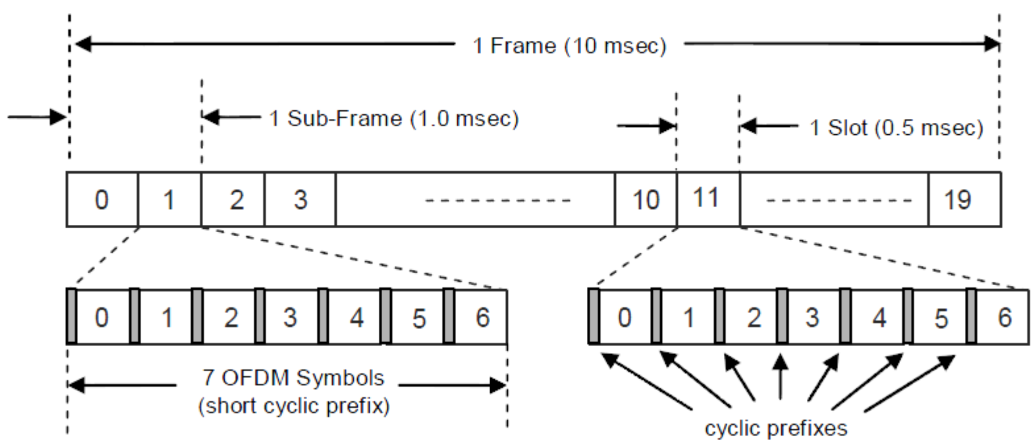

Figure 12. LTE generic frame structure. From [15].

2. Physical Channels

Physical channels convey information from higher layers in the LTE stack and have defined algorithms for bit scrambling, modulation, layer mapping, cyclic delay diversity (CDD) pre-coding, and resource element assignment. Generally, the channels are defined into three types: the physical downlink shared channel (PDSCH), which is mainly for data and multimedia transport and is designed for very high data rates with modulation options including quadrature phase-shift keying (QPSK), sixteen-quadrature amplitude modulation (16QAM), 64-quadrature amplitude modulation (64QAM), and spatial multiplexing; the physical downlink control channel (PDCCH), which conveys UE-specific control information such as uplink power control commands, requires robustness as its main consideration, and has QPSK as the only available modulation format; and the common control physical channel (CCPCH), which carries cell-wide control information, also has robustness as the main consideration, and has QPSK as the only available modulation format.

Uplink physical channels are used to transmit information originating in layers above the physical layer, and there are two types of channels defined for uplink: the physical uplink shared channel (PUSCH); and the physical uplink control channel (PUCCH), which conveys control information such as channel quality indication (CQI) and uplink scheduling requests.

3. Physical Signals (Signaling)

Unlike physical channels, physical signals convey information that is used exclusively within the physical layer and are defined into two types: the reference signals to determine the channel impulse response (CIR), where each such signal is uniquely assigned to each cell in a network and acts as a cell-specific identifier; and the synchronization signals to convey network timing information.

4. Transport Channels

Transport channels included in the physical layer act as service access points (SAPs) for higher layers by providing a structure for passing data across higher layers. They provide a mechanism by which higher layers can configure the physical layer and provide status indicators on packet errors to higher layers. They also support higher layer peer-to-peer signaling. The mapping of the downlink transport channels to the downlink physical channels is shown in Figure 13, while the mapping of the uplink transport channels to the uplink physical channels is shown in Figure 14.

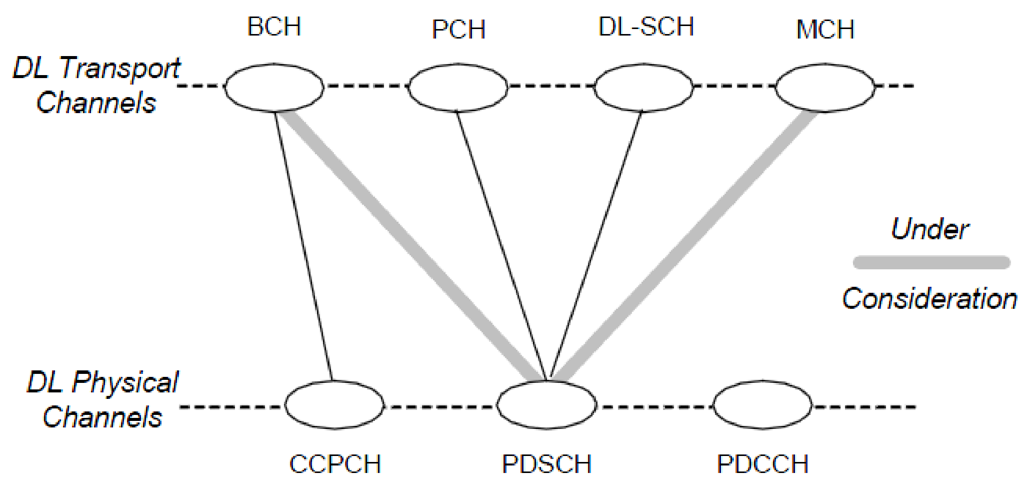

Figure 13. Mapping downlink transport channels to physical channels. From [15].

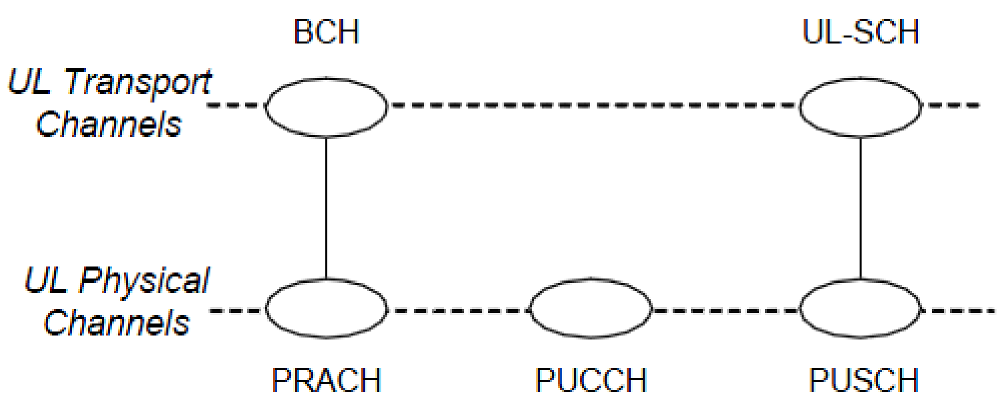

Figure 14. Mapping of UL transport channels to UL physical channels. From [15].

F. LAYER 2 (MAC, RLC, PDCP) [7]

The LTE layer 2 consists of three sub-layers called Medium Access Control layer (MAC), Radio Link Control (RLC), and Packet Data Convergence Protocol (PDCP). Its functions include the mapping between transparent and logical channels, performing error correction through hybrid ARQ, executing priority handling with dynamic scheduling, and performing logical channel prioritization. [16] [17]

1. Mapping between Transparent and Logical Channels

The MAC offers services to RLC in the form of a logical channel, which is generally defined as a control channel or a traffic channel, depending on the type of information it carries. A control channel is used for transmission of control and configuration information required for operating an LTE system, while a traffic channel is used for the transmission of user data.

2. Error Correction through Hybrid ARQ

The Hybrid ARQ (HARQ) process between the MAC and physical layers retransmits transport blocks for error recovery. While the physical layer performs the retention and recombination with incremental redundancy, the MAC layer performs the management and signaling. In HARQ operation, the retransmission does not have to be fully correct. It has to be correct enough that it can be combined mathematically with the previous transport block in order to produce a good transport block, making it an efficient way of providing the ARQ function[7].

3. Priority Handling with Dynamic Scheduling

Priority handling between UEs done at the eNB for both downlink and uplink, as well as priority handling between the logical channels of one of the UEs for both downlink and uplink, are done using dynamic scheduling in the RLC sub-layer. A dynamic scheduling operation assigns resources in the downlink when data is available, and the UE dynamically requests transmission opportunities when data arrives in its uplink buffer. This reduces control channel signaling greatly.

4. Logical Channel Prioritization

The Logical Channel Prioritization procedure is applied when there is a new transmission to be performed, and this is based on the configured priority and Prioritized Bit Rate (PBR). Logical channels are served in the order of their priority such that the Quality of Service (QoS) is maintained.

G. LATIN SQUARES [21]

A Latin Square is a matrix (of dimension N_c sub-carriers) with entries from the set of virtual channels, namely 0, 1, …, N_c - 1, for periodic virtual channel hopping over the sub-carriers every OFDM symbol time. Five virtual channels over five OFDM symbol times are shown in Figure 15, with each row of the hopping matrix corresponding to a sub-carrier and each column representing an OFDM symbol time. The entries represent the virtual channels that use that sub-carrier in different OFDM symbol times for maximal frequency diversity, and at any OFDM symbol time, the virtual channels occupy different sub-carriers.

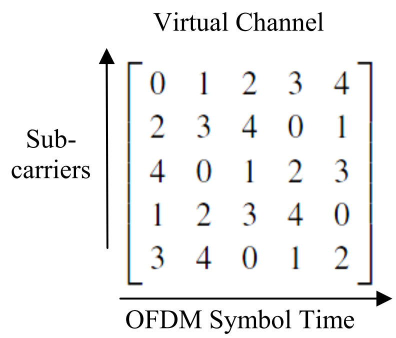

Figure 15. Latin Square. After [21].

To further illustrate the hopping pattern concept of the Latin Square, assume there are five virtual channels utilizing five OFDM symbol times (that is, $N_c = 5$), as shown in Figure 16, with the corresponding hopping pattern matrix as shown in Figure 15. Virtual channel 0 is assigned the OFDM symbol and sub-carrier pairs (0,0), (1,2), (2,4), (3,1), and (4,3) as shown in Figure 16. The design rule here is to maximize diversity by having minimal overlap between virtual channels of the neighboring eNBs, where each eNB has its own hopping Latin Square matrix.

For the case when N_c is prime, there is a family of N_c - 1 mutually quasi-orthogonal Latin Squares. For a = 1, …, N_c - 1, there are N_c - 1 matrices R^a of size $N_c \times N_c$ with the (i,j)th entry computed from

$$R_{ij}^{a} = (ai + j) \text{ modulo } N_c \qquad (3.1)$$

where i and j are the row and column indices, respectively.

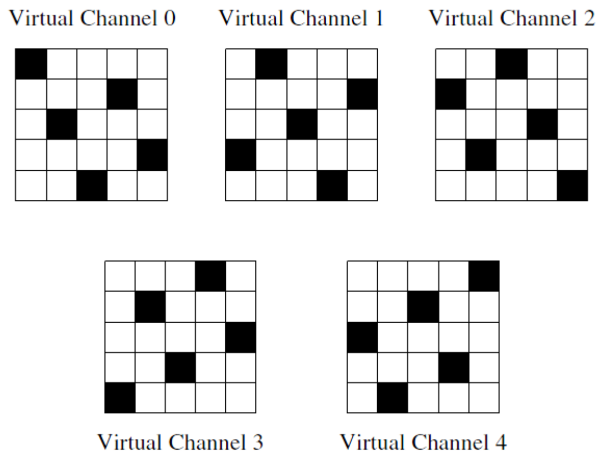

Figure 16. Virtual hopping patterns for N_c=5. From [21].

THIS PAGE INTENTIONALLY LEFT BLANK

IV. LINK ANALYSIS FOR 120°-SECTORING

A. NETWORK POWER PLANNING

The frequency reuse scheme of Alcatel's proposal, called Network Power Planning [2], is shown in Figure 17 with two tiers for the purpose of analysis. Each cell has an eNB at the cell center that serves a number of UEs uniformly distributed in the cell. Each cell is also partitioned into a center area and an edge area, where frequency reuse factor-1 is used in the center area. Since sectoring is used for the edge area, the frequency reuse pattern here is 3/7, where three is the number of sectors per cell, and seven is the number of frequency sub-channels available per cluster. It is worthwhile to note that, in addition to sectoring, with no adjacent edge areas sharing the same set of sub-channels, the performance of the cell edge users (CEUs) is expected to improve.

Sub-channels 1, 2, and 6 are allocated, respectively, for cell edge users in cell O with full power according to the sector in which the UEs transmit and receive. A reduced power is used for the UEs in the center cell.

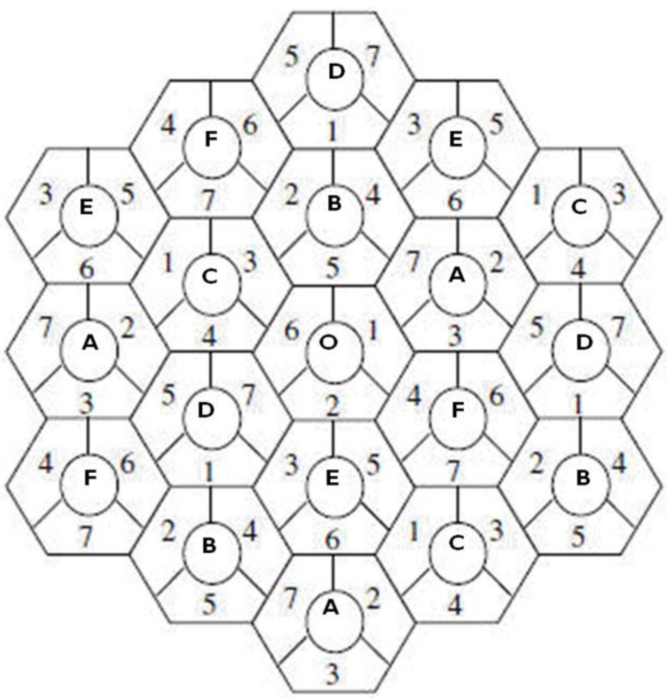

Figure 17. Frequency reuse scheme of Alcatel's proposal. After [2].

1. Interference Analysis for the Forward Channel

Assuming that the traffic load is uniformly distributed in each cell and is proportional to the cell area, we let the cell of interest be O. The positions where the highest level of CCI is experienced for center area and edge area are marked by a triangle and a star, respectively. The inner cell radius is labeled as *r*, while the outer cell radius is denoted as *R*. This is represented in Figure 18.

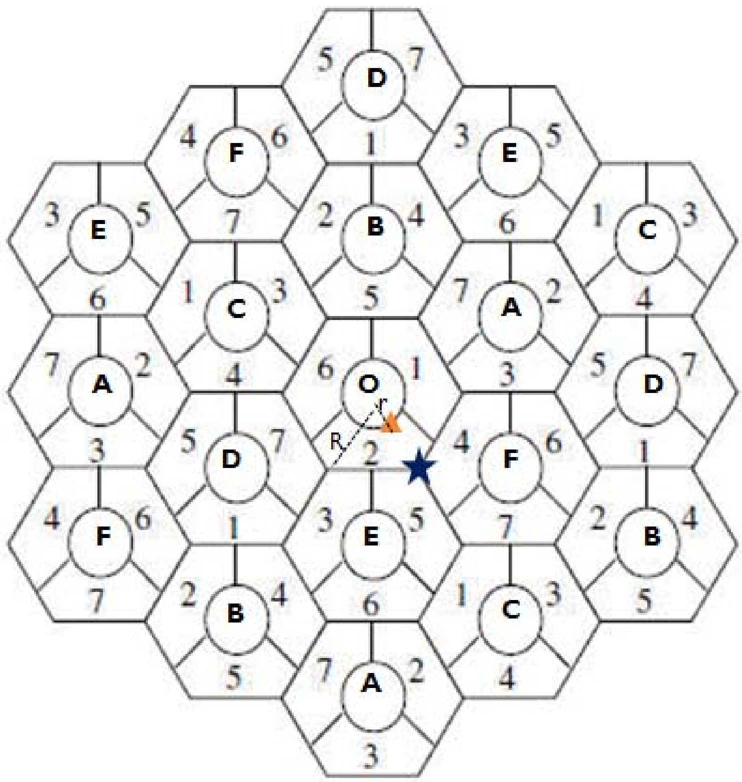

Figure 18. Positions of UEs in center and edge areas for analysis. After [2].

Assuming all eNB have the same transmit antenna gains, we have the desired power received from eNB at cell O (eNB_O) $P_{R,O}$ as

$$P_{R,O} = \frac{G_T G_R P_{T,O}}{L_O} \tag{4.1}$$

where G_T is the gain of the transmitter at eNB, G_R is the gain of the receiver of the UE, $P_{T,O}$ is the transmitted power of eNB_O, and L_O is the propagation loss from eNB_O to the UE.

The co-channel interference power received from eNB at cell A (eNB_A) $P_{R,A}$ is

$$P_{R,A} = \frac{G_T G_R P_{T,A}}{L_A} \tag{4.2}$$

where $P_{T,A}$ is the transmitted power of eNB_A; L_A is the propagation loss from eNB_A to the UE.

The co-channel interference power received from eNB at cell B (eNB_B) $P_{R,B}$ is

$$P_{R,B} = \frac{G_T G_R P_{T,B}}{L_B} \tag{4.3}$$

where $P_{T,B}$ is the transmitted power of eNB_B; L_B is the propagation loss from eNB_B to the UE.

The co-channel interference power received from eNB at cell C (eNB_C) $P_{R,C}$ is

$$P_{R,C} = \frac{G_T G_R P_{T,C}}{L_C} \tag{4.4}$$

where $P_{T,C}$ is the transmitted power of eNB_C; L_C is the propagation loss from eNB_C to the UE.

The co-channel interference power received from eNB at cell D (eNB_D) $P_{R,D}$ is

$$P_{R,D} = \frac{G_T G_R P_{T,D}}{L_D} \tag{4.5}$$

where $P_{T,D}$ is the transmitted power of eNB_D; L_D is the propagation loss from eNB_D to the UE.

The co-channel interference power received from eNB at cell E (eNB_E) $P_{R,E}$ is

$$P_{R,E} = \frac{G_T G_R P_{T,E}}{L_E} \tag{4.6}$$

where $P_{T,E}$ is the transmitted power of eNB_E; L_E is the propagation loss from eNB_E to the UE.

The co-channel interference power received from eNB at cell F (eNB_F) $P_{R,F}$ is

$$P_{R,F} = \frac{G_T G_R P_{T,F}}{L_F} \tag{4.7}$$

where $P_{T,F}$ is the transmitted power of eNB_F; L_F is the propagation loss from eNB_F to the UE.

2. Forward channel Signal-to-Interference Ratio (SIR) analysis for cell-center users (CCU)

Other than the sub-channels assigned to the edge areas of the cells, the remaining sub-channels 3, 4, 5 and 7 for eNB_O, are used for the entire center area irrespective of the sector. Hence, the cell-center user (CCU) shown as the triangle in Figure 19 receives co-channel interference (CCI) from the eNB in the six cells (A to F) in the first tier.

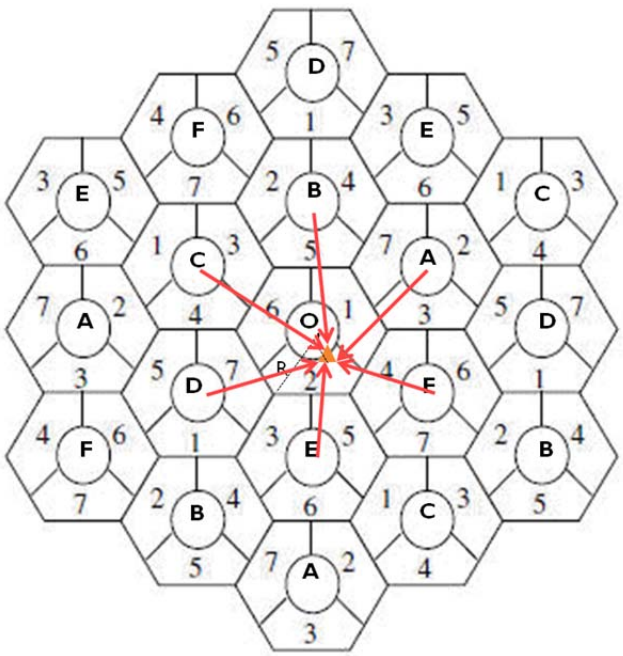

Figure 19. Forward channel interference experienced by the CCU. After [2].

Since the interference from the second tier cells are small compared to the first tier, they are negligible and, thus, ignored. Therefore, by summing Equations (4.2) to (4.7), the total co-channel interference I received by the CCU due to first tier eNB in cells A to F is

$$I = \left(\frac{G_T G_R P_{T,A}}{L_A}\right) + \left(\frac{G_T G_R P_{T,B}}{L_B}\right) + \left(\frac{G_T G_R P_{T,C}}{L_C}\right) + \left(\frac{G_T G_R P_{T,D}}{L_D}\right) + \left(\frac{G_T G_R P_{T,E}}{L_E}\right) + \left(\frac{G_T G_R P_{T,F}}{L_F}\right). \quad (4.8)$$

Grouping the common terms $G_T G_R$ together in Equation (4.8), we get

$$I = \left(G_T G_R\right)\left(L_A^{-1} P_{T,A} + L_B^{-1} P_{T,B} + L_C^{-1} P_{T,C} + L_D^{-1} P_{T,D} + L_E^{-1} P_{T,E} + L_F^{-1} P_{T,F}\right). \quad (4.9)$$

The forward channel SIR of the CCU $SIR_{CCU,120^\circ}$ is derived as follows:

$$SIR_{CCU,120^\circ} = \left(\frac{P_{R,O}}{I} \right). \tag{4.10}$$

Substituting Equations (4.1) and (4.9) into Equation (4.10), we get

$$SIR_{CCU,120^\circ} = \left(\frac{L_O^{-1} P_{T,O}}{\left(L_A^{-1} P_{T,A} + L_B^{-1} P_{T,B} + L_C^{-1} P_{T,C} + L_D^{-1} P_{T,D} + L_E^{-1} P_{T,E} + L_F^{-1} P_{T,F} \right)} \right). \tag{4.11}$$

The power law equation is determined as

$$L = \beta d^n \tag{4.12}$$

where β is a proportionality constant that is a function of the antenna heights of both transmitter and receiver and the carrier frequency; d is the distance between the transmitter and the receiver, and n is the path loss component factor.

Substituting Equation (4.12) into Equation (4.11), we have

$$SIR_{CCU,120^\circ} = \left(\frac{\left(\beta_O^{-1} r^{-n}\right) P_{T,O}}{\left(\left(\beta_A^{-1}\left(\sqrt{3R^2+r^2}\right)^{-n}\right) P_{T,A} + \left(\beta_B^{-1}\left(\sqrt{3R^2+r^2+3Rr}\right)^{-n}\right) P_{T,B} + \left(\beta_C^{-1}\left(\sqrt{3R^2+r^2+3Rr}\right)^{-n}\right) P_{T,C} + \left(\beta_D^{-1}\left(\sqrt{3R^2+r^2}\right)^{-n}\right) P_{T,D} + \left(\beta_E^{-1}\left(\sqrt{3R^2+r^2-3Rr}\right)^{-n}\right) P_{T,E} + \left(\beta_F^{-1}\left(\sqrt{3R^2+r^2-3Rr}\right)^{-n}\right) P_{T,F} \right)} \right). \tag{4.13}$$

Since $\beta_O = \beta_A = \beta_B = \beta_C = \beta_D = \beta_E = \beta_F$ by assumption, for homogeneous clusters, we obtain

$$SIR_{CCU,120^\circ} = \left(\frac{\left(r^{-n}\right) P_{T,O}}{\left(\left(\sqrt{3R^2+r^2}\right)^{-n} P_{T,A} + \left(\sqrt{3R^2+r^2+3Rr}\right)^{-n} P_{T,B} + \left(\sqrt{3R^2+r^2+3Rr}\right)^{-n} P_{T,C} + \left(\sqrt{3R^2+r^2}\right)^{-n} P_{T,D} + \left(\sqrt{3R^2+r^2-3Rr}\right)^{-n} P_{T,E} + \left(\sqrt{3R^2+r^2-3Rr}\right)^{-n} P_{T,F} \right)} \right). \tag{4.14}$$

By rearranging the common term r^{-n} in Equation (4.14), we get

$$SIR_{CCU,120^{\circ}} = \left(\frac{P_{T,O}}{\left(\left(\sqrt{3\left(\frac{R}{r}\right)^2+1}\right)^{-n} P_{T,A} + \left(\sqrt{3\left(\frac{R}{r}\right)^2+3\left(\frac{R}{r}\right)+1}\right)^{-n} P_{T,B} + \left(\sqrt{3\left(\frac{R}{r}\right)^2+3\left(\frac{R}{r}\right)+1}\right)^{-n} P_{T,C} + \left(\sqrt{3\left(\frac{R}{r}\right)^2+1}\right)^{-n} P_{T,D} + \left(\sqrt{3\left(\frac{R}{r}\right)^2-3\left(\frac{R}{r}\right)+1}\right)^{-n} P_{T,E} + \left(\sqrt{3\left(\frac{R}{r}\right)^2-3\left(\frac{R}{r}\right)+1}\right)^{-n} P_{T,F} \right)} \right). \quad (4.15)$$

3. Forward channel Signal-to-Interference Ratio (SIR) analysis for cell edge users (CEU)

Cell edge users (CEUs) are only allowed to use their assigned sub-channel, and as shown in Figure 20, the CEU is denoted as a star and is using sub-channel 2. Only cells A and B in the first tier have sectors using the same sub-channel 2, but because of sectoring, the transmission of signals by the eNB in these two cells is in a direction away from the CEU. Hence, they do not interfere with the CEU.

Moving the analysis to the second tier, we see that two A cells and two B cells use the same sub-channel 2, but cell B in the bottom left has its sector facing away from the CEU. As such, the CEU has interference due to two A cells and one B cell on the bottom right only.

Therefore, the total co-channel interference I received by the CEU due to second tier eNB (two A cells and one B cell on the lower right only) is given by

$$I = \left(\frac{G_T G_R P_{T,A}}{L_A} \right) + \left(\frac{G_T G_R P'_{T,A}}{L'_A} \right) + \left(\frac{G_T G_R P_{T,B}}{L_B} \right) \quad (4.16)$$

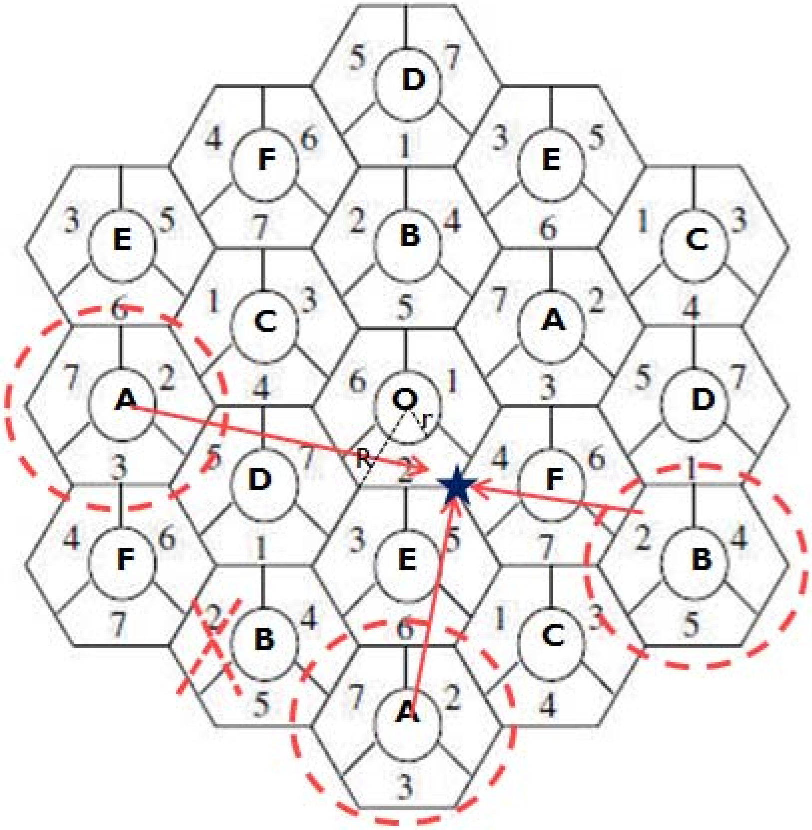

Figure 20. Forward channel interference experienced by the CEU. After [2].

where, referring to Figure 20, $P_{T,A}$ is the transmitted power of eNB_A on the left and L_A is the propagation loss from eNB_A on the left to the UE, $P'_{T,A}$ is the transmitted power of eNB_A on the bottom and L'_A is the propagation loss from eNB_A on the bottom to the UE, and $P_{T,B}$ is the transmitted power of eNB_B on the right and L_B is the propagation loss from eNB_B on the right to the UE. Grouping the common terms $G_T G_R$ together in Equation (4.16), we get

$$I = \left(G_T G_R\right)\left(L_A^{-1} P_{T,A} + L_A'^{-1} P'_{T,A} + L_B^{-1} P_{T,B}\right). \tag{4.17}$$

The forward channel SIR of the CEU $SIR_{CEU,120^\circ}$ is derived from

$$SIR_{CEU,120^\circ} = \left(\frac{P_{R,O}}{I}\right). \tag{4.18}$$

Substituting Equations (4.1) and (4.17) into Equation (4.18), we get

$$SIR_{CEU,120^\circ} = \left(\frac{L_O^{-1} P_{T,O}}{\left(L_A^{-1} P_{T,A} + L_A^{'-1} P_{T,A}^{'} + L_B^{-1} P_{T,B} \right)} \right). \tag{4.19}$$

Substituting Equation (4.12) into Equation (4.19), we have

$$SIR_{CEU,120^\circ} = \left(\frac{\left(\beta_O^{-1} R^{-n} \right) P_{T,O}}{\left(\left(\beta_A^{-1} \left(\sqrt{13} R \right)^{-n} \right) P_{T,A} + \left(\beta_A^{'-1} \left(\sqrt{7} R \right)^{-n} \right) P_{T,A}^{'} + \left(\beta_B^{-1} \left(\sqrt{7} R \right)^{-n} \right) P_{T,B} \right)} \right). \tag{4.20}$$

Since $\beta_O = \beta_A = \beta'_A = \beta_B$ by assumption, for homogeneous clusters, we obtain

$$SIR_{CEU,120^\circ} = \left(\frac{R^{-n} P_{T,O}}{\left(\left(\sqrt{13} R \right)^{-n} P_{T,A} + \left(\sqrt{7} R \right)^{-n} P_{T,A}^{'} + \left(\sqrt{7} R \right)^{-n} P_{T,B} \right)} \right). \tag{4.21}$$

By rearranging the common term R^{-n} in Equation (4.21), we get

$$SIR_{CEU,120^\circ} = \left(\frac{P_{T,O}}{\left(\left(\sqrt{13} \right)^{-n} P_{T,A} + \left(\sqrt{7} \right)^{-n} P_{T,A}^{'} + \left(\sqrt{7} \right)^{-n} P_{T,B} \right)} \right). \tag{4.22}$$

4. Interference Analysis for the Reverse Channel

In the reverse channel analysis, it is also assumed that the traffic load is uniformly distributed in each cell and is proportional to the cell area. Referring back to Figure 18, we let the cell of interest be O again, and the positions where the highest level of CCI is experienced for the center area and the edge area are marked by a triangle and a star, respectively. Similar to the analysis for the forward channel, the inner cell radius is labeled as *r*, while the outer cell radius is denoted as *R*. The desired power received by the eNB in cell O is given by Equation (4.1), and the interference power received from other UEs from cells A to F is the same Equations (4.2) to (4.7).

5. Reverse Channel Signal-to-Interference Ratio (SIR) Analysis for the Center Area

From Figure 21, the desired UE is located at the corner of the center area in cell O (shown as the triangle), with the undesirable center area UEs (shown as the squares) in their respective cells at positions nearest to the eNB in cell O, and emitting interference to the eNB in cell O.

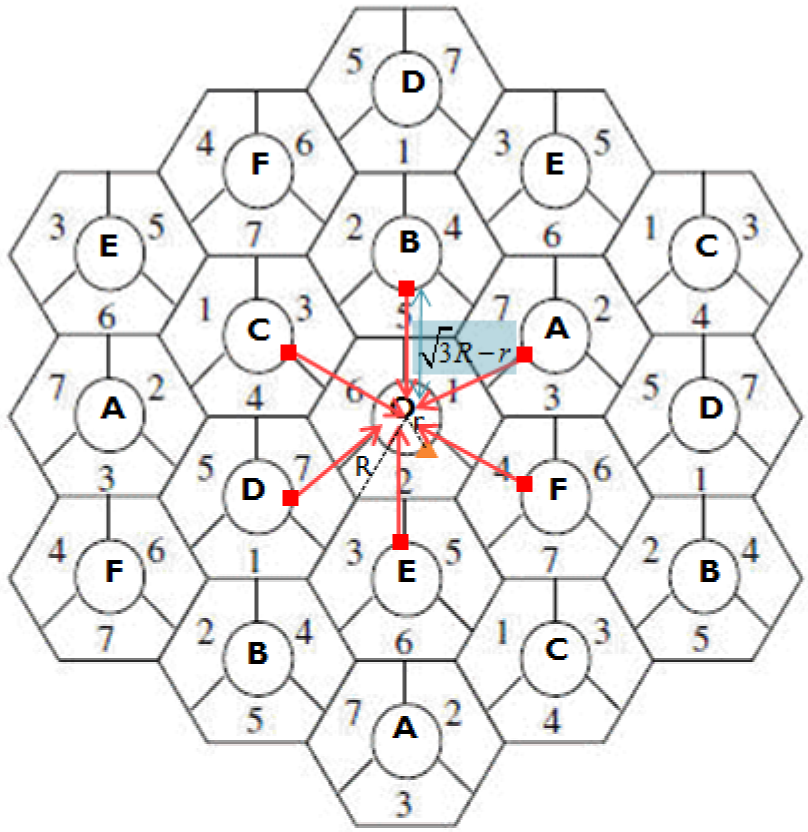

Figure 21. Reverse channel interference analysis for center area.

Assuming one UE from each sector interfering with the eNB in cell O, we see that the total co-channel interference I received by this eNB due to the first tier UE (A to F) is the same as Equation (4.9), and is repeated here for convenience:

$$I = \left(G_T G_R\right)\left(L_A^{-1} P_{T,A} + L_B^{-1} P_{T,B} + L_C^{-1} P_{T,C} + L_D^{-1} P_{T,D} + L_E^{-1} P_{T,E} + L_F^{-1} P_{T,F}\right). \qquad (4.23)$$

When there are multiple UEs at the edge causing interference, I increases.

The reverse channel SIR of the cell center area (CC) SIR_{CC} is derived as follows:

$$SIR_{CC} = \left(\frac{P_{R,O}}{I}\right). \qquad (4.24)$$

Substituting Equations (4.1) and (4.23) into Equation (4.24), we get

$$SIR_{CC} = \left(\frac{L_O^{-1} P_{T,O}}{\left(L_A^{-1} P_{T,A} + L_B^{-1} P_{T,B} + L_C^{-1} P_{T,C} + L_D^{-1} P_{T,D} + L_E^{-1} P_{T,E} + L_F^{-1} P_{T,F}\right)}\right). \qquad (4.25)$$

Substituting Equation (4.12) into Equation (4.25), we have

$$SIR_{CC}=\left(\frac{\left(\beta_O^{-1}r^{-n}\right)P_{T,O}}{\left(\left(\beta_A^{-1}\left(\sqrt{3}R-r\right)^{-n}\right)P_{T,A}+\left(\beta_B^{-1}\left(\sqrt{3}R-r\right)^{-n}\right)P_{T,B}+\left(\beta_C^{-1}\left(\sqrt{3}R-r\right)^{-n}\right)P_{T,C}+\left(\beta_D^{-1}\left(\sqrt{3}R-r\right)^{-n}\right)P_{T,D}+\left(\beta_E^{-1}\left(\sqrt{3}R-r\right)^{-n}\right)P_{T,E}+\left(\beta_F^{-1}\left(\sqrt{3}R-r\right)^{-n}\right)P_{T,F}\right)}\right).\quad(4.26)$$

Since $\beta_O = \beta_A = \beta_B = \beta_C = \beta_D = \beta_E = \beta_F$ by assumption, for homogeneous clusters, we obtain

$$SIR_{CC}=\left(\frac{\left(r^{-n}\right)P_{T,O}}{\left(\left(r^{-n}\right)\left(\sqrt{3}\left(\frac{R}{r}\right)-1\right)^{-n}\right)\left(P_{T,A}+P_{T,B}+P_{T,C}+P_{T,D}+P_{T,E}+P_{T,F}\right)}\right).\quad(4.27)$$

By rearranging the common term r^{-n} in Equation (4.27), we get

$$SIR_{CCU}=\left(\frac{P_{T,O}}{\left(\left(\sqrt{3}\left(\frac{R}{r}\right)-1\right)^{-n}\right)\left(P_{T,A}+P_{T,B}+P_{T,C}+P_{T,D}+P_{T,E}+P_{T,F}\right)}\right).\quad(4.28)$$

6. Reverse Channel Signal-to-Interference Ratio Analysis for the Edge Area

In Figure 22, the desired UE is located at the corner of the outer sector in cell O (shown as the star). Since cell edge users (CEUs) adopt a sectoring approach, only cells D, E and F in the first tier that are facing the intended sector (sub-channel 2) contribute to the CCI. However, since none of these three cells are using sub-channel 2, the analysis is moved on to the second tier, where the bottom cells A, two B cells, C, and F are all facing the intended sector. Since only A and two B cells use sub-channel 2, the positions where the UE interferes the most are marked as squares as shown.

Therefore, the total co-channel interference I received by the eNB in cell O is

$$I=\left(\frac{G_T G_R P_{T,B}}{L_B}\right)+\left(\frac{G_T G_R P_{T,A}}{L_A}\right)+\left(\frac{G_T G_R P'_{T,B}}{L'_B}\right)\quad(4.29)$$

where, referring to Figure 22, $P_{T,B}$ is the transmitted power of the UE in cell B on the left and L_B is the propagation loss from the UE in cell B on the left to eNB_O; $P_{T,A}$ is the transmitted power of the UE in cell A on the bottom and L_A is the propagation loss from the UE in cell A on the bottom to eNB_O; and $P'_{T,B}$ is the transmitted power of the UE in cell B on the right and L'_B is the propagation loss from the UE in cell B on the right to eNB_O.

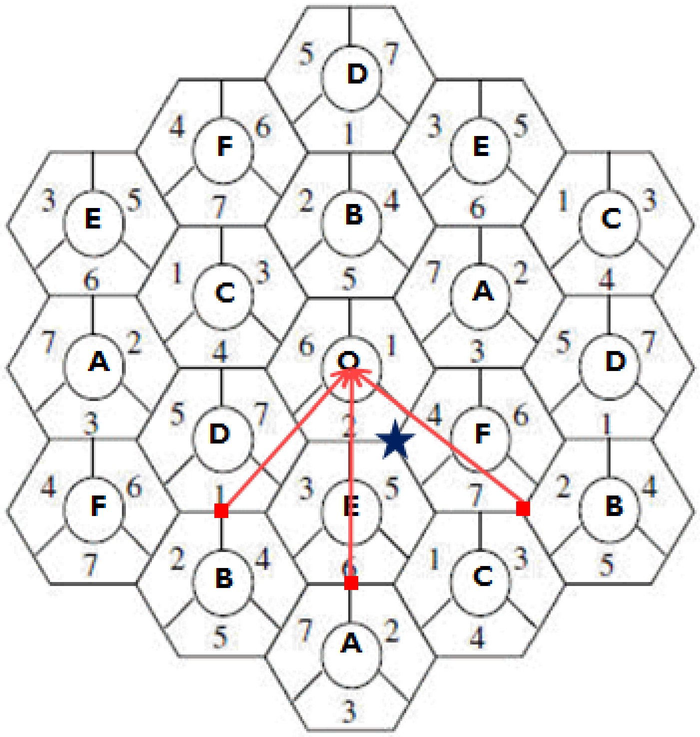

Figure 22. Reverse channel interference analysis for edge area.

Grouping the common terms $G_T G_R$ together in Equation (4.29), we get

$$I = \left(G_T G_R\right)\left(L_B^{-1} P_{T,B} + L_A^{-1} P_{T,A} + L_B'^{-1} P'_{T,B}\right). \quad (4.30)$$

The reverse channel SIR of the cell edge area (CE) $SIR_{CE,120^\circ}$ is defined as

$$SIR_{CE,120^\circ} = \left(\frac{P_{R,O}}{I}\right). \quad (4.31)$$

Substituting Equations (4.1) and (4.30) into Equation (4.31), we get

$$SIR_{CE,120^\circ} = \left(\frac{L_O^{-1} P_{T,O}}{\left(L_B^{-1} P_{T,B} + L_A^{-1} P_{T,A} + L_B'^{-1} P'_{T,B}\right)}\right). \quad (4.32)$$

Substituting Equation (4.12) into Equation (4.32), we have

$$SIR_{CE,120^\circ} = \left(\frac{\left(\beta_O^{-1} R^{-n}\right) P_{T,O}}{\left(\left(\beta_B^{-1}\left(\frac{\sqrt{21}}{2}R\right)^{-n}\right) P_{T,B} + \left(\beta_A^{-1}\left(\frac{3\sqrt{3}}{2}R\right)^{-n}\right) P_{T,A} + \left(\beta_B'^{-1}\left(\sqrt{7}R\right)^{-n}\right) P'_{T,B}\right)}\right). \quad (4.33)$$

Since $\beta_O = \beta_A = \beta_B = \beta'_B$ by assumption, for homogeneous clusters, we obtain

$$SIR_{CE,120^\circ} = \left(\frac{R^{-n} P_{T,O}}{\left(\left(\frac{\sqrt{21}}{2} R \right)^{-n} P_{T,B} + \left(\frac{3\sqrt{3}}{2} R \right)^{-n} P_{T,A} + \left(\sqrt{7} R \right)^{-n} P'_{T,B} \right)} \right). \tag{4.34}$$

By rearranging the common term R^{-n} in Equation (4.34), we get

$$SIR_{CE,120^\circ} = \left(\frac{P_{T,O}}{\left(\left(\frac{\sqrt{21}}{2} \right)^{-n} P_{T,B} + \left(\frac{3\sqrt{3}}{2} \right)^{-n} P_{T,A} + \left(\sqrt{7} \right)^{-n} P'_{T,B} \right)} \right). \tag{4.35}$$

V. LINK ANALYSIS FOR 60°-SECTORING

A. EXTENDING THE NETWORK POWER PLANNING CONCEPT

Expanding the frequency reuse scheme of Alcatel's proposal discussed in Section III, we can develop a frequency reuse scheme for 60°-sectoring as shown in Figure 23. Similar to the previous discussion, each cell has an eNB at the cell center that serves a number of UEs assumed to be uniformly distributed in the cell. Each cell is also partitioned into a center area and an edge area, where frequency reuse factor-1 is used in the center area. Since sectoring is used for the edge area, the frequency reuse pattern here is 6/7, where six is the number of sectoring per cell, and seven is the number of frequency sub-channels available per cell. It is worthwhile to note that in addition to sectoring, with no adjacent edge areas sharing the same set of sub-channels, the performance in terms of SIR of the cell-edge users (CEUs) is expected to improve more than that for 120°-sectoring.

Sub-channels 1 to 6 are allocated, respectively, for the cell edge users in each cell with full power according to the sector in which the UEs transmit and receive. Reduced power is used for the UEs in the center cell.

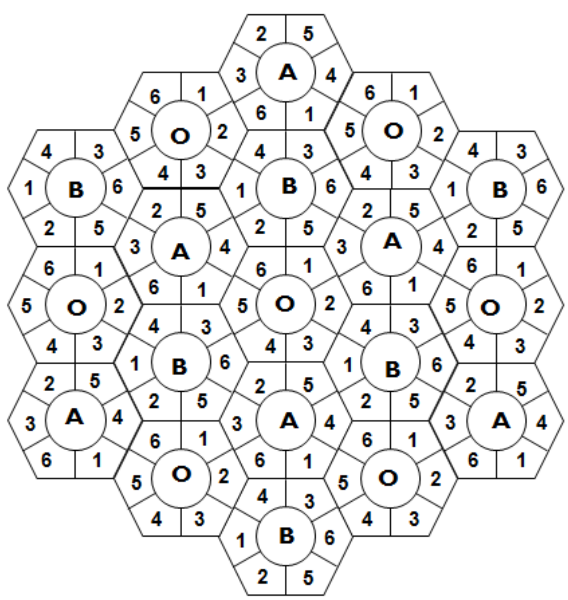

Figure 23. Frequency reuse scheme for 60°-sectoring.

1. Methodology for Sub-Channel Assignment

The design rule to achieve the frequency planning outcome as shown in Figure 25 is to allocate the sub-channels 1 to 6 in such a way that the same sub-channel in the adjacent cell is facing totally away from the intended sector. For example, if a sector is assigned to be sub-channel 1 in one cell, then the sector in the adjacent cell to be assigned the same sub-channel 1 must be one that is facing completely away from the former. This illustration is further elaborated with the help of Figure 26. To assign sub-channel 1 in the cell on the right (Cell A), the three possible sectors to be assigned are highlighted in green. The sector that is most out of the way from the intended sector highlighted in yellow for sub-channel 1 in Cell O is the bottom right sector, which is marked "1." This same concept applies for sub-channel 2, where the top left sector in Cell A faces totally away from the portion highlighted in green for sub-channel 2. In this way, there is minimal co-channel interference from adjacent cells.

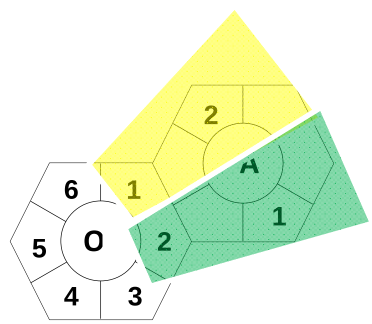

Figure 24. An example of sub-channel assignment for 60° sectoring.

By repeating this approach for each sub-channel in the first tier followed by the second tier, the cell structure as shown in Figure 23 can be achieved.

2. Interference Analysis for the Forward Channel

Assuming that the traffic load is uniformly distributed in each cell and is proportional to the cell area, we let the cell of interest be O situated in the heart of the structure, and the positions where the highest level of CCI are experienced for the center area and the edge area be marked by a triangle and a star, respectively. The inner cell radius is labeled as *r*, while the outer cell radius is denoted as *R*. This is represented in Figure 25.

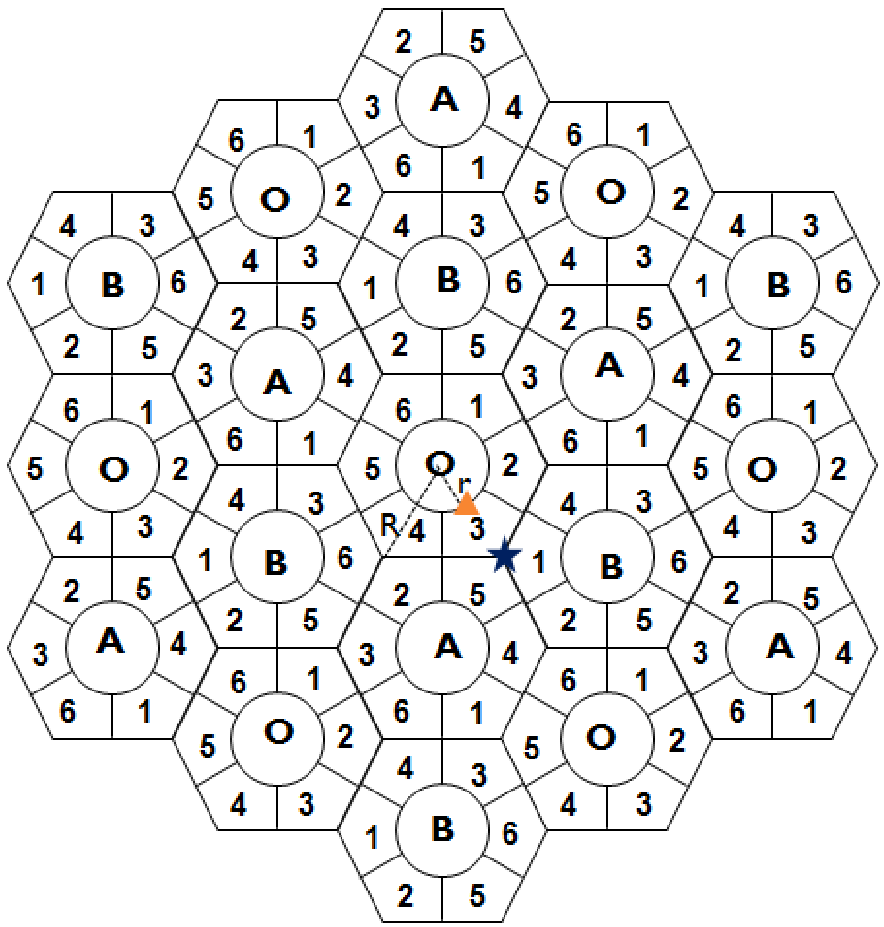

Figure 25. Positions of UEs in center and edge areas for analysis.

The desired power received by the eNB in cell O is given by Equation (4.1), and the interference powers received from other UEs from the six cells in the first tier is the same Equations (4.2) to (4.7).

3. Forward Channel Signal-to-Interference Ratio Analysis for Cell Center Users

Other than the sub-channels assigned to the edge areas of the cells, the remaining sub-channel, which is sub-channel 7, is used for the entire center area irrespective of the sector, hence, the CCU shown as the triangle in Figure 26 receives co-channel interference from the eNB in the six cells (three A cells and three B cells) in the first tier.

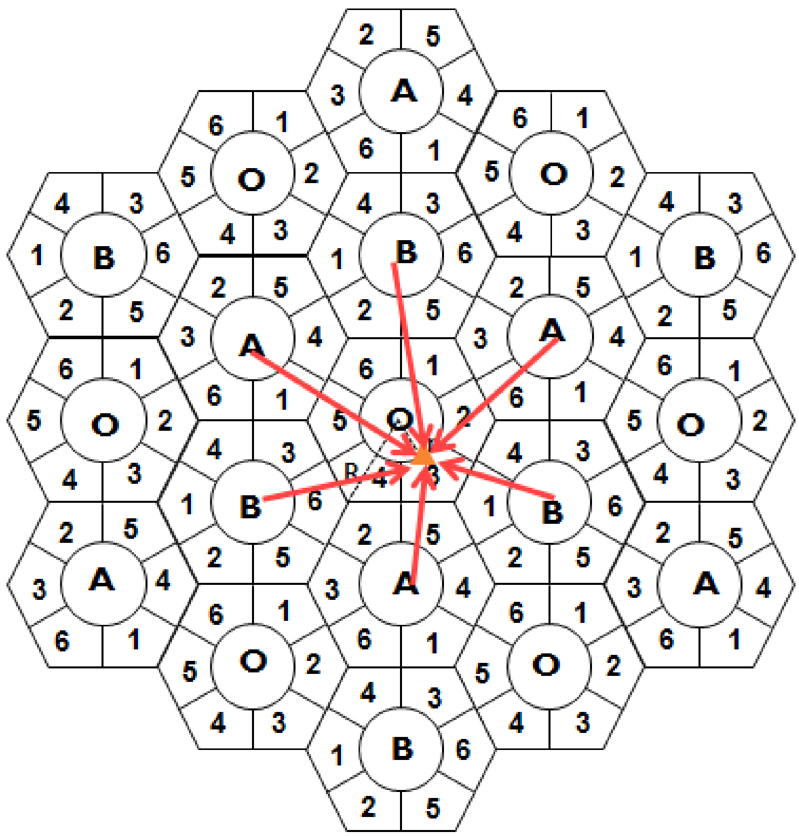

Figure 26. Forward channel interference experienced by CCU.

Since the interference from the second tier cells is small compared to the first tier, it is negligible and thus ignored. Therefore, the total co-channel interference I received by the CCU due to the eNBs in three A and three B cells in the first tier is the given by Equation (4.9), repeated here for convenience:

$$I = (G_T G_R)\left(L_A^{-1} P_{T,A} + L_B^{-1} P_{T,B} + L_A'^{-1} P'_{T,A} + L_B'^{-1} P'_{T,B} + L_A''^{-1} P''_{T,A} + L_B''^{-1} P''_{T,B}\right). \quad (5.1)$$

As such, the forward channel SIR of the CCU $SIR_{CCU,60^\circ}$ is also the same as Equation (4.15):

$$SIR_{CCU,60^\circ} = \left(\frac{P_{T,O}}{\left(\left(\sqrt{3\left(\frac{R}{r}\right)^2+1}\right)^{-n} P_{T,A} + \left(\sqrt{3\left(\frac{R}{r}\right)^2+3\left(\frac{R}{r}\right)+1}\right)^{-n} P_{T,B} + \left(\sqrt{3\left(\frac{R}{r}\right)^2+3\left(\frac{R}{r}\right)+1}\right)^{-n} \dot{P}_{T,A} + \left(\sqrt{3\left(\frac{R}{r}\right)^2+1}\right)^{-n} \dot{P}_{T,B} + \left(\sqrt{3\left(\frac{R}{r}\right)^2-3\left(\frac{R}{r}\right)+1}\right)^{-n} \ddot{P}_{T,A} + \left(\sqrt{3\left(\frac{R}{r}\right)^2-3\left(\frac{R}{r}\right)+1}\right)^{-n} \ddot{P}_{T,B}\right)} \right). \quad (5.2)$$

4. Forward Channel Signal-to-Interference Ratio Analysis for Cell Edge Users

CEUs are only allowed to use their assigned sub-channel. In Figure 27, the CEU shown as the star uses sub-channel 3. All six cells in the first tier have sectors using the same sub-channel 3, but because of sectoring, the transmission of signal by the eNB in these cells is in a direction away from the CEU. Hence, they do not interfere with the CEU.

Moving the analysis to the second tier, we see that all 12 cells have the same sub-channel 3, but nine cells have their sector facing away from the CEU. As such, the CEU is interfered by one A cell on the bottom right, one B cell on the bottom, and one O cell on the top left only.

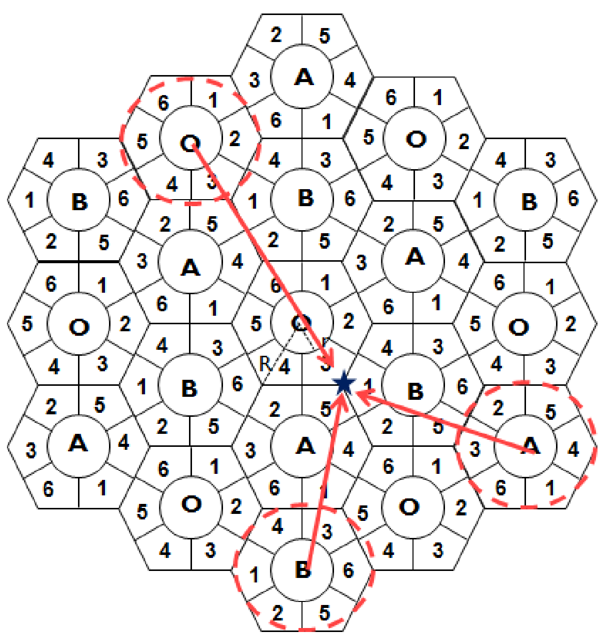

Figure 27. Forward channel interference experienced by CEU.

Therefore, the total co-channel interference I received by the CEU due to second tier eNB (one A cell on the bottom right, one B cell on the bottom, and one O cell on the top left only) is given by

$$I = \left(\frac{G_T G_R P_{T,O}^{'}}{L_O^{'}} \right) + \left(\frac{G_T G_R P_{T,A}}{L_A} \right) + \left(\frac{G_T G_R P_{T,B}}{L_B} \right) \tag{5.3}$$

where, referring to Figure 27, $P_{T,A}$ is the transmitted power of eNB_A on the bottom right and L_A is the propagation loss from eNB_A on the bottom right to the UE; $P_{T,B}$ is the transmitted power of eNB_B on the bottom and L_B is the propagation loss from eNB_B on the right to the UE; and $P^{'}_{T,O}$ is the transmitted power of eNB_O on the top left and $L^{'}_O$ is the propagation loss from eNB_O on the top left to the UE. Grouping the common terms $G_T G_R$ together in Equation (5.3), we get

$$I = \left(G_T G_R \right) \left(L_O^{'-1} P_{T,O}^{'} + L_A^{-1} P_{T,A} + L_B^{-1} P_{T,B} \right). \tag{5.4}$$

The forward channel SIR of the CEU $SIR_{CEU,60^\circ}$ is defined as

$$SIR_{CEU,60^\circ} = \left(\frac{P_{R,O}}{I} \right). \tag{5.5}$$

Substituting Equations (4.1) and (5.4) into Equation (5.5), we get

$$SIR_{CEU,60^\circ} = \left(\frac{L_O^{-1} P_{T,O}}{\left(L_O^{'-1} P_{T,O}^{'} + L_A^{-1} P_{T,A} + L_B^{-1} P_{T,B} \right)} \right). \tag{5.6}$$

Substituting Equation (4.12) into Equation (5.6), we have

$$SIR_{CEU,60^\circ} = \left(\frac{\left(\beta_O^{-1} R^{-n} \right) P_{T,O}}{\left(\left(\beta_O^{'-1} (4R)^{-n} \right) P_{T,O}^{'} + \left(\beta_A^{-1} (\sqrt{7}R)^{-n} \right) P_{T,A} + \left(\beta_B^{-1} (\sqrt{7}R)^{-n} \right) P_{T,B} \right)} \right). \tag{5.7}$$

Since $\beta_O = \beta_A = \beta_B = \beta^{'}_O$ by assumption, for homogeneous clusters, we obtain

$$SIR_{CEU,60^\circ} = \left(\frac{R^{-n} P_{T,O}}{\left((4R)^{-n} P_{T,O}^{'} + (\sqrt{7}R)^{-n} P_{T,A} + (\sqrt{7}R)^{-n} P_{T,B} \right)} \right). \tag{5.8}$$

By rearranging the common term R^{-n} in Equation (5.8), we get

$$SIR_{CEU,60^\circ} = \left(\frac{P_{T,O}}{\left((4)^{-n} P'_{T,O} + \left(\sqrt{7}\right)^{-n} P_{T,A} + \left(\sqrt{7}\right)^{-n} P_{T,B} \right)} \right). \tag{5.9}$$

5. Interference Analysis for the Reverse Channel

In the reverse channel analysis, it is also assumed that the traffic load is uniformly distributed in each cell and is proportional to the cell area. Referring back to Figure 25, we let the cell of interest be cell O situated at the heart of the structure again, and the positions where the highest level of CCI are experienced for center area and edge area are marked by a triangle and star, respectively. Similar to the analysis for the forward channel, the inner cell radius is labeled as *r*, while the outer cell radius is denoted as *R*. The desired power received by the eNB in cell O is the given as Equation (4.1), and the interference powers received from other UEs from the six cells in the first tier is given by Equations (4.2) to (4.7).

6. Reverse Channel Signal-to-Interference Ratio (SIR) Analysis for Center Area

In Figure 28, the desired UE is located at the corner of the center area in cell O (shown as the triangle), with the undesired center area UEs (shown as the squares) in their respective cells at positions nearest to the eNB in cell O and emitting interference to the eNB base station in cell O.

Assuming one UE from each sector interfering with the eNB in cell O, we see that the total co-channel interference I received by this eNB due to the first tier UEs is given by Equation (4.9), repeated here for convenience:

$$I = \left(G_T G_R\right)\left(L_A^{-1} P_{T,A} + L_B^{-1} P_{T,B} + L_A'^{-1} P'_{T,A} + L_B'^{-1} P'_{T,B} + L_A''^{-1} P''_{T,A} + L_B''^{-1} P''_{T,B}\right). \tag{5.10}$$

When there are multiple UEs at the edge causing interference, I increases.

The reverse channel SIR of the cell center area (CC) SIR_{CCU} is given by

$$SIR_{CCU} = \left(\frac{P_{T,O}}{\left(\left(\sqrt{3}\left(\frac{R}{r}\right) - 1 \right)^{-n} \right) \left(P_{T,A} + P_{T,B} + P'_{T,A} + P'_{T,B} + P''_{T,A} + P''_{T,B} \right)} \right). \quad (5.11)$$

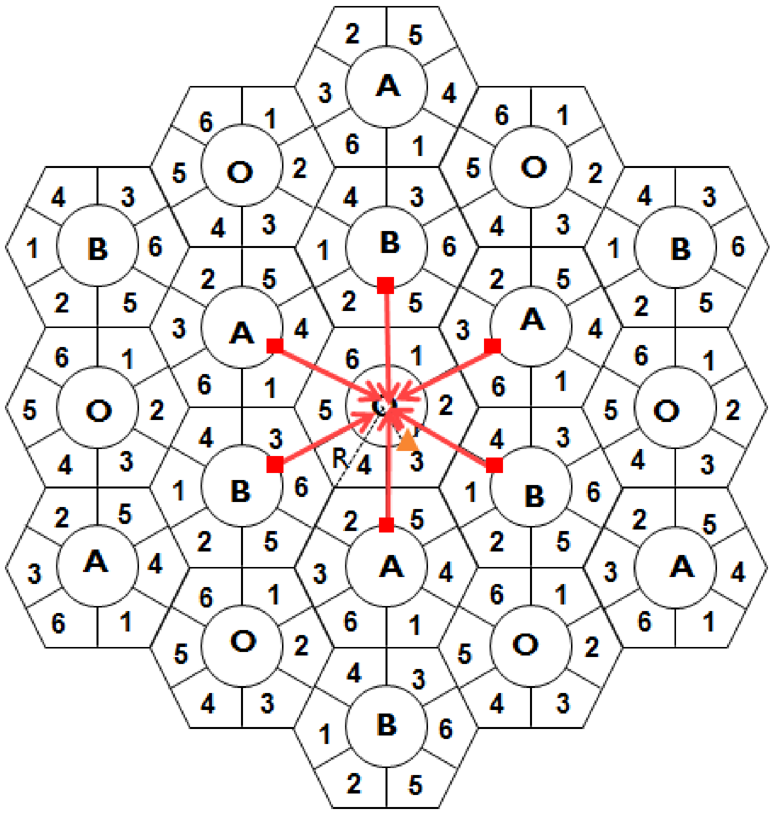

Figure 28. Reverse channel interference analysis for center area.

7. Reverse Channel Signal-to-Interference Ratio Analysis for Edge Area

In Figure 29, the desired UE is located at the corner of the outer cell in cell O (shown as the star). Since cell edge users adopt a sectoring approach, only cells A and B at the bottom right in the first tier which are facing the intended sector (sub-channel 3) contribute to the CCI. However, since the sectors using sub-channel 3 are facing away from the intended sector, the analysis is moved on to the second tier, where the bottom cells A, B, and O have their sector with sub-channel 3 facing the intended sector. The positions where the UE interfere most are marked as squares.

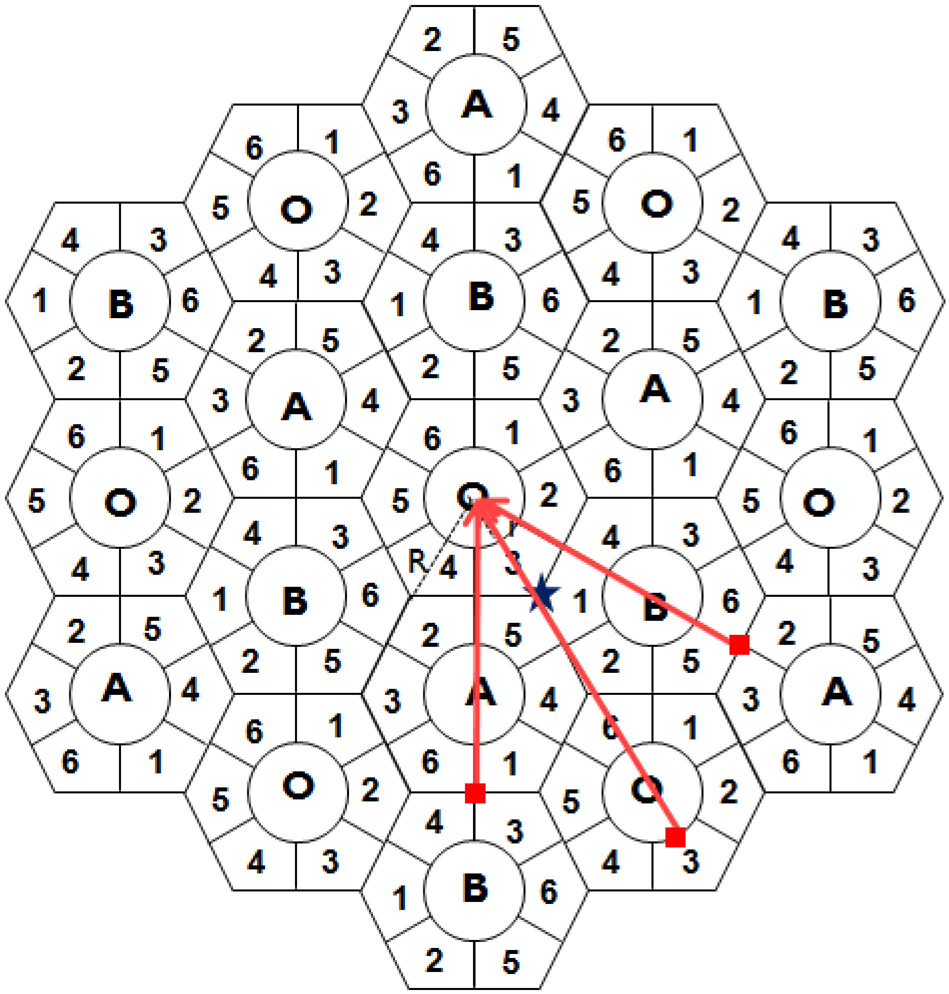

Figure 29. Reverse channel interference analysis for edge area.

Therefore, the total co-channel interference I received by the eNB in cell O is

$$I = \left(\frac{G_T G_R P_{T,A}}{L_A}\right) + \left(\frac{G_T G_R P_{T,B}}{L_B}\right) + \left(\frac{G_T G_R P'_{T,O}}{L'_O}\right) \tag{5.12}$$

where, referring to Figure 29, $P_{T,A}$ is the transmitted power of the UE in cell A on the right and L_A is the propagation loss from the UE on the right to eNB_O; $P_{T,B}$ is the transmitted power of the UE in cell B on the bottom and L_B is the propagation loss from the UE in cell B on the bottom to eNB_O; and $P'_{T,O}$ is the transmitted power of the UE in cell O on the bottom right and L'_O is the propagation loss from the UE in cell O on the bottom right to eNB$_O$. Grouping the common terms $G_T G_R$ together in Equation (4.12), we get

$$I = \left(G_T G_R\right)\left(L_A^{-1} P_{T,A} + L_B^{-1} P_{T,B} + L_O^{'-1} P_{T,O}^{'}\right). \tag{5.13}$$

The reverse channel SIR of the cell edge area $SIR_{CE,60^\circ}$ is defined as

$$SIR_{CE,60^\circ} = \left(\frac{P_{R,O}}{I}\right). \tag{5.14}$$

Substituting Equations (4.1) and (5.13) into Equation (5.14), we get

$$SIR_{CE,60^\circ} = \left(\frac{L_O^{-1} P_{T,O}}{\left(L_A^{-1} P_{T,A} + L_B^{-1} P_{T,B} + L_O^{'-1} P_{T,O}^{'}\right)}\right). \tag{5.15}$$

Substituting Equation (4.12) into Equation (5.15), we have

$$SIR_{CE,60^\circ} = \left(\frac{\left(\beta_O^{-1} R^{-n}\right) P_{T,O}}{\left(\left(\beta_A^{-1}\left(\frac{3\sqrt{3}}{2}R\right)^{-n}\right) P_{T,A} + \left(\beta_B^{-1}\left(\frac{3\sqrt{3}}{2}R\right)^{-n}\right) P_{T,B} + \left(\beta_O^{'-1}\left(3R+r\right)^{-n}\right) P_{T,O}^{'}\right)}\right). \tag{5.16}$$

Since $\beta_O = \beta_A = \beta_B = \beta'_O$ by assumption, for homogeneous clusters, we obtain

$$SIR_{CE,60^\circ} = \left(\frac{R^{-n} P_{T,O}}{\left(\left(\frac{3\sqrt{3}}{2}R\right)^{-n} P_{T,A} + \left(\frac{3\sqrt{3}}{2}R\right)^{-n} P_{T,B} + \left(3R+r\right)^{-n} P_{T,O}^{'}\right)}\right). \tag{5.17}$$

By rearranging the common term R^{-n} in Equation (5.17), we get

$$SIR_{CE,60^\circ} = \left(\frac{P_{T,O}}{\left(\left(\frac{3\sqrt{3}}{2}\right)^{-n} P_{T,A} + \left(\frac{3\sqrt{3}}{2}\right)^{-n} P_{T,B} + \left(3+\frac{r}{R}\right)^{-n} P_{T,O}^{'}\right)}\right). \tag{5.18}$$

VI. MAC SUB-LAYER ANALYSIS

A. SCHEDULING STRATEGY

To complement the sectoring techniques discussed in Chapters IV and V, the proposed MAC sub-layer design aims to maximize interference diversity with the use of a Latin Square hopping scheme. Furthermore, as the Latin Squares are maintained by each eNB, where each virtual channel is able to hop over different sub-carriers at different OFDM symbol times, no single strong interference from a virtual channel can cause degradation in performance [21].

1. Brief Illustration

As discussed in Chapter III, LTE makes use of OFDMA to allocate the resource blocks to the users in both time and frequency domains such that different users can use the same sub-channel at different time while minimizing the chance of co-channel interference. However, in a worst case scenario, there may be two users, user A1 in eNB_A and user B1 in eNB_B, being assigned the same resources at the same frequency and time, as shown in Figure 30. This is known as co-channel interference.

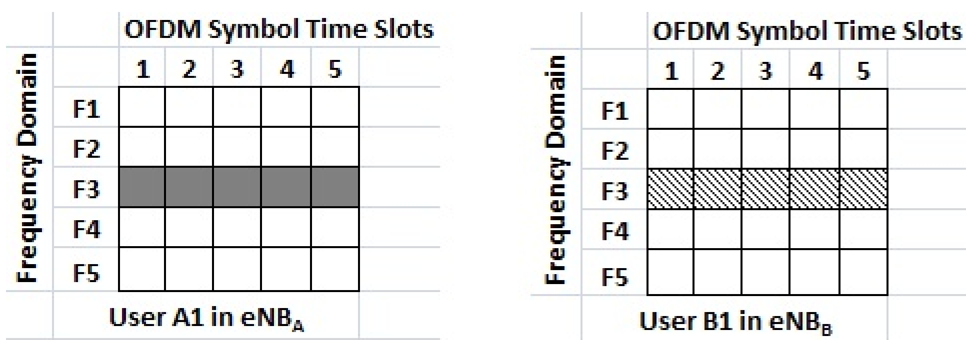

Figure 30. An example of the worst case resource allocation for one user per eNB.

Therefore, the allocation of frequencies for the users should be as spread out as possible. Furthermore, these frequencies should be hopped every OFDM symbol time. In this manner, the hop patterns for the neighboring eNBs are as far "apart" as possible, minimizing the chances of co-channel interference even more. This is the concept of the

Latin Square frequency hopping scheme. An illustration of a possible resource allocation with Latin Square for the scenario in the previous paragraph is shown in Figure 31.

Each user sends its data using the allocated frequency channel in the particular time slot. As seen from the Latin Square for user A1 in eNB_A, colored in solid grey in Figure 31, the assigned frequency channel changes each time frame to allow for frequency diversity. For example, the data sent out by user A1 in eNB_A is first done in F1 in time slot 1, then F2 in time slot 2, F3 in time slot 3, F4 in time slot 4, and F5 in time slot 5.

Similarly, for user B1 in eNB_B, shaded with stripes in Figure 31, the assigned frequency channel changes each time frame to allow for frequency diversity. The data sent out by user B1 in eNB_B is first done in F5 in time slot 1, then F1 in time slot 2, F2 in time slot 3, F3 in time slot 4, and F4 in time slot 5.

With this MAC sub-layer design of resource scheduling as illustrated in Figure 31, co-channel interference can be reduced significantly. The frequency hopping technique via Latin Square allows the *n* sub-carriers allocated for the user to be as spread out as possible. Furthermore, these *n* sub-carriers are hopped every OFDM symbol time. Although the amount of SIR improvement decreases as the number of users per Latin Square increases, due to the minimal chance of channel overlap, CCI is generally reduced.

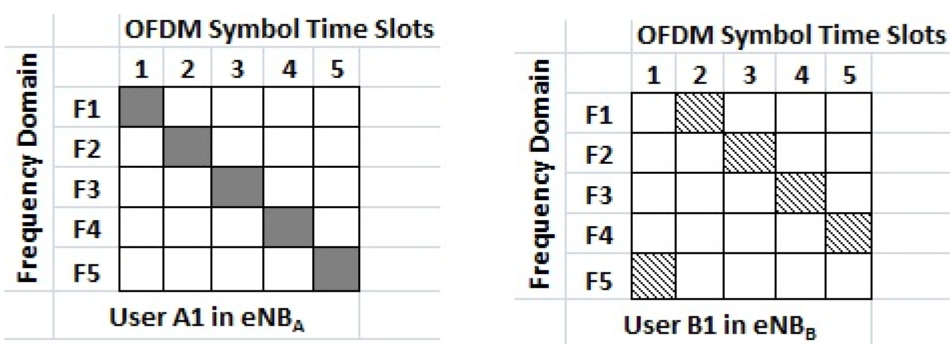

Figure 31. An example of resource allocation for one user per cell with Latin Square.

As seen in 3G cellular networks [8]-[9] where a 60°-sectoring scheme is able to achieve better SIR performance than a 120°-sectoring scheme, the following analysis with a Latin Square frequency hopping scheme can only be done only for the 60°-sectoring scheme. Furthermore, since the CEU faces the worst SIR as compared to the CCU, this analysis is performed on the CEU only for both forward and reverse channels.

Using the forward channel analysis for the CEU shown in Figure 27 and discussed in Chapter V to further illustrate the Latin Square scheme used, the hopping pattern for the users in each eNB is unique as shown in Figure 32.

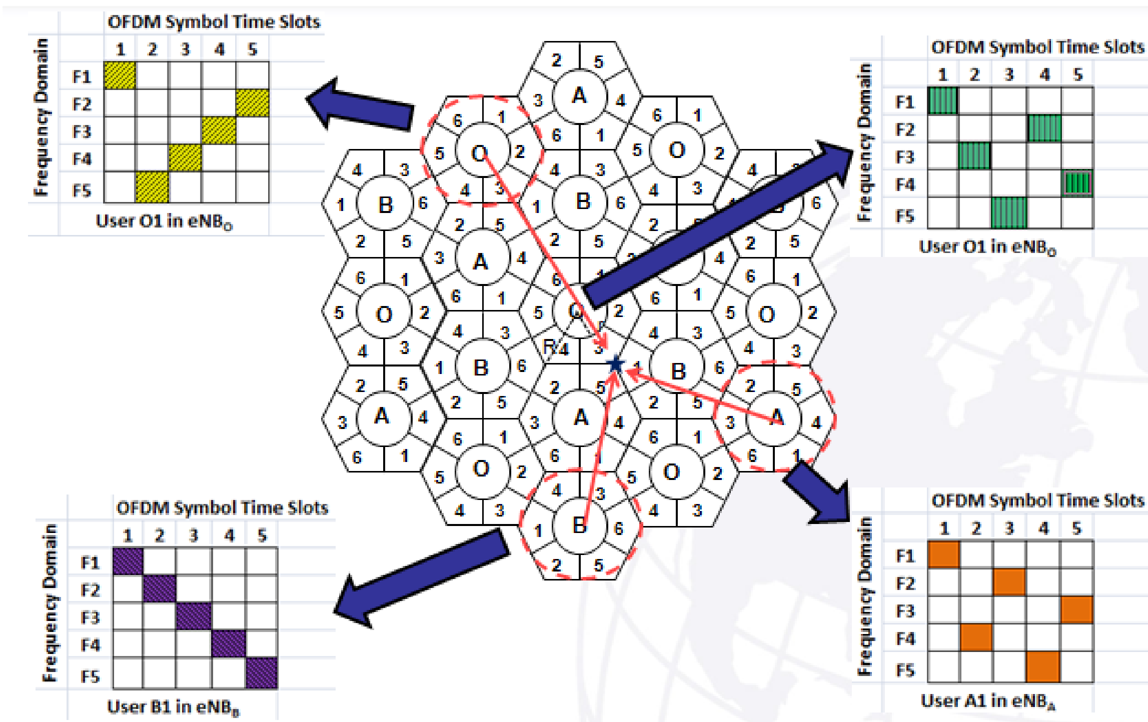

Figure 32. Unique hopping patterns for different eNBs with Latin Square scheme.

Mapping the matrices together as shown in Figure 33, we see that there is only one instance when the same channel in the same frequency slot and time slot happens. This clearly shows that with Latin Square Scheme used, the probability of overlapped channels is reduced, reducing the effect of CCI.

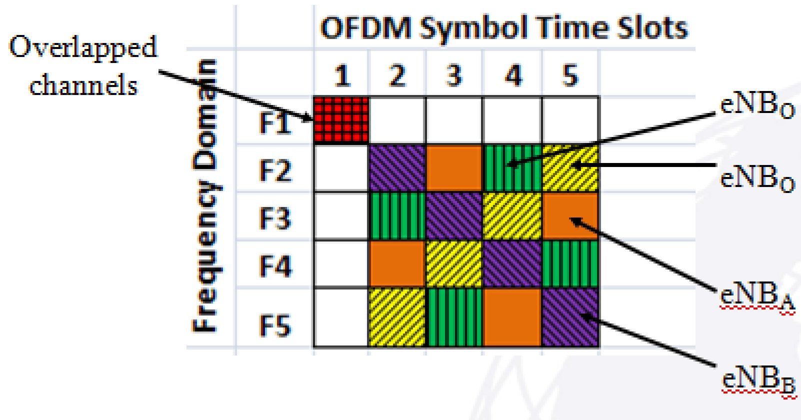

Figure 33. Mapped matrices.

2. Virtual Channel Assignment Approach (Scenario 1)

Assuming a channel bandwidth of 3 MHz with 15 resource blocks (a resource block has 12 subcarriers) and for a Latin Square of size 5, we see that a family of four distinct quasi-orthogonal Latin Squares is available: one for the eNB under consideration and three for three co-channel eNBs. According to [21], we can create these Latin Squares when the square size is prime, allowing each eNB a unique Latin square.

The channel bandwidth of 3 MHz with 15 resource blocks (15 12-subcarrier-blocks over 20 time slots per frame) can accommodate a total of 12 identical Latin Squares. With one virtual channel assigned to each user, 12 Latin squares can support a maximum of 60 users per sector per eNB. In the case of the maximum number of users, the probability of co-channel interference is the highest, and the utilization of the virtual channel is also at the highest. This illustration is depicted in Figure 34.

Assuming the same parameters where the channel bandwidth is 3 MHz with 15 resource blocks, but this time the Latin Square size is 7, we see that a family of six distinct quasi-orthogonal Latin Squares is available: one for the eNB under consideration, three for three co-channel eNBs, and two unused. Due to the frame length of 20 time slots and the frequency constrained by the number of resource blocks defined in each channel bandwidth, each frame can accommodate two full Latin Squares and five partial Latin

Time slots per frame

Number of 12-subcarrier-blocks

1	2	3	4	5	6	7	8	9	10	11	12	13	14	15	16	17	18	19	20
0	1	2	3	4	0	1	2	3	4	0	1	2	3	4	0	1	2	3	4
2	3	4	0	1	2	3	4	0	1	2	3	4	0	1	2	3	4	0	1
4	0	1	2	3	4	0	1	2	3	4	0	1	2	3	4	0	1	2	3
1	2	3	4	0	1	2	3	4	0	1	2	3	4	0	1	2	3	4	0
3	4	0	1	2	3	4	0	1	2	3	4	0	1	2	3	4	0	1	2
0	1	2	3	4	0	1	2	3	4	0	1	2	3	4	0	1	2	3	4
2	3	4	0	1	2	3	4	0	1	2	3	4	0	1	2	3	4	0	1
4	0	1	2	3	4	0	1	2	3	4	0	1	2	3	4	0	1	2	3
1	2	3	4	0	1	2	3	4	0	1	2	3	4	0	1	2	3	4	0
3	4	0	1	2	3	4	0	1	2	3	4	0	1	2	3	4	0	1	2
0	1	2	3	4	0	1	2	3	4	0	1	2	3	4	0	1	2	3	4
2	3	4	0	1	2	3	4	0	1	2	3	4	0	1	2	3	4	0	1
4	0	1	2	3	4	0	1	2	3	4	0	1	2	3	4	0	1	2	3
1	2	3	4	0	1	2	3	4	0	1	2	3	4	0	1	2	3	4	0
3	4	0	1	2	3	4	0	1	2	3	4	0	1	2	3	4	0	1	2

Figure 34. An example of resource allocation for a channel bandwidth of 3 MHz per sector per eNB, with Latin Square size 5 (Scenario 1).

Squares, where some of the resource blocks in a Latin Square are not used. These unusable resource blocks are shaded in Figure 35. The two partial Latin Squares on the right border can still serve seven users each, but each user is only allocated six timeslots with seven 12-subcarrier blocks instead of seven timeslots as in the full Latin Square. Similarly, two partial Latin Squares on the bottom border can also serve seven users each, but each user is only allocated one timeslot and only one 12-subcarrier block. Lastly, the partial Latin Square on the bottom right border can only serve six users with one timeslot each and only one 12-subcarrier block. In this case, a maximum of 62 users per sector per eNB can be supported, but only 28 users receive seven resource blocks each, 14 users with six resource blocks each, and 20 users with one resource block each.

In the case of the maximum number of users, the probability of co-channel interference is the highest, and the utilization of the virtual channels is also at the highest.

3. Resource Block Assignment Approach (Scenario 2)

Again, assuming a channel bandwidth of 3 MHz with 15 resource blocks and the users assigned one resource block per timeslot each, we see that the maximum number of users supported is 300, i.e., 20 × 15. In order to minimally support this number of users, a Latin Square of size 19, which is the next prime of square root of 300, is used. At this size, however, the probability of co-channel interference is high. This is because the probability of multiple users being assigned the same resource block increases when the number of users in the network increases. As such, the best case with the lowest effect of co-channel interference is the next prime number of the square root of the number of users multiplied by the number of interfering sources plus one, which indicates the reference source.

Time slots per frame

Number of 12-subcarrier-blocks

1	2	3	4	5	6	7	8	9	10	11	12	13	14	15	16	17	18	19	20	
0	1	2	3	4	5	6	0	1	2	3	4	5	6	0	1	2	3	4	5	6
2	3	4	5	6	0	1	2	3	4	5	6	0	1	2	3	4	5	6	0	1
4	5	6	0	1	2	3	4	5	6	0	1	2	3	4	5	6	0	1	2	3
6	0	1	2	3	4	5	6	0	1	2	3	4	5	6	0	1	2	3	4	5
1	2	3	4	5	6	0	1	2	3	4	5	6	0	1	2	3	4	5	6	0
3	4	5	6	0	1	2	3	4	5	6	0	1	2	3	4	5	6	0	1	2
5	6	0	1	2	3	4	5	6	0	1	2	3	4	5	6	0	1	2	3	4
0	1	2	3	4	5	6	0	1	2	3	4	5	6	0	1	2	3	4	5	6
2	3	4	5	6	0	1	2	3	4	5	6	0	1	2	3	4	5	6	0	1
4	5	6	0	1	2	3	4	5	6	0	1	2	3	4	5	6	0	1	2	3
6	0	1	2	3	4	5	6	0	1	2	3	4	5	6	0	1	2	3	4	5
1	2	3	4	5	6	0	1	2	3	4	5	6	0	1	2	3	4	5	6	0
3	4	5	6	0	1	2	3	4	5	6	0	1	2	3	4	5	6	0	1	2
5	6	0	1	2	3	4	5	6	0	1	2	3	4	5	6	0	1	2	3	4
0	1	2	3	4	5	6	0	1	2	3	4	5	6	0	1	2	3	4	5	6
2	3	4	5	6	0	1	2	3	4	5	6	0	1	2	3	4	5	6	0	1
4	5	6	0	1	2	3	4	5	6	0	1	2	3	4	5	6	0	1	2	3
6	0	1	2	3	4	5	6	0	1	2	3	4	5	6	0	1	2	3	4	5
1	2	3	4	5	6	0	1	2	3	4	5	6	0	1	2	3	4	5	6	0
3	4	5	6	0	1	2	3	4	5	6	0	1	2	3	4	5	6	0	1	2
5	6	0	1	2	3	4	5	6	0	1	2	3	4	5	6	0	1	2	3	4

Figure 35. An example of resource allocation for a channel bandwidth of 3 MHz per sector per eNB. with Latin Square size 7 (Scenario 1).

For example, if the number of interfering sources is three, then to have the lowest effect of co-channel interference, the size of the Latin Square in this case is the next prime number of the square root of (300 × 4), which equates to 37. The size of the Latin Square is then varied from the prime numbers between 19 and 37, which are 19, 23, 29, 31, and 37, to investigate the behavior of co-channel interference and resource utilization. Although a bigger Latin Square size means a lower effect of co-channel interference, it also means that the utilization of the resources decreases. Taking Latin Squares of sizes 23 and 29 as shown in Figure 36, we see that each lighter shaded small square represents one resource block per user (300 of them in this case and bounded by the frame length of 20 time slots and channel frequency). The darker shaded small squares are the unutilized resource blocks from the remaining Latin Square sizes of 23 and 29, respectively.

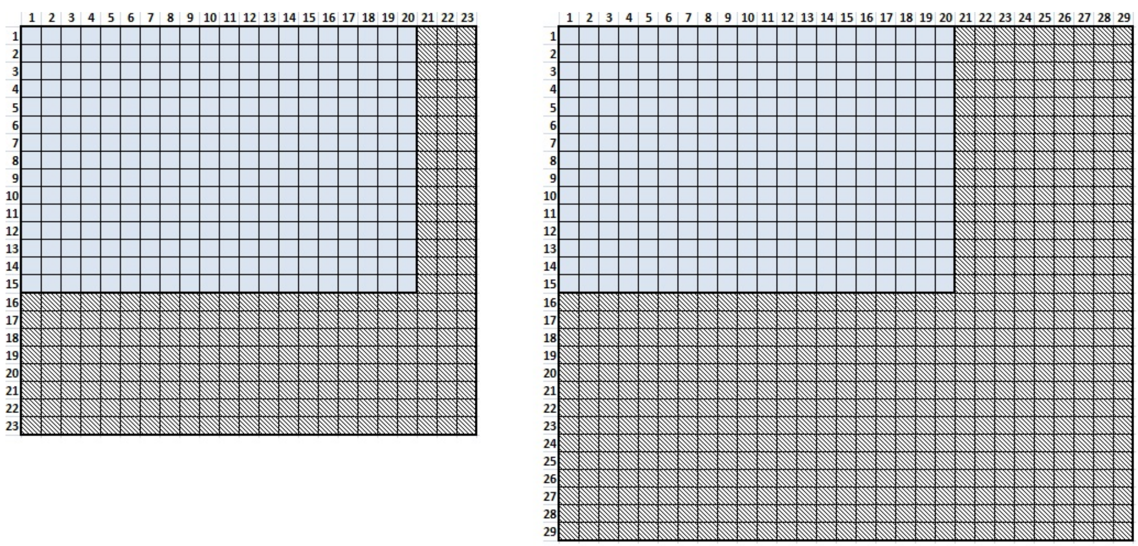

Figure 36. An example of resource allocation for a channel bandwidth of 3 MHz per sector per eNB, with various Latin Square sizes (Scenario 2).

4. Proposed Algorithm for 60°-sectoring

The SIR equations derived in Section IV and V have the general form

$$SIR = \frac{P_{desired}}{(p_1 I_1) + (p_2 I_2) + (p_3 I_3) + (p_4 I_4) + \cdots}. \tag{6.1}$$

Without the use of the Latin Square frequency hopping scheme to diversify the sub-carriers' assignment, the worst case where an eNB becomes an interfering source has a probability p_i 1. However, with the use of the Latin Square frequency hopping scheme, the resources are allocated to the users in a staggered manner as shown previously in Figure 33. This means that the probability p_i of two users in two eNBs (one user per eNB) being allocated the same resources in the same frequency and time symbol is reduced. Certainly, this probability p_i of the eNB becoming an interfering source increases when the number of users per Latin Square increases or when the size of Latin Square decreases.

Figure 27 and Equation (5.9) show that there are three interfering sources in the second tier. The SIR for the CEU in the forward channel for the 60°-sectoring becomes

$$SIR_{CEU,60^\circ} = \left(\frac{P_{T,O}}{\left(p_O (4)^{-n} P'_{T,O} + p_A \left(\sqrt{7}\right)^{-n} P_{T,A} + p_B \left(\sqrt{7}\right)^{-n} P_{T,B} \right)} \right). \tag{6.2}$$

Similarly, for the reverse channel for 60°-sectoring, as seen in Figure 29 and Equation (5.18), there are also three interfering sources in the second tier. The SIR for the cell edge in the reverse channel for the 60°-sectoring becomes

$$SIR_{CE,60^\circ} = \left(\frac{P_{T,O}}{\left(p_A \left(\frac{3\sqrt{3}}{2}\right)^{-n} P_{T,A} + p_B \left(\frac{3\sqrt{3}}{2}\right)^{-n} P_{T,B} + p_O \left(3+\frac{r}{R}\right)^{-n} P'_{T,O} \right)} \right). \tag{6.3}$$

VII. SIMULATION AND ANALYSIS

A. TEST SETUP AND OBJECTIVE

Based on the final forward and reverse channel SIR equations derived in Chapters IV and V, it can be seen that the SIR is dependent upon the power transmitted by the eNB and UE, respectively. As such, the average SIR is computed as

$$SIR_{Average} = \sum_{i=1}^{M} p_i SIR_i \quad (7.1)$$

where p_i is the probability of the SIR value computed over the number of transmitted power intervals, M.

It is also observed from the SIR equations that the SIR is dependent upon the path loss exponent, whose value is normally in the range of two to four, where two is for propagation in free space and four is for relatively lossy environments. For the purpose of the simulations for this thesis, a path loss exponent of four is used. In addition, for the cell center areas, the SIR is dependent on the cell edge area radius to the cell center area radius ratio *R/r*. Since the cell area is divided into two portions with a center area and an edge area, it is pertinent to investigate the relationship between the average SIR and *R/r* and identify the optimal ratio point for cell center areas. A simulation code in Matlab was written to calculate the average SIR for cell edge areas and is listed in the Appendix.

B. RESULTS AND ANALYSIS FOR 120°-SECTORING APPROACH

1. Forward Channel SIR for CCU

In LTE, an eNB typically transmits power from 5 W to 60 W. Assuming a discrete uniform distribution of power at an interval of 5 W, we see that p_i is 1/12. A path loss exponent of four and Equation (4.15) are used to plot the average SIR in dB against the ratio of *R/r* ranging from 1 to 5 as shown in Figure 37 and tabulated in Table 3.

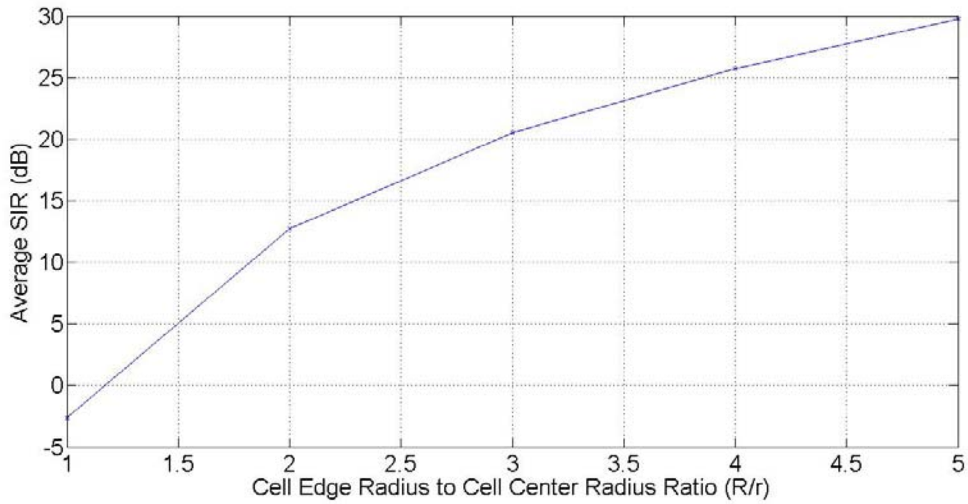

Figure 37. Forward channel average SIR as a function of the ratio of *R/r* (120°-sectoring).

Table 3. Forward channel average at its respective ratio of *R/r* (120°-sectoring).

R/r	1	2	3	4	5
Average SIR (dB)	-2.6	12.8	20.5	25.8	29.8

As expected, with a bigger center area, co-channel interference is higher. The center area cannot be unrealistically small, however, as this means a higher power level is required for cell edge users. As such, to achieve an acceptable SIR performance for the CCU in the forward channel, the *R/r* has to be at least two, where the corresponding SIR is 12.8 dB as found in Table 3.

2. Forward Channel SIR for CEU

From Equation (4.22), the average SIR is independent of the *R/r* ratio. Similar to the cell center analysis performed in the previous section, a discrete uniform power distribution at intervals of 5 W is assumed from 5 W to 60 W, p_i is 1/12 and a path loss exponent of four is used in the computation. From the Matlab simulation of Equation (4.22), the average forward channel SIR for cell center users with 120°-sectoring was computed to be 14.0 dB.

3. Reverse Channel SIR Center Area

From LTE (Rel-10) [10], the maximum power that the UE can transmit is 23 dBm or 200 mW. Assuming a discrete uniform distribution of power at an interval of 10 mW from 10 mW to 200 mW, we have p_i is 1/20. A path loss exponent of four and Equation (4.28) are used to plot the average SIR in dB against the ratio of *R/r* ranging from 1 to 6 as shown in Figure 38, and tabulated in Table 4.

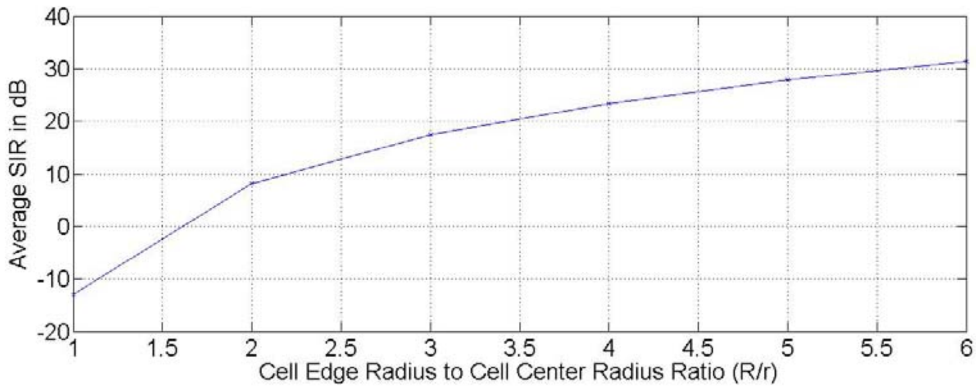

Figure 38. Reverse channel average SIR as a function of the ratio of *R/r* (120°-sectoring).

Table 4. Reverse channel average at its respective ratio of *R/r* (120°-sectoring).

R/r	1	2	3	4	5	6
Average SIR (dB)	-13.0	8.1	17.4	23.4	27.8	31.4

Again, as expected, with a bigger center area, the CCI is higher. The center area cannot be unrealistically small however, as this means a higher power level is required for eNB to receive a signal from the cell edge areas. As such, for the reverse link to achieve an acceptable SIR performance, the *R/r* has to be at least three, where the corresponding SIR is 17.4 dB as found in Table 4.

To reconcile the forward and reverse channel analysis for the CCU, the acceptable *R/r* is three because anything less than this ratio has an adverse effect on the SIR for the CCU in the reverse channel, as seen in Table 4. Therefore, with *R/r* = 3, the SIR for the

CCU in the forward channel is 20.5 dB (from Table 3), while the SIR for the CCU in the reverse channel is 17.4 dB (from Table 4). This means that the center cell is reverse-channel limited.

4. Reverse Channel SIR for Edge Area

As seen in Equation (4.35), the average SIR is independent of *R/r*. Similar to the cell center analysis done in the previous section, a discrete uniform power distribution at intervals of 10 mW is assumed from 10 mW to 200 mW; p_i is then 1/20, and a path loss exponent of four is used in the computation. From the Matlab simulation on Equation (4.35), the average reverse channel SIR for a cell edge area with 120°-sectoring is computed to be 11.7 dB.

C. RESULTS AND ANALYSIS FOR THE 60°-SECTORING APPROACH

1. Forward Channel SIR for CCU

Similar to the analysis for the 120°-sectoring approach, the eNB typically transmits power from 5 W to 60 W, and p_i = 1/12. Assuming a discrete uniform distribution of power at intervals of 5 W and a path loss exponent of four, we use Equation (5.2) to plot the average SIR in dB versus *R/r* for ranging from 1 to 5 as shown in Figure 39, and tabulated in Table 5.

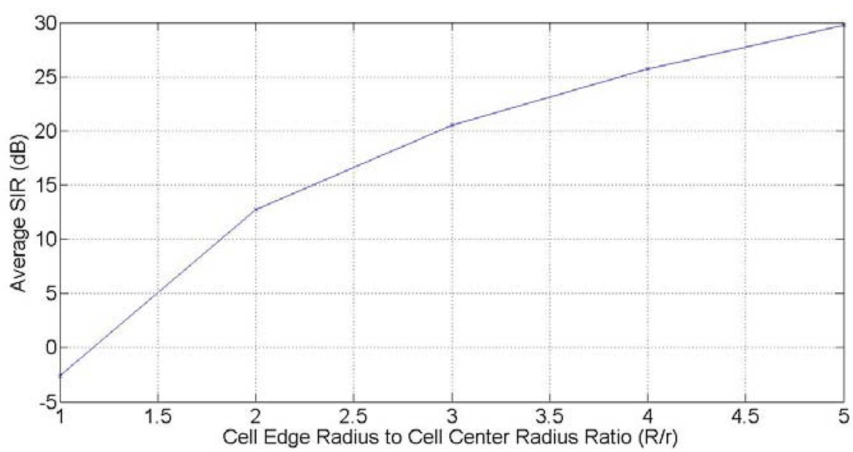

Figure 39. Forward channel average SIR as a function of the ratio of *R/r* (60°-sectoring).

Table 5. Forward channel average at its respective ratio of *R/r* (60°-sectoring).

R/r	1	2	3	4	5
Average SIR (dB)	-2.6	12.8	20.5	25.8	29.8

As the methodology used here for center users is the same for both 120°-sectoring and 60°-sectoring, the results presented here are the same as those for 120°-sectoring. With the same argument, with a bigger center area, the co-channel interference is higher and, thus, less desired. The center area cannot be unrealistically small, however, as this means a higher power level is required for cell edge users. As such, to achieve an acceptable SIR performance for the CCU in the forward channel, *R/r* has to be at least two, where the corresponding SIR is 12.8 dB as found in Table 5.

2. Forward Channel SIR for the CEU

The average SIR is independent of *R/r* as shown in Equation (5.9). Similar to the cell center analysis performed in the previous section, a discrete uniform power distribution at intervals of 5 W is assumed from 5 W to 60 W. This gives $p_i = 1/12$, and a path loss exponent of four is used in the computation. From the Matlab simulation of Equation (5.9), the average forward channel SIR for cell center users with 60°-sectoring is found to be 14.2 dB.

3. Reverse Channel SIR for the Center Area

From LTE (Rel-8), the maximum power that the UE can transmit is 23 dBm or 200 mW. Assuming a discrete uniform distribution of power at intervals of 10 mW from 10 mW to 200 mW, we have $p_i = 1/20$. For a path loss exponent of four and using equation (5.11), the average SIR in dB is plotted against *R/r* ranging from 1 to 6 as shown in Figure 40 and tabulated in Table 6.

Again, since the methodology used for the center area is the same for both 120°-sectoring and 60°-sectoring, the results presented here are the same as those for 120°-sectoring.

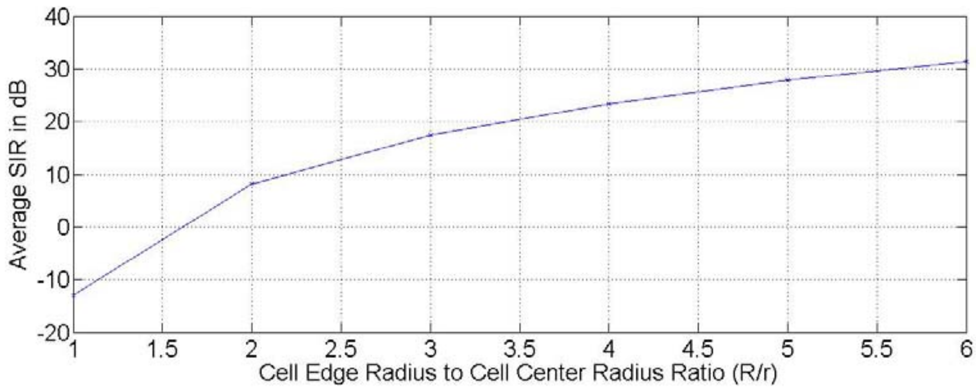

Figure 40. Reverse channel average SIR as a function of the ratio of *R/r* (60°-sectoring).

Table 6. Reverse channel average at its respective ratio of *R/r* (60°-sectoring).

R/r	1	2	3	4	5	6
Average SIR (dB)	-13.0	8.1	17.4	23.4	27.8	31.4

Again, with a larger center area, the co-channel interference is higher and, thus, less desired. The center area cannot be unrealistically small, however, as this means a higher power level is required for the eNB to receive a signal from the cell edge areas. As such, for the reverse link to achieve an acceptable SIR performance, *R/r* must be at least three, where the corresponding SIR is 17.4dB as found in Table 6.

To reconcile the forward and reverse channel analyses for the CCU, the acceptable *R/r* is three, because anything less than this ratio has an adverse effect on the SIR for the CCU in the reverse channel, as seen in Table 6. Therefore, with *R/r* = 3, the SIR for the CCU in the forward channel is 20.5 dB (from Table 5), while the SIR for the CCU in the reverse channel is 17.4 dB (from Table 6). This means that the center cell is reverse-channel limited.

4. Reverse Channel SIR for Edge Area

As seen in Equation (5.18), the average SIR is dependent on the *r/R* ratio. Similar to the cell center analysis performed in the previous section, a discrete uniform power distribution at intervals of 10 mW is assumed from 10 mW to 200 mW. As a result, p_i = 1/20, and a path loss exponent of four is used in the computation. As mentioned in the previous section, the optimal average SIR for the reverse channel for center area is obtained when R/r = 3, so r/R = 1/3. Therefore, using the Matlab simulation of equation (5.18) with r/R = 1/3, the average reverse channel SIR for the cell edge area with 60°-sectoring was computed to be 13.4 dB.

D. RESULTS AND ANALYSIS FOR MAC-LAYER PROPOSED DESIGN

1. Virtual Channel Assignment Approach (Scenario 1) for the Forward Channel

Using Equation (6.2), we obtain the behavior of the SIR and the resource allocation for the channel bandwidths of 3 MHz, 10 MHz, and 20 MHz for the forward channel shown in Figures 41 to 46. In each channel bandwidth, the number of users per Latin Square is varied between 5 and 7 to illustrate the SIR and the resource utilization behavior.

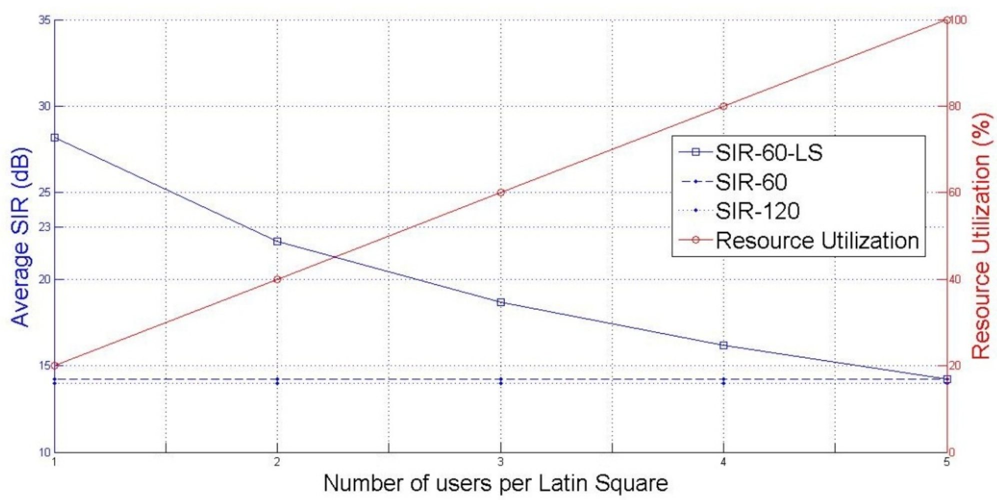

Figure 41. SIR performance and resource utilization for forward channel, with 3 MHz channel bandwidth per sector, Latin Square size 5.

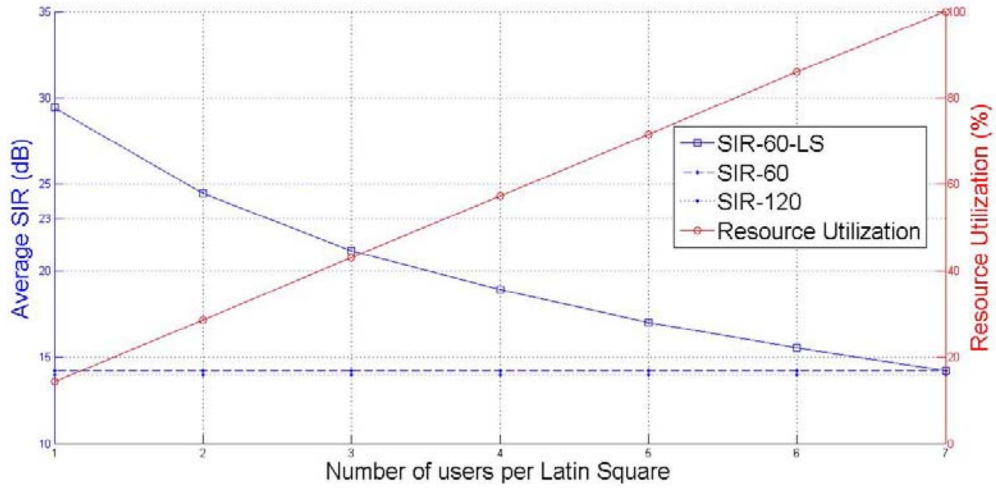

Figure 42. SIR performance and resource utilization for forward channel, with 3 MHz channel bandwidth per sector, Latin Square size 7.

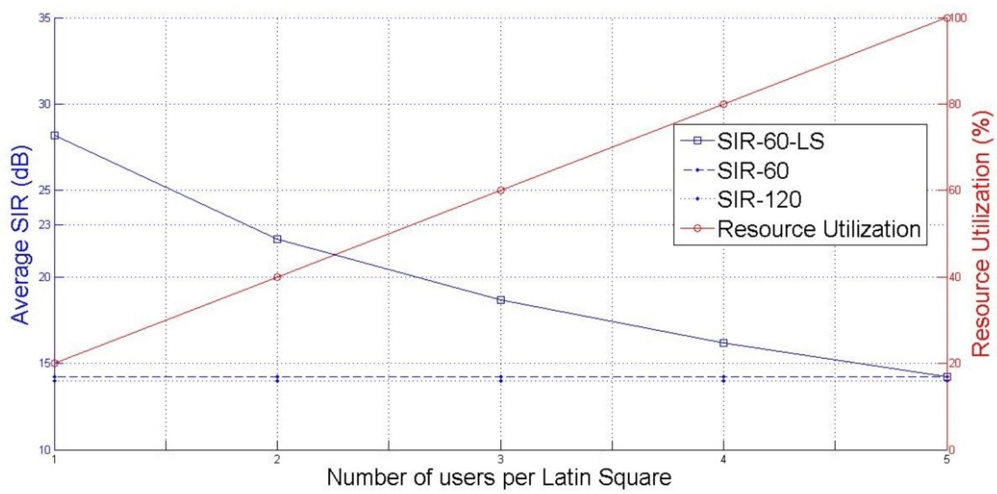

Figure 43. SIR performance and resource utilization for forward channel, with 10 MHz channel bandwidth per sector, Latin Square size 5.

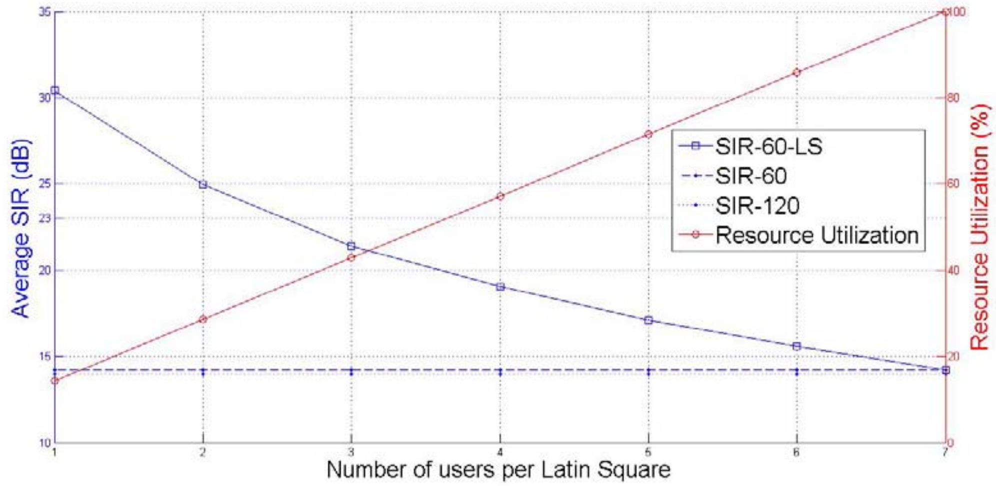

Figure 44. SIR performance and resource utilization for forward channel, with 10 MHz channel bandwidth per sector, Latin Square size 7.

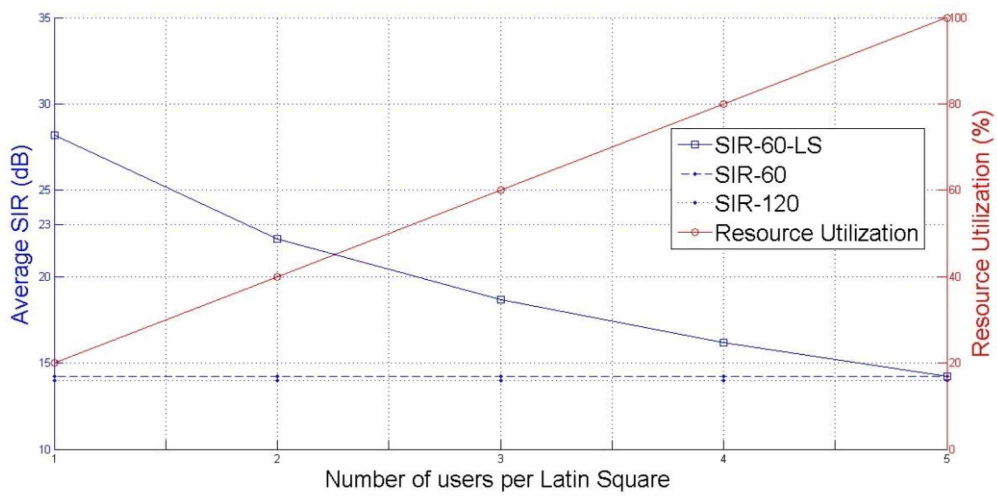

Figure 45. SIR performance and resource utilization for forward channel, with 20 MHz channel bandwidth per sector, Latin Square size 5.

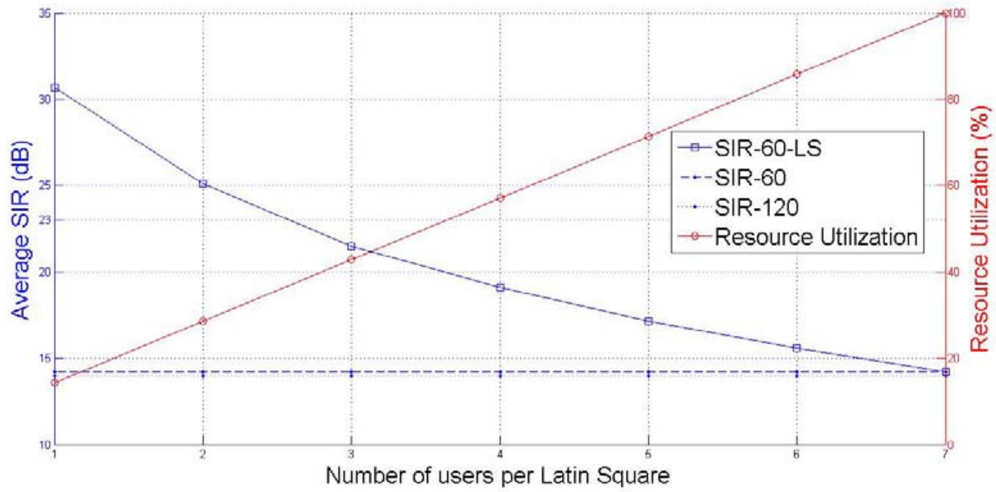

Figure 46. SIR performance and resource utilization for forward channel, with 20 MHz channel bandwidth per sector, Latin Square size 7.

From Figures 41 to 46, it can be observed that with the Latin Square scheme applied, the SIR improves in general. In fact, by looking at the number of users from one to five only for both Latin Square sizes of 5 and 7, the SIR improves more with the Latin Square size 7 and slightly more when the channel bandwidth increases. This shows that with a bigger Latin Square size, the probability that users are assigned the same virtual channel is reduced as the number of virtual channels assigned is increased from five to seven. Furthermore, when the channel bandwidth increases, the number of resource blocks increases too, diffusing the probability of overlapped resources. Having said this, we note that with a range of users from one to five, the resource utilization for Latin Square size 7 drops by about 20% of that of Latin Square size 5. Also, the number of users supported is reduced since a transmission frame of 20 time slots and 15 resource blocks fits a smaller number of (7×7) Latin Squares as compared to (5×5).

The extent that the SIR improves is greater as the number of users per Latin Square decreases. This makes sense because, when there are fewer users per eNB, the probability of the users being assigned the same virtual channel decreases, reducing the effect of co-channel interference. On the other hand, when the number of users per Latin Square increases, the resources are better utilized, therefore, the increase in the resource utilization.

2. Resource Block Assignment Approach (Scenario 2) for the Forward Channel

Using Equation (6.2), we show the behavior of the SIR and the resource allocation for the various channel bandwidths from 1.4 MHz to 20 MHz for the forward channel in Figures 47 to 52.

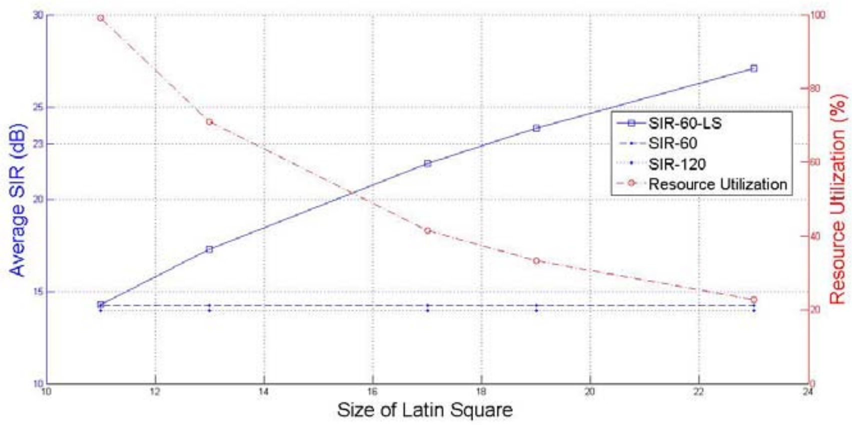

Figure 47. SIR performance and resource utilization for forward channel, with 1.4 MHz channel bandwidth per sector.

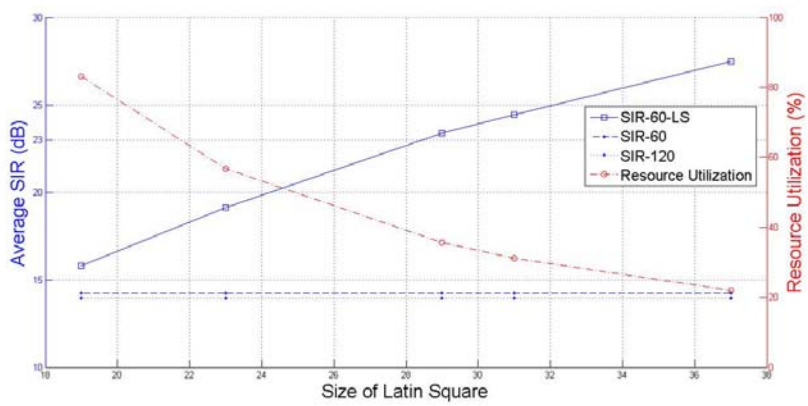

Figure 48. SIR performance and resource utilization for forward channel, with 3 MHz channel bandwidth per sector.

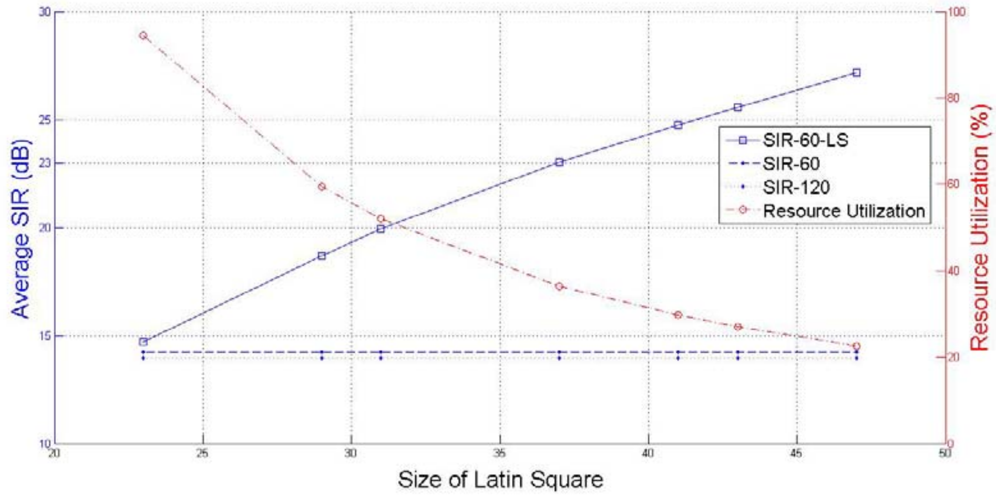

Figure 49. SIR performance and resource utilization for forward channel, with 5 MHz channel bandwidth per sector.

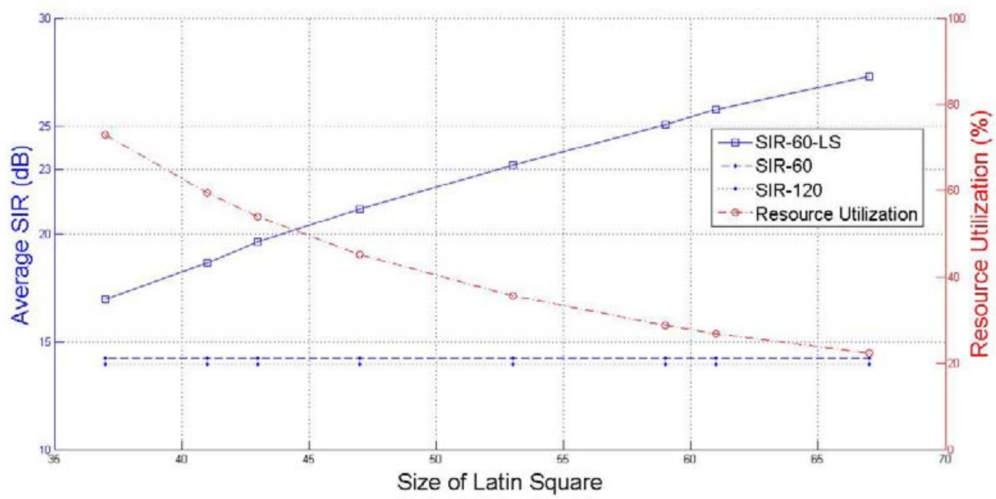

Figure 50. SIR performance and resource utilization for forward channel, with 10 MHz channel bandwidth per sector.

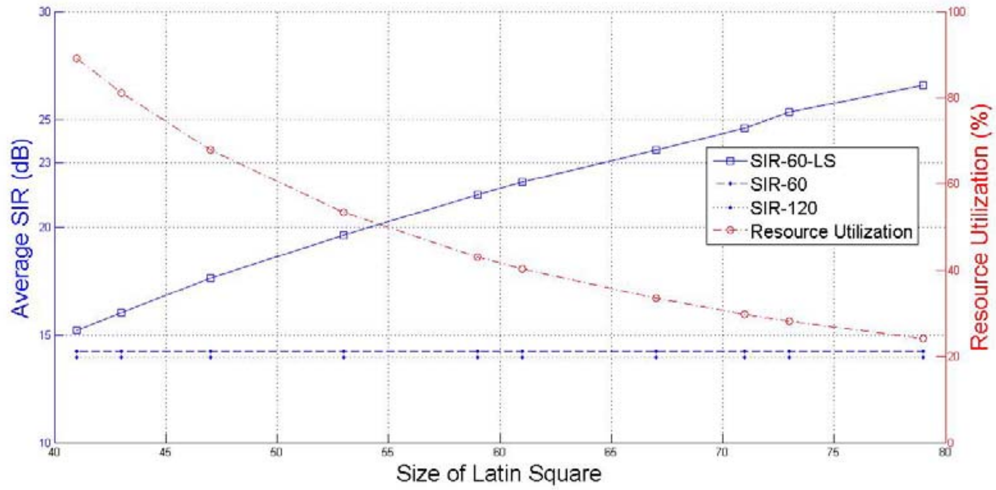

Figure 51. SIR performance and resource utilization for forward channel, with 15 MHz channel bandwidth per sector.

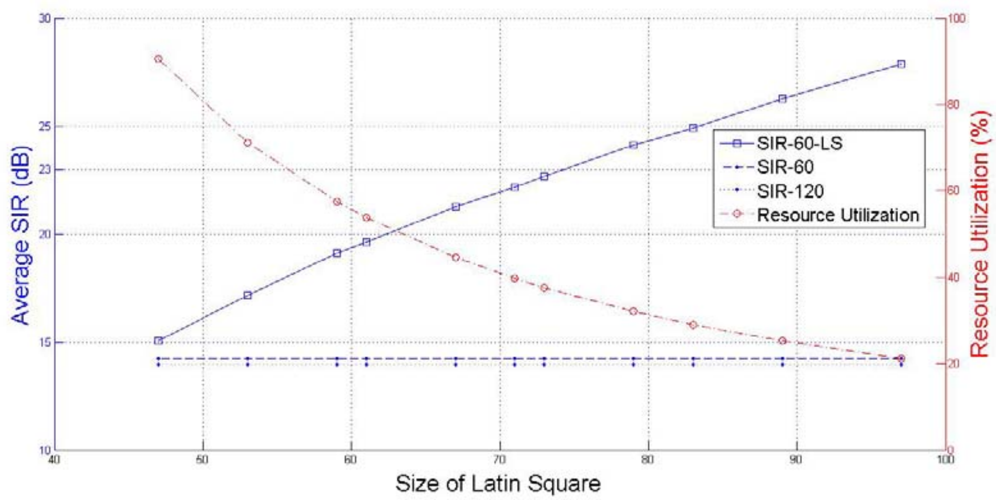

Figure 52. SIR performance and resource utilization for forward channel, with 20 MHz channel bandwidth per sector.

From Figures 47 to 52, it can be observed that with the Latin Square scheme applied, the SIR improves in general. In fact, the SIR improves more as the size of the Latin Square increases. This makes sense because when the Latin Square is large, the probability that the users are assigned the same resources decreases, reducing the effect of co-channel interference. On the other hand, when the size of the Latin Square increases, the resources are less utilized, therefore, there is a decrease in the resource utilization. Furthermore, it can also be observed from Figure 50 that the resource utilization is lower when the channel bandwidth is 10 MHz. This is because at the channel bandwidth of 10 MHz, the maximum number of users supported is 1000, i.e., 20 × 50. As discussed in Chapter VI, in order to minimally support this number of users, a Latin Square of size 37, which is the next prime number of square root 1000, is used. As such, comparing to the other channel bandwidth sizes, the resource utilization appears to be lower.

3. Virtual Channel Assignment Approach (Scenario 1) for the Reverse Channel

The same analysis is applied in the reverse channel, and by using Equation (6.3), the behavior of the SIR and the resource allocation for the channel bandwidths of 3 MHz, 10 MHz, and 20 MHz for the reverse channel are shown in Figures 53 to 58. Again, for each channel bandwidth, the number of users per Latin Square is varied between 5 and 7 to illustrate the SIR and the resource utilization behavior.

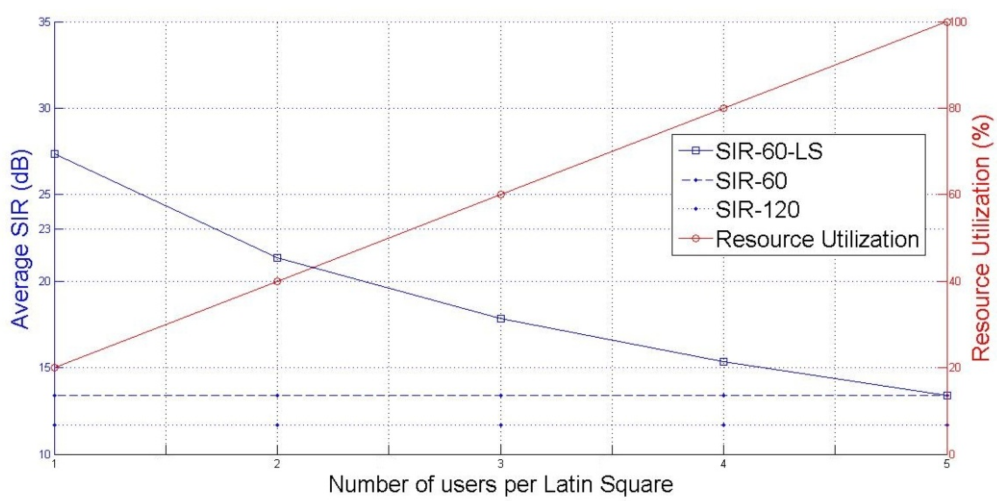

Figure 53. SIR performance and resource utilization for reverse channel, with 3 MHz channel bandwidth per sector, Latin Square size 5.

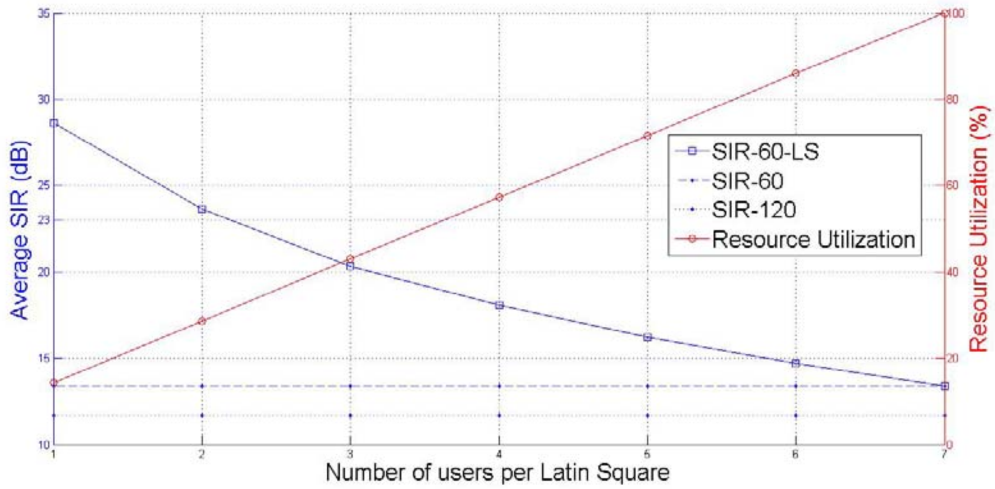

Figure 54. SIR performance and resource utilization for reverse channel, with 3 MHz channel bandwidth per sector, Latin Square size 7.

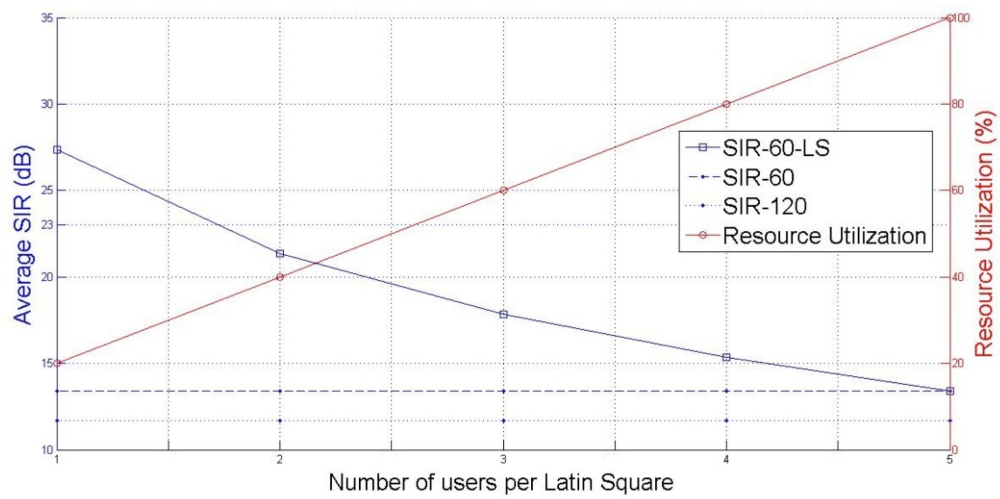

Figure 55. SIR performance and resource utilization for reverse channel, with 10 MHz channel bandwidth per sector, Latin Square size 5.

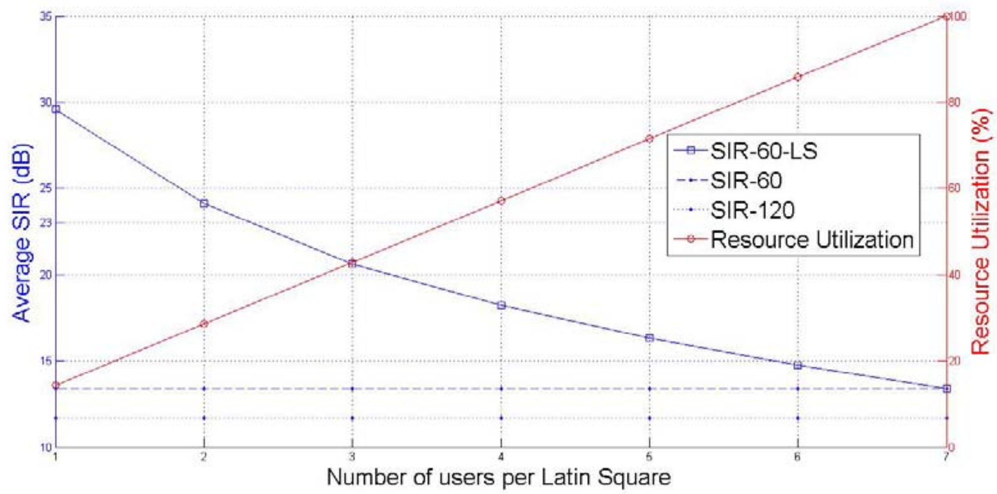

Figure 56. SIR performance and resource utilization for reverse channel, with 10 MHz channel bandwidth per sector, Latin Square size 7.

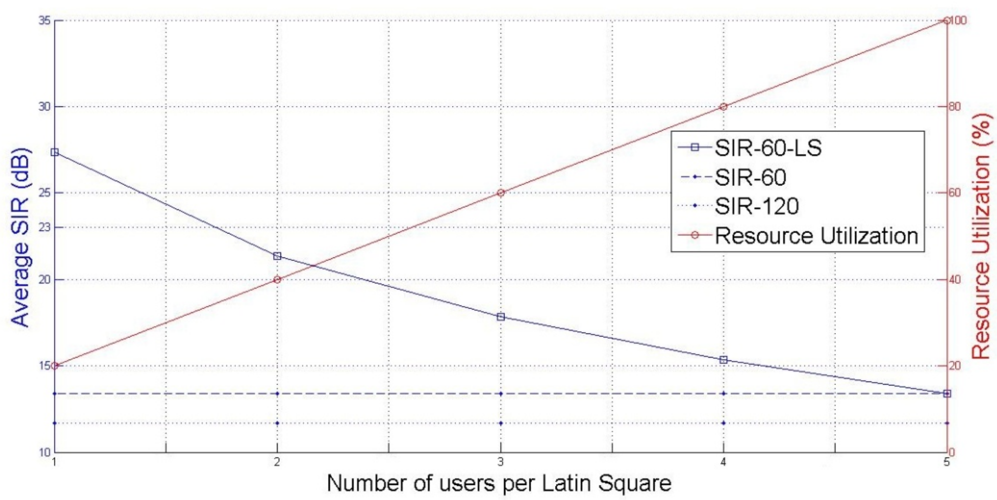

Figure 57. SIR performance and resource utilization for reverse channel, with 20 MHz channel bandwidth per sector, Latin Square size 5.

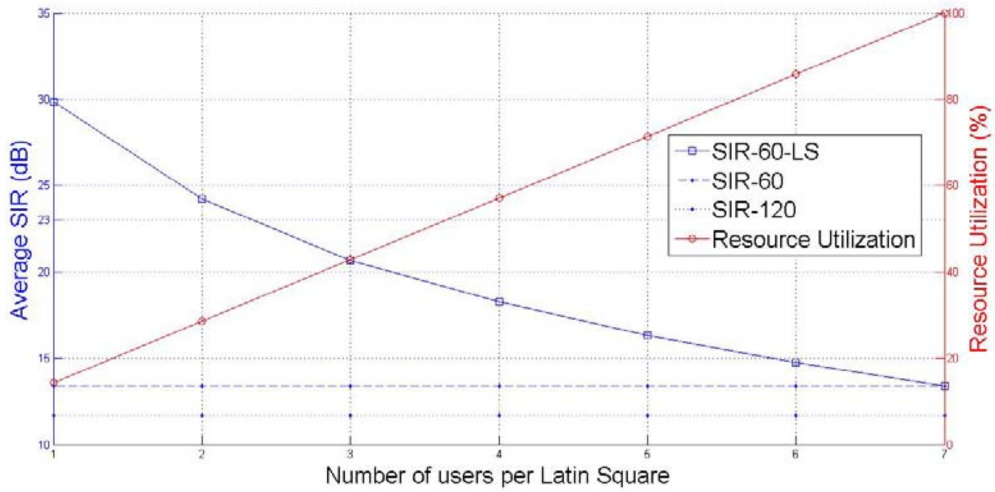

Figure 58. SIR performance and resource utilization for reverse channel, with 20 MHz channel bandwidth per sector, Latin Square size 7.

From Figures 53 to 58, the same observation on the forward channel can be made for the reverse channel. When the Latin Square scheme is applied, the SIR improves in general. By comparing the SIR for the one to five users range for Latin Square sizes 5 and 7, we see that the SIR improves more with Latin Square of size 7 and slightly more when the channel bandwidth increases. This shows that with a larger Latin Square size, the probability that the users are assigned the same virtual channel is reduced as the number of virtual channels assignment is increased from five to seven. Furthermore, when the channel bandwidth increases, the number of resource blocks increases too, diffusing the probability of overlapped resources. It is also important to note that from the user range of one to five, the resource utilization for Latin Square size 7 drops by about 20% of that of Latin Square size 5.

Furthermore, the extent that the SIR improves is greater as the number of users per Latin Square decreases. When there are fewer users per eNB, the probability that the users are assigned the same virtual channel decreases, reducing the effect of co-channel interference. On the other hand, when the number of users per Latin Square increases, the resources are better utilized, therefore, the increase in the resource utilization.

4. Resource Block Assignment Approach (Scenario 2) for the Reverse Channel

By using Equation (6.3), we show the behavior of the SIR and the resource allocation for the various channel bandwidths from 1.4 MHz to 20 MHz for the reverse channel in Figures 59 to 64.

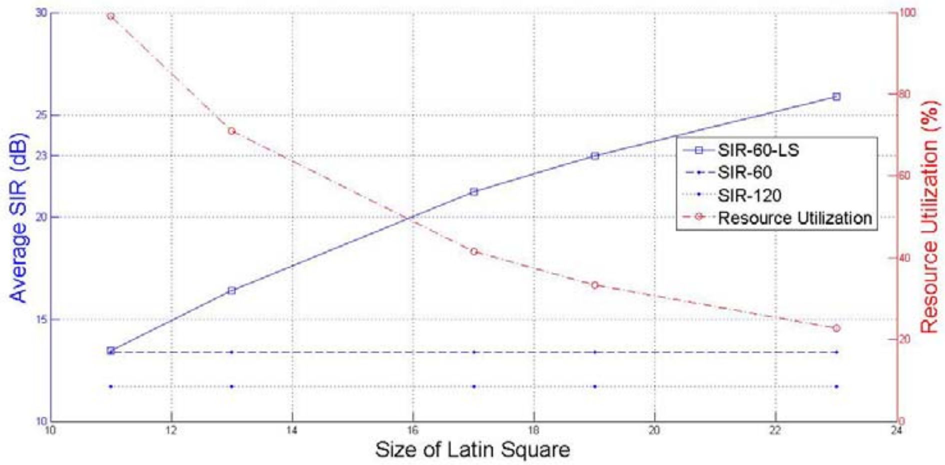

Figure 59. SIR performance and resource utilization for reverse channel, with 1.4 MHz channel bandwidth per sector.

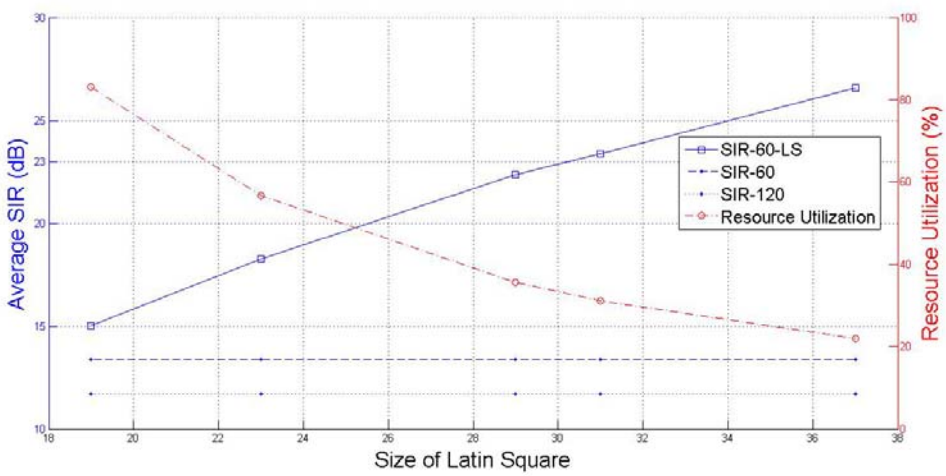

Figure 60. SIR performance and resource utilization for reverse channel, with 3 MHz channel bandwidth per sector.

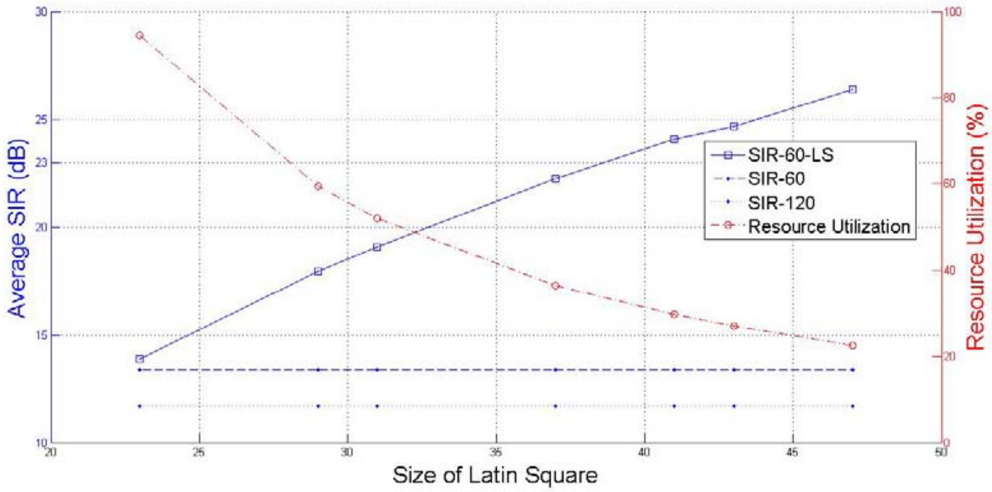

Figure 61. SIR performance and resource utilization for reverse channel, with 5 MHz channel bandwidth per sector.

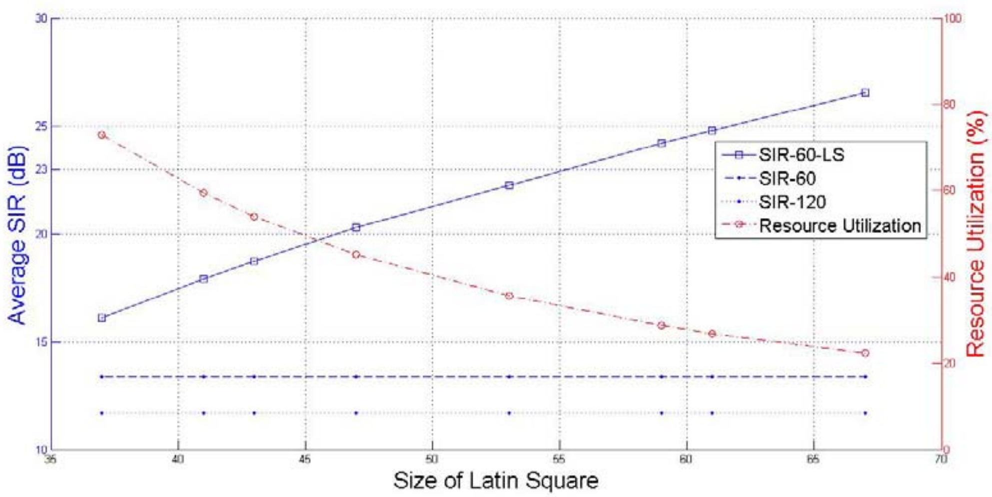

Figure 62. SIR performance and resource utilization for reverse channel, with 10 MHz channel bandwidth per sector.

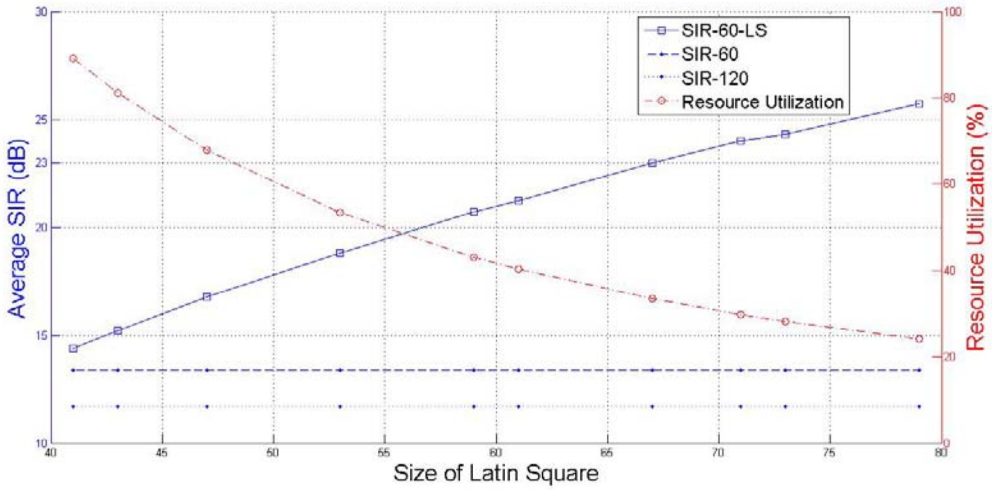

Figure 63. SIR performance and resource utilization for reverse channel, with 15 MHz channel bandwidth per sector.

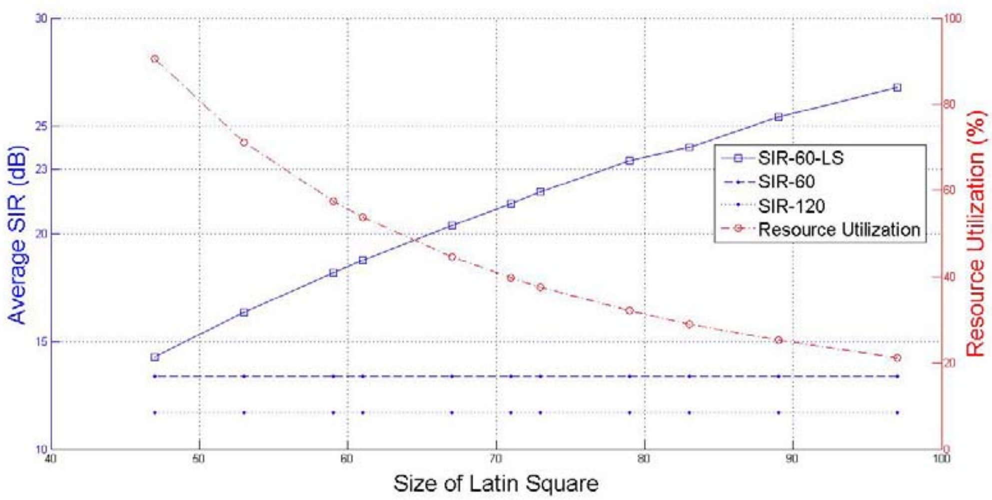

Figure 64. SIR performance and resource utilization for reverse channel, with 20 MHz channel bandwidth per sector.

In Figures 59 to 64, it can be observed that with the Latin Square scheme applied, the SIR again improves in general. In fact, the SIR improves more as the size of the Latin Square increases. This makes sense because when the Latin Square is larger, the probability that the users are assigned the same resources decreases, reducing the effect of co-channel interference. On the other hand, when the size of the Latin Square increases, the resources are less utilized, therefore, the decrease in the resource utilization. Furthermore, it can also be observed from Figure 64 that the resource utilization is lower when the channel bandwidth is 10 MHz. This is because at a channel bandwidth of 10 MHz, the maximum number of users supported is 1000, i.e., 20 × 50. As discussed in Chapter VI, in order to minimally support this number of users, a Latin Square of size 37, which is the next prime number of square root 1000, is used. As such, compared to the other channel bandwidth sizes, the resource utilization appears to be lower.

E. SUMMARY

Since each use case is unique, it is crucial to identify the best methodology to be adopted.

1. Forward Channel SIR for CCU

In both cell structures discussed, sectoring is not adopted for the center area, therefore, it is expected that the average SIR for each ratio of *R/r* is the same. This is shown in Table 7. From the simulations for the forward channel, the boundary of the cell center area is optimum with a high SIR of 20.5 dB when this inner cell distance is one-third of the cell radius.

Table 7. Comparison for forward channel average at its respective ratio of *R/r*.

R/r	1	2	3	4	5
Average SIR (dB) for 120°-sectoring	-2.6	12.8	20.5	25.8	29.8
Average SIR (dB) for 60°-sectoring	-2.6	12.8	20.5	25.8	29.8

2. Forward Channel SIR for the CEU

For the cell edge users, different degrees of sectoring are adopted; therefore, it is expected that the average SIR will be different. In fact, it is expected that the average SIR for the CEU in 60°-sectoring would be better. This is shown in Table 8, where the average SIR for the 60°-sectoring is 0.3 dB better than that for 120°-sectoring. This is equivalent to 1.06 ($10^{0.25/10}$ = 1.06) times better than 120°-sectoring approach, a 6% improvement.

In addition, in Scenario 1 where each virtual channel is assigned to each user, the SIR improves more than without the Latin Square scheme applied. As seen in Figures 42, 44, and 46, the SIR is better when the Latin Square size 7 is applied as compared to a Latin Square size 5; the resource utilization in the former case is about 20% poorer than in the latter. Furthermore, with the Latin Square size 7, there is a full-and-partial Latin Square situation, where some of the users are allocated 7 resource blocks each, while others are allocated six, or even one resource block each. In this case, some form of QoS needs to be implemented, which can add to further complexity. As such, since a Latin Square size 5 can still achieve an improved SIR with better resource utilization, this size is preferred.

In Scenario 2 where the users are assigned one resource block per time slot each, there is also a tradeoff between the improved SIR with the Latin Square scheme applied and the resource utilization. In general, the size of the Latin Square is kept at the next prime number that is able to accommodate the number of users that can be supported in each channel bandwidth in order to better utilize the resources available. As seen in Figures 49 to 54, the general improvement in SIR is between 11 dB and 23 dB. A summary of SIR results is shown in Table 8.

Table 8. Comparison for forward channel SIR for CEU.

Average SIR (dB) for 120°-sectoring	**Average SIR (dB) for 60°-sectoring**	**Average SIR (dB) for 60°-sectoring with Latin Square (One Virtual Channel per user)**	**Average SIR (dB) for 60°-sectoring with Latin Square (One Resource Block per time slot per user)**
14.0	14.2	14.2 dB to 31.0 dB (Depends on the number of users per Latin Square)	16.0 dB to 28.0 dB (Depends on the size of Latin Square)

3. Reverse Channel SIR for the Center Area

Similar to the analysis made in the forward channel, sectoring is not adopted for the center area in the reverse channel for both techniques; hence, it is expected that the average SIR at each ratio of *R/r* is the same. This is shown in Table 9. From the simulations done for the reverse link, to achieve an acceptable SIR performance, the *R/r* has to be at least three, where the corresponding SIR is 17.4 dB as summarized in Table 9.

Table 9. Comparison for reverse channel average at its respective ratio of *R/r*.

R/r	1	2	3	4	5	6
Average SIR (dB) for 120°-sectoring	-13.0	8.1	17.4	23.4	27.8	31.4
Average SIR (dB) for 60°-sectoring	-13.0	8.1	17.4	23.4	27.8	31.4

To reconcile the forward and reverse channel analyses for the CCU, the acceptable *R/r* = 3 because anything less than this ratio has an adverse effect on the SIR for the CCU in the reverse channel, as seen in Table 9. Therefore, with the *R/r* = 3, the SIR for the CCU in the forward channel would be 20.5 dB (from Table 7), while the SIR for the CCU in the reverse channel would be 17.4 dB (from Table 9).

4. Reverse Channel SIR for Edge Area

Similarly, different degrees of sectoring are adopted for the cell edge area in the reverse channel; therefore, it is expected that the average SIR would be different. As mentioned earlier, it is expected that the average SIR for the CEU in 60°-sectoring will be better. This is shown in Table 10, where the average SIR for 60°-sectoring is 5.7dB better than that for 120°-sectoring. This is equivalent to 1.48 ($10^{1.7/10} = 1.48$) times better than the 120°-sectoring approach, a 48% improvement.

In addition, in Scenario 1 where each virtual channel is assigned to each user, the SIR improves more than without the Latin Square scheme applied. As seen in Figures 54, 56, and 58, the SIR is better when a Latin Square size 7 is applied as compared to a Latin Square size 5; the resource utilization in the former is about 20% poorer than the latter. Furthermore, with a Latin Square size 7, there is a full-and-partial Latin Square situation, where some of the users are allocated 7 resource blocks each, while others are allocated six, or even one resource block each. In this case, some form of QoS needs to be implemented, which can add to further complexity. As such, since a Latin Square size 5 can achieve an improved SIR with better resource utilization, this size is preferred.

In Scenario 2 where the users are assigned one resource block per time slot each, there is also a tradeoff between the improved SIR with the Latin Square scheme applied and the resource utilization. In general, the size of the Latin Square is kept at the next prime number that is able to accommodate the number of users which can be supported in each channel bandwidth in order to better utilize the resources available. As seen in Figures 59 to 64, the general improvement in SIR is between 15 dB and 28 dB. A summary of SIR results is shown in Table 10.

Table 10. Comparison for reverse channel SIR for CEU.

Average SIR (dB) for 120°-sectoring	**Average SIR (dB) for 60°-sectoring**	**Average SIR (dB) for 60°-sectoring with Latin Square (One Virtual Channel per user)**	**Average SIR (dB) for 60°-sectoring with Latin Square (One Resource Block per time slot per user)**
11.7	13.4	13.4 dB to 30.0 dB (Depends on the number of users per Latin Square)	15.0 dB to 28.0 dB (Depends on the size of Latin Square)

VIII. CONCLUSION AND RECOMMENDATIONS

A. CONCLUSION

The feasibility of the proposed solution of using 60°- sectoring on the physical layer for an LTE cell structure, and the resulting performance improvements in terms of SIR were demonstrated in this thesis. At the MAC layer, the proposal to adopt a Latin Square with OFDMA and sectorization in the physical layer further reduces the effect of co-channel interference and achieves better SIR. By doing this cross-layer optimization solution, physical and MAC layer control decisions are able to reach their full potential when they are designed in an integrated manner.

B. SIGNIFICANT FINDINGS

With the OFDMA technique adopted in the LTE network, a frequency reuse approach can be used. Furthermore, with the use of sectorization, a higher frequency reuse factor can be achieved, increasing the capacity to handle more users with a low effect of co-channel interference. With proper resource management and using a Latin Square at the MAC layer, the effect of co-channel interference can be reduced even more, although, with some impact on resource utilization.

C. RECOMMENDATIONS

At the physical layer, the allocation of the sub-channels can be further analyzed and refined to achieve even better SIR solely based on sectorization. Referring to Figure 23, we see that it is possible that sub-channel 7 does not always have to be assigned in the center area. Instead, the seven sub-channels can take turns to be allocated to the center area, and the remaining six sub-channels will fall into each sector accordingly. A simulation can then be run to determine if there is further improvement to the SIR in this layer.

As seen from the results in this work, the use of a Latin Square was shown to improve the SIR significantly, and the consideration of resource utilization was taken into account in this thesis. Another good area for further study would be to understand the impact on the transmission throughput given a bit error rate. This includes the consideration of the modulation coding scheme and bit error rate. This would give an even better picture with which to ascertain the right size of Latin Square to be implemented for each eNB, thus achieving an optimum point between SIR, resource utilization, and transmission throughput.

APPENDIX

The Matlab code that uses the SIR equations found in Chapters IV, V, and VI to understand the relationship between the average SIR and the ratio of *R/r* for cell center area for both forward and reverse channels is contained in this Appendix. The codes to understand the behavior of the SIR and the resource utilization for the cell edge users for both the forward and reverse channels are also included in this Appendix.

For Forward Channel, 120°-sectoring, CCU

```
%To calculate the Forward Channel SIR for LTE-Advanced
%120-sectoring
%CCU

clear all;
close all;

n = 4;      %Path loss exponent
Rr=1:5;     %Rr is the ratio of R over r, where R=outer cell radius,
r=inner cell radius
P=5:5:60;

Z=0;
for i=1:length(Rr)
for Pto=5:5:60
    for Pta=5:5:60
        for Ptb=5:5:60
            for Ptc=5:5:60
                for Ptd=5:5:60
                    for Pte=5:5:60
                        for Ptf=5:5:60
                        SIR_ccu1(i) = (Pto/(((sqrt(3*(Rr(i))^2 + 1))^-
n)*Pta + ((sqrt(3*(Rr(i))^2 + 3*(Rr(i)) + 1))^-n)*Ptb +
((sqrt(3*(Rr(i))^2 + 3*(Rr(i)) + 1))^-n)*Ptc +((sqrt(3*(Rr(i))^2 + 1))^-
n)*Ptd + ((sqrt(3*(Rr(i))^2 - 3*(Rr(i)) + 1))^-n)*Pte +
((sqrt(3*(Rr(i))^2 - 3*(Rr(i)) + 1))^-n)*Ptf))+Z;
                        Z=SIR_ccu1(i);
                        end
                    end
                end
            end
        end
    end
end
    Z=0;
end
```

```
SIR_ccu1_dB= 10*log10(SIR_ccu1);
SIR_ccu1_dB_average=10*log10(SIR_ccu1*(1/length(P))^7);

figure,
plot(Rr,SIR_ccu1_dB_average, 'bx-')
grid on;
xlabel('Cell Edge Radius to Cell Center Radius Ratio
(R/r)','fontsize',20)
ylabel('Average SIR (dB)','fontsize',20)
%title('Forward Channel Average SIR as a function of cell edge to cell
center radius ratio for Cell-Center User (CCU) in cell O (120 deg-
sectoring)','fontsize',20)
```

For Forward Channel, 120°-sectoring, CEU

```
%To calculate the Forward Channel SIR for LTE-Advanced
%120-sectoring
%CEU

clear all;
close all;

n = 4;      %Path loss exponent
P=5:5:60;

Z1=0;

for Pto=5:5:60
    for Pta=5:5:60
        for Ptb=5:5:60
            for Ptal=5:5:60
                SIR_ceu1 = (Pto/((((sqrt(13))^-n)*Ptal) + (((sqrt(7))^-
n)*Pta) + (((sqrt(7))^-n)*Ptb)))+Z1;
                Z1=SIR_ceu1;
            end
        end
    end
end

SIR_ceu1_dB= 10*log10(SIR_ceu1);
SIR_ceu1_dB_average=10*log10(SIR_ceu1*(1/length(P))^4);
```

For Reverse Channel, 120°-sectoring, CCU

```
%To calculate the Reverse Channel SIR for LTE-Advanced
%120-sectoring
%CCU

clear all;
close all;
```

```
n = 4;      %Path loss exponent
Rr=1:6;     %Rr is the ratio of R over r, where R=outer cell radius,
r=inner cell radius
P=0.01:0.01:0.2;   %From LTE (Rel-8), the maximum UE transmit power is
23dBm, that is, 200mW.

Z_rev=0;
for i=1:length(Rr)
for Pto=0.01:0.01:0.2
    for Pta=0.01:0.01:0.2
        for Ptb=0.01:0.01:0.2
            for Ptc=0.01:0.01:0.2
                for Ptd=0.01:0.01:0.2
                    for Pte=0.01:0.01:0.2
                        for Ptf=0.01:0.01:0.2
                            SIR_ccu1_rev(i) =
(Pto/(((((sqrt(3))*(Rr(i)))-1)^-n)*(Pta+Ptb+Ptc+Ptd+Pte+Ptf)))+Z_rev;
                            Z_rev=SIR_ccu1_rev(i);
                        end
                    end
                end
            end
        end
    end
end
    Z_rev=0;
end

SIR_ccu1_rev_dB= 10*log10(SIR_ccu1_rev);
SIR_ccu1_rev_dB_average=10*log10(SIR_ccu1_rev*(1/length(P))^7);

figure,
plot(Rr,SIR_ccu1_rev_dB_average, 'bx-')
grid on;
xlabel('Cell Edge Radius to Cell Center Radius Ratio
(R/r)','fontsize',20)
ylabel('Average SIR in dB','fontsize',20)
%title('Reverse Channel Average SIR as a function of cell edge to cell
center radius ratio for Cell-Center User (CCU) in cell O')
```

For Reverse Channel, 120°-sectoring, CEU

```
%To calculate the Reverse Channel SIR for LTE-Advanced
%120-sectoring
%CEU

clear all;
close all;

n = 4;      %Path loss exponent
Rr=1:6;     %Rr is the ratio of R over r, where R=outer cell radius,
r=inner cell radius
```

```
P=0.01:0.01:0.2;   %From LTE (Rel-8), the maximum UE transmit power is
23dBm, that is, 200mW.

Z1_rev=0;

for Pto=0.01:0.01:0.2
    for Pta=0.01:0.01:0.2
        for Ptb=0.01:0.01:0.2
            for Ptbl=0.01:0.01:0.2
                SIR_ceu1_rev = (Pto/(((((sqrt(21))/2)^-n)*Ptbl) +
((((3/2)*(sqrt(3)))^-n)*Pta) + (((sqrt(7))^-n)*Ptb)))+Z1_rev;
                Z1_rev=SIR_ceu1_rev;
            end
        end
    end
end

SIR_ceu1_rev_dB= 10*log10(SIR_ceu1_rev);
SIR_ceu1_rev_dB_average=10*log10(SIR_ceu1_rev*(1/length(P))^4);
```

For Forward Channel, 60°-sectoring, CCU

```
%To calculate the Forward Channel SIR for LTE-Advanced
%CCU -- 60-sectoring

clear all;
close all;

n = 4;      %Path loss exponent
Rr=1:5;     %Rr is the ratio of R over r, where R=outer cell radius,
r=inner cell radius
P=5:5:60;

Z=0;
for i=1:length(Rr)
for Pto=5:5:60
    for Pta=5:5:60
        for Ptb=5:5:60
            for Pta1=5:5:60
                for Ptb1=5:5:60
                    for Pta2=5:5:60
                        for Ptb2=5:5:60

                        SIR_ccu1(i) = (Pto/(((sqrt(3*(Rr(i))^2 + 1))^-
n)*Pta + ((sqrt(3*(Rr(i))^2 + 3*(Rr(i)) + 1))^-n)*Ptb +
((sqrt(3*(Rr(i))^2 + 3*(Rr(i)) + 1))^-n)*Pta1 +((sqrt(3*(Rr(i))^2 +
1))^-n)*Ptb1 + ((sqrt(3*(Rr(i))^2 - 3*(Rr(i)) + 1))^-n)*Pta2 +
((sqrt(3*(Rr(i))^2 - 3*(Rr(i)) + 1))^-n)*Ptb2))+Z;
                        Z=SIR_ccu1(i);

                        end
                    end
```

```
                end
            end
        end
    end
end
    Z=0;
end

SIR_ccu1_dB= 10*log10(SIR_ccu1);
SIR_ccu1_dB_average=10*log10(SIR_ccu1*(1/length(P))^7);

figure,
plot(Rr,SIR_ccu1_dB_average, 'bx-')
grid on;

xlhand = get(gca,'xlabel')
set(xlhand,'string','X','fontsize',20)

xlabel('Cell Edge Radius to Cell Center Radius Ratio
(R/r)','fontsize',20)
ylabel('Average SIR (dB)','fontsize',20)
%title('Forward Channel Average SIR as a function of cell edge to cell
center radius ratio for Cell-Center User (CCU) in cell O (60o-
sectoring)','fontsize',20)
```

Forward Channel, 60°-sectoring, CEU

```
%To calculate the Forward Channel SIR for LTE-Advanced
%CEU -- 60-SECTORING

clear all;
close all;

n = 4;      %Path loss exponent
P=5:5:60;

Z1=0;

for Pto=5:5:60
    for Pta=5:5:60
        for Ptb=5:5:60
            for Ptoo=5:5:60
            SIR_ceu1 = (Pto/((((sqrt(16))^-n)*Ptoo) + (((sqrt(7))^-
n)*Pta) + (((sqrt(7))^-n)*Ptb)))+Z1;
            Z1=SIR_ceu1;
            end
        end
    end
end

SIR_ceu1_dB= 10*log10(SIR_ceu1);
SIR_ceu1_dB_average=10*log10(SIR_ceu1*(1/length(P))^4);
```

Reverse Channel, 60°-sectoring, CCU

```
%To calculate the Reverse Channel SIR for LTE-Advanced
%CCU  -- 60-SECTORING

clear all;
close all;

n = 4;      %Path loss exponent
Rr=1:6;     %Rr is the ratio of R over r, where R=outer cell radius,
r=inner cell radius
P=0.01:0.01:0.2;   %From LTE (Rel-8), the maximum UE transmit power is
23dBm, that is, 200mW.

Z_rev=0;
for i=1:length(Rr)
for Pto=0.01:0.01:0.2
    for Pta=0.01:0.01:0.2
        for Ptb=0.01:0.01:0.2
             for Pta1=0.01:0.01:0.2
                for Ptb1=0.01:0.01:0.2
                     for Pta2=0.01:0.01:0.2
                        for Ptb2=0.01:0.01:0.2

                            SIR_ccu1_rev(i) =
(Pto/(((((sqrt(3))*(Rr(i)))-1)^-
n)*(Pta+Ptb+Pta1+Ptb1+Pta2+Ptb2)))+Z_rev;
                            Z_rev=SIR_ccu1_rev(i);
                        end
                     end
                end
             end
        end
    end
end
    Z_rev=0;
end

SIR_ccu1_rev_dB= 10*log10(SIR_ccu1_rev);
SIR_ccu1_rev_dB_average=10*log10(SIR_ccu1_rev*(1/length(P))^7);

figure,
plot(Rr,SIR_ccu1_rev_dB_average, ‘bx-’)
grid on;
xlabel(‘Cell Edge Radius to Cell Center Radius Ratio
(R/r)’,’fontsize’,20)
ylabel(‘Average SIR in dB’,’fontsize’,20)
%title(‘Reverse Channel Average SIR as a function of cell edge to cell
center radius ratio for Cell-Center User (CCU) in cell O (60o-
sectoring)’)
```

Reverse Channel, 60°-sectoring, CEU

```
%To calculate the Reverse Channel SIR for LTE-Advanced
%60-sectoring
%CEU

clear all;
close all;

n = 4;       %Path loss exponent
Rr=1:6;      %Rr is the ratio of R over r, where R=outer cell radius,
r=inner cell radius
P=0.01:0.01:0.2;   %From LTE (Rel-8), the maximum UE transmit power is
23dBm, that is, 200mW.

Z1_rev=0;

for Pto=0.01:0.01:0.2
    for Pta=0.01:0.01:0.2
        for Ptb=0.01:0.01:0.2
            for Ptoo=0.01:0.01:0.2
                SIR_ceu1_rev = (Pto/( ((((3/2)*(sqrt(3)))^-n)*Pta) +
((((3/2)*(sqrt(3)))^-n)*Ptb) + (((3+1/3)^-n)*Ptoo)))+Z1_rev;
                Z1_rev=SIR_ceu1_rev;
            end
        end
    end
end

SIR_ceu1_rev_dB= 10*log10(SIR_ceu1_rev);
SIR_ceu1_rev_dB_average=10*log10(SIR_ceu1_rev*(1/length(P))^4);
```

Forward Channel, 60°-sectoring, CEU, Latin Square Scenario 1

```
clear all, close all;

%Forward Channel - CEU (60-sectoring)
%One virtual channel per user

%Determine the number of users per sector (User input here)
%RB=6;             %For Channel BW of 1.4MHz  (input)
RB=15;             %For Channel BW of 3MHz  (input)
%RB=25;             %For Channel BW of 5MHz  (input)
%RB=50;             %For Channel BW of 10MHz  (input)
%RB=75;             %For Channel BW of 15MHz  (input)
%RB=100;             %For Channel BW of 20MHz  (input)

timeslots=20;       %No. of time slots per LTE frame
users=RB*timeslots;          %max no. of users per sector

%Varying the size of Latin Squares to accomodate the users per sector
```

```
Nc=5;    %User input here

load=0;
for load=1:Nc;

    % Generate a Latin Square for reference eNB_O
    a=2;                        %Latin Square Formula Ra_ij = ai+j mod Nc
    i=0;
    j=0;
    for i=1:Nc
        for j=1:Nc
            Ro(i,j) = mod((a*(i-1) + (j-1)),Nc);
        end
    end

    f=ceil(RB/Nc);
    t=ceil(20/Nc);
    for ii=1:f;
        for jj=1:t;
            Ro_big(((ii-1)*Nc)+1:(ii*Nc),((jj-1)*Nc)+1:(jj*Nc)) = Ro;
        end
    end

    k=1;
    for col=1:20                %time slots
        for row=1:RB
            Ro_actual(k) = Ro_big(row, col);
            k=k+1;
        end
    end
    Ro_actual=reshape(Ro_actual,RB,20);

    % Generate a Latin Square for eNB_A  in tier 2
    a=1;                        %Latin Square Formula Ra_ij = ai+j mod Nc
    i=0;
    j=0;
    for i=1:Nc
        for j=1:Nc
            Ra(i,j) = mod((a*(i-1) + (j-1)),Nc);
        end
    end

    f=ceil(RB/Nc);
    t=ceil(20/Nc);
    for ii=1:f;
        for jj=1:t;
            Ra_big(((ii-1)*Nc)+1:(ii*Nc),((jj-1)*Nc)+1:(jj*Nc)) = Ra;
        end
    end

    k=1;
    for col=1:20                %time slots
        for row=1:RB
```

```
        Ra_actual(k) = Ra_big(row, col);
        k=k+1;
    end
end
Ra_actual=reshape(Ra_actual,RB,20);

% Generate a Latin Square for eNB_O  in tier 2
a=3;                        %Latin Square Formula Ra_ij = ai+j mod Nc
i=0;
j=0;
for i=1:Nc
    for j=1:Nc
        Ro2(i,j) = mod((a*(i-1) + (j-1)),Nc);
    end
end

f=ceil(RB/Nc);
t=ceil(20/Nc);
for ii=1:f;
    for jj=1:t;
        Ro2_big(((ii-1)*Nc)+1:(ii*Nc),((jj-1)*Nc)+1:(jj*Nc)) = Ro2;
    end
end

k=1;
for col=1:20                %time slots
    for row=1:RB
        Ro2_actual(k) = Ro2_big(row, col);
        k=k+1;
    end
end
Ro2_actual=reshape(Ro2_actual,RB,20);

% Generate a Latin Square for eNB_B  in tier 2
a=4;                        %Latin Square Formula Ra_ij = ai+j mod Nc
i=0;
j=0;
for i=1:Nc
    for j=1:Nc
        Rb(i,j) = mod((a*(i-1) + (j-1)),Nc);
    end
end

f=ceil(RB/Nc);
t=ceil(20/Nc);
for ii=1:f;
    for jj=1:t;
        Rb_big(((ii-1)*Nc)+1:(ii*Nc),((jj-1)*Nc)+1:(jj*Nc)) = Rb;
    end
end

k=1;
for col=1:20                %time slots
```

```
    for row=1:RB
        Rb_actual(k) = Rb_big(row, col);
        k=k+1;
    end
end
Rb_actual=reshape(Rb_actual,RB,20);

%1 for overlap, 0 for no overlap
kk=0;
matchA=0;
matchB=0;
matchO2=0;
for kk=1:users
    if Ro_actual(kk) <= load-1
        Roactual(kk)=1;
    else Roactual(kk)=0;
    end

    if Ra_actual(kk) <= load-1
        Raactual(kk)=1;
    else Raactual(kk)=0;
    end

    if Rb_actual(kk) <= load-1
        Rbactual(kk)=1;
    else Rbactual(kk)=0;
    end

    if Ro2_actual(kk) <= load-1
        Ro2actual(kk)=1;
    else Ro2actual(kk)=0;
    end

    if (Roactual(kk)==1) &&(Raactual(kk)==1)
    matchA=matchA+1;
    end

    if (Roactual(kk)==1) &&(Rbactual(kk)==1)
    matchB=matchB+1;
    end

    if (Roactual(kk)==1) &&(Ro2actual(kk)==1)
    matchO2=matchO2+1;
    end

end

p_A(load) = (sum(matchA))/users;
p_O2(load) = (sum(matchO2))/users;
p_B(load) = (sum(matchB))/users;

%To find utilization
```

```
        utilization(load) = ((sum(Roactual))/users)*100;

    %To calculate the Forward Channel SIR for LTE-Advanced
    %Frequency Reuse Scheme 1-CEU -- 60-SECTORING

    n = 4;      %Path loss exponent
    P=5:5:60;

    Z1=0;

    for Pto=5:5:60
        for Pta=5:5:60
            for Ptb=5:5:60
                for Ptoo=5:5:60
                SIR_ceu1 = (Pto/((((sqrt(16))^-n)*Ptoo*p_O2(load)) +
(((sqrt(7))^-n)*Pta*p_A(load)) + (((sqrt(7))^-n)*Ptb*p_B(load))))+Z1;
                Z1=SIR_ceu1;
                end
            end
        end
    end

    SIR_ceu1_dB(load)= 10*log10(SIR_ceu1);
    SIR_ceu1_dB_average(load)=10*log10(SIR_ceu1*(1/length(P))^4);
end

%************************************************

SIR_ceu1_dB_average_without = 14.22*(ones(1,Nc));

SIR_ceu1_dB_average_without_120 = 13.97*(ones(1,Nc));


%*************************************************************

xaxis= 1:Nc;

display('Plotting');

figure;
grid on;
ax1 = gca;
get(ax1,'Position')
set(ax1,'XColor','k',...
    'YColor','b',...
    'YLim',[10,35],...
    'YTick',[10, 15, 20, 23, 25, 30,35]);
ylabel('Average SIR (dB)','fontsize',20)
a=line(xaxis, SIR_ceu1_dB_average, 'Color', 'b', 'LineStyle', '-',
'Marker', 'sq', 'Parent', ax1);
```

```
ax2 = axes('Position',get(ax1,'Position'),...
           'XAxisLocation','bottom',...
           'YAxisLocation','left',...
           'Color','none',...
           'XColor','k',...
           'YColor','b',...
           'YLim',[10,35],...
           'YTick',[10, 15, 20, 23, 25, 30,35],...
           'XTick',[],'XTickLabel',[]);
b=line(xaxis,SIR_ceu1_dB_average_without, 'Color', 'b', 'LineStyle', '--
', 'Marker', '.', 'Parent', ax2);


ax3 = axes('Position',get(ax1,'Position'),...
           'XAxisLocation','bottom',...
           'YAxisLocation','left',...
           'Color','none',...
           'XColor','k',...
           'YColor','b',...
           'YLim',[10,35],...
           'YTick',[10, 15, 20, 23, 25, 30, 35],...
           'XTick',[],'XTickLabel',[]);
c=line(xaxis,SIR_ceu1_dB_average_without_120, 'Color', 'b', 'LineStyle',
':', 'Marker', '.', 'Parent', ax3)

ax4 = axes('Position',get(ax1,'Position'),...
           'XAxisLocation','bottom',...
           'YAxisLocation','right',...
           'Color','none',...
           'XColor','k',...
           'YColor','r',...
           'YLim',[0,100],...
           'YTick',[0, 20, 40, 60, 80, 100],...
           'XTick',[],'XTickLabel',[]);
ylabel('Resource Utilization (%)','fontsize',20)
d=line(xaxis, utilization, 'Color', 'r', 'LineStyle', '-', 'Marker',
'o', 'Parent', ax4)

Leg = legend([a;b;c;d], {'SIR-60-LS','SIR-60','SIR-120','Resource
Utilization'},'fontsize',20);


xlabel('Number of users per Latin Square', 'fontsize',20)
%title('SIR Performance and Resource Utilization for Forward Channel,
with
%20MHz Channel Bandwidth per sector','fontsize',20)
```

Forward Channel, 60°-sectoring, CEU, Latin Square Scenario 2

```
clear all, close all;

%Forward Channel - CEU (60-sectoring)
%One RB per user

%Determine the number of users per sector (User input here)
RB=6;             %For Channel BW of 1.4MHz  (input)
%RB=15;              %For Channel BW of 3MHz  (input)
%RB=25;              %For Channel BW of 5MHz  (input)
%RB=50;              %For Channel BW of 10MHz  (input)
%RB=75;              %For Channel BW of 15MHz  (input)
%RB=100;              %For Channel BW of 20MHz  (input)

%End of user input

timeslots=20;       %No. of time slots per LTE frame
users=RB*timeslots;          %max no. of users per sector

%Determine the sizes of Latin Squares to accomodate the users per sector
PrimeNo=primes(100);
minN = ceil(sqrt(users));
maxN = ceil(sqrt(4*users));     %4 Base stations

j=0;
for j=1:length(PrimeNo)
    if (PrimeNo(j)>=minN) && (PrimeNo(j)<=maxN)
        N(j)= PrimeNo(j);
    end
end

N_loc = find(N~=0);
maxNprime = find(PrimeNo>maxN);
maxNprime = PrimeNo(maxNprime(1));

N=[N(N_loc) maxNprime];             %Prime value for the size of the
square
Nsq = N.*N;  %max no . of users allowable per sector

k=0;

for size = 1:length(N)
    mO = randperm(Nsq(size));
    mA = randperm(Nsq(size));
    mB = randperm(Nsq(size));
    mO2 = randperm(Nsq(size));

for k=1:50  %k number of runs for each latin square
    matchA=0;
    matchB=0;
    matchO2=0;
```

```
    i=0;
    for i=1:Nsq(size)

        if mO(i) <= users
            m_O(i)=1;
        else m_O(i)=0;
        end

        if mA(i) <= users
            m_A(i)=1;
        else m_A(i)=0;
        end

        if mB(i) <= users
            m_B(i)=1;
        else m_B(i)=0;
        end

        if mO2(i) <= users
            m_O2(i)=1;
        else m_O2(i)=0;
        end

        if (m_O(i)==1) &&(m_A(i)==1)
            matchA=matchA+1;
        end

        if (m_O(i)==1) &&(m_B(i)==1)
            matchB=matchB+1;
        end

        if (m_O(i)==1) &&(m_O2(i)==1)
            matchO2=matchO2+1;
        end

    end

    p_A(k) = matchA/Nsq(size);       %probability of overlaps
    p_B(k) = matchB/Nsq(size);       %probability of overlaps
    p_O2(k) = matchO2/Nsq(size);       %probability of overlaps

end

p_A_ave(size) = sum(p_A)/k;
p_B_ave(size) = sum(p_B)/k;
p_O2_ave(size) = sum(p_O2)/k;

n = 4;      %Path loss exponent
    P=5:5:60;

    Z1=0;
```

```
    for Pto=5:5:60
        for Pta=5:5:60
            for Ptb=5:5:60
                for Ptoo=5:5:60
                SIR_ceu1 = (Pto/((((sqrt(16))^-n)*Ptoo*p_O2_ave(size)) +
(((sqrt(7))^-n)*Pta*p_A_ave(size)) + (((sqrt(7))^-
n)*Ptb*p_B_ave(size))))+Z1;
                Z1=SIR_ceu1;
                end
            end
        end
    end

    SIR_ceu1_dB(size)= 10*log10(SIR_ceu1);
    SIR_ceu1_dB_average(size)=10*log10(SIR_ceu1*(1/length(P))^4);
end

%**************************************************************

SIR_ceu1_dB_average_without = 14.22*(ones(1,length(N)));

SIR_ceu1_dB_average_without_120 = 13.97*(ones(1,length(N)));

%**************************************************************

%Calculate the resource utilization with Latin Square
k1=0;
for k1=1:length(N)
    utilization(k1) = (users./Nsq(k1))*100;
end

%**************************************************************

display('Plotting');

figure;
grid on;
ax1 = gca;
get(ax1,'Position')
set(ax1,'XColor','k',...
    'YColor','b',...
    'YLim',[10,30],...
    'YTick',[10, 15, 20, 23, 25,30]);
ylabel('Average SIR (dB)','fontsize',20)
a = line(N, SIR_ceu1_dB_average, 'Color', 'b', 'LineStyle', '-',
'Marker', 'sq', 'Parent', ax1);


ax2 = axes('Position',get(ax1,'Position'),...
           'XAxisLocation','bottom',...
           'YAxisLocation','left',...
```

```
           'Color','none',...
           'XColor','k',...
           'YColor','b',...
           'YLim',[10,30],...
           'YTick',[10, 15, 20, 23, 25,30],...
           'XTick',[],'XTickLabel',[]);
b = line(N,SIR_ceu1_dB_average_without, 'Color', 'b', 'LineStyle', '--',
'Marker', '.', 'Parent', ax2);


ax3 = axes('Position',get(ax1,'Position'),...
           'XAxisLocation','bottom',...
           'YAxisLocation','left',...
           'Color','none',...
           'XColor','k',...
           'YColor','b',...
           'YLim',[10,30],...
           'YTick',[10, 15, 20, 23, 30],...
           'XTick',[],'XTickLabel',[]);
c = line(N,SIR_ceu1_dB_average_without_120, 'Color', 'b', 'LineStyle',
':', 'Marker', '.', 'Parent', ax3)

ax4 = axes('Position',get(ax1,'Position'),...
           'XAxisLocation','bottom',...
           'YAxisLocation','right',...
           'Color','none',...
           'XColor','k',...
           'YColor','r',...
           'YLim',[0,100],...
           'YTick',[0, 20, 40, 60, 80, 100],...
           'XTick',[],'XTickLabel',[]);
ylabel('Resource Utilization (%)','fontsize',20)
d = line(N, utilization, 'Color', 'r', 'LineStyle', '-.', 'Marker', 'o',
'Parent', ax4)

Leg = legend([a;b;c;d], {'SIR-60-LS','SIR-60','SIR-120','Resource
Utilization'},'fontsize',16 );

xlabel('Size of Latin Square','fontsize',20)
%title('SIR Performance and Resource Utilization for Forward Channel,
with 5MHz Channel Bandwidth per sector','fontsize',20)
```

Reverse Channel, 60°-sectoring, CEU, Latin Square Scenario 1

```
clear all, close all;

%Reverse Channel - CEU (60-sectoring)
%One virtual channel per user

%Determine the number of users per sector (User input here)
%RB=6;             %For Channel BW of 1.4MHz  (input)
```

```
%RB=15;             %For Channel BW of 3MHz  (input)
%RB=25;             %For Channel BW of 5MHz  (input)
%RB=50;             %For Channel BW of 10MHz  (input)
%RB=75;             %For Channel BW of 15MHz  (input)
RB=100;             %For Channel BW of 20MHz  (input)

timeslots=20;       %No. of time slots per LTE frame
users=RB*timeslots;          %max no. of users per sector

%Varying the size of Latin Squares to accomodate the users per sector
Nc=7;    %User input here

load=0;
for load=1:Nc;

    % Generate a Latin Square for reference eNB_O
    a=2;                      %Latin Square Formula Ra_ij = ai+j mod Nc
    i=0;
    j=0;
    for i=1:Nc
        for j=1:Nc
            Ro(i,j) = mod((a*(i-1) + (j-1)),Nc);
        end
    end

    f=ceil(RB/Nc);
    t=ceil(20/Nc);
    for ii=1:f;
        for jj=1:t;
            Ro_big(((ii-1)*Nc)+1:(ii*Nc),((jj-1)*Nc)+1:(jj*Nc)) = Ro;
        end
    end

    k=1;
    for col=1:20              %time slots
        for row=1:RB
            Ro_actual(k) = Ro_big(row, col);
            k=k+1;
        end
    end
    Ro_actual=reshape(Ro_actual,RB,20);

    % Generate a Latin Square for eNB_A  in tier 2
    a=1;                      %Latin Square Formula Ra_ij = ai+j mod Nc
    i=0;
    j=0;
    for i=1:Nc
        for j=1:Nc
            Ra(i,j) = mod((a*(i-1) + (j-1)),Nc);
        end
    end

    f=ceil(RB/Nc);
```

```
t=ceil(20/Nc);
for ii=1:f;
    for jj=1:t;
        Ra_big(((ii-1)*Nc)+1:(ii*Nc),((jj-1)*Nc)+1:(jj*Nc)) = Ra;
    end
end

k=1;
for col=1:20            %time slots
    for row=1:RB
        Ra_actual(k) = Ra_big(row, col);
        k=k+1;
    end
end
Ra_actual=reshape(Ra_actual,RB,20);

% Generate a Latin Square for eNB_O  in tier 2
a=3;                    %Latin Square Formula Ra_ij = ai+j mod Nc
i=0;
j=0;
for i=1:Nc
    for j=1:Nc
        Ro2(i,j) = mod((a*(i-1) + (j-1)),Nc);
    end
end

f=ceil(RB/Nc);
t=ceil(20/Nc);
for ii=1:f;
    for jj=1:t;
        Ro2_big(((ii-1)*Nc)+1:(ii*Nc),((jj-1)*Nc)+1:(jj*Nc)) = Ro2;
    end
end

k=1;
for col=1:20            %time slots
    for row=1:RB
        Ro2_actual(k) = Ro2_big(row, col);
        k=k+1;
    end
end
Ro2_actual=reshape(Ro2_actual,RB,20);

% Generate a Latin Square for eNB_B  in tier 2
a=4;                    %Latin Square Formula Ra_ij = ai+j mod Nc
i=0;
j=0;
for i=1:Nc
    for j=1:Nc
        Rb(i,j) = mod((a*(i-1) + (j-1)),Nc);
    end
end
```

```
f=ceil(RB/Nc);
t=ceil(20/Nc);
for ii=1:f;
    for jj=1:t;
        Rb_big(((ii-1)*Nc)+1:(ii*Nc),((jj-1)*Nc)+1:(jj*Nc)) = Rb;
    end
end

k=1;
for col=1:20            %time slots
    for row=1:RB
        Rb_actual(k) = Rb_big(row, col);
        k=k+1;
    end
end
Rb_actual=reshape(Rb_actual,RB,20);

%1 for overlap, 0 for no overlap
kk=0;
matchA=0;
matchB=0;
matchO2=0;
for kk=1:users
    if Ro_actual(kk) <= load-1
        Roactual(kk)=1;
    else Roactual(kk)=0;
    end

    if Ra_actual(kk) <= load-1
        Raactual(kk)=1;
    else Raactual(kk)=0;
    end

    if Rb_actual(kk) <= load-1
        Rbactual(kk)=1;
    else Rbactual(kk)=0;
    end

    if Ro2_actual(kk) <= load-1
        Ro2actual(kk)=1;
    else Ro2actual(kk)=0;
    end

    if (Roactual(kk)==1) &&(Raactual(kk)==1)
    matchA=matchA+1;
    end

    if (Roactual(kk)==1) &&(Rbactual(kk)==1)
    matchB=matchB+1;
    end

    if (Roactual(kk)==1) &&(Ro2actual(kk)==1)
    matchO2=matchO2+1;
```

```
        end

    end

    p_A(load) = (sum(matchA))/users;
    p_O2(load) = (sum(matchO2))/users;
    p_B(load) = (sum(matchB))/users;

    %To find utilization
        utilization(load) = ((sum(Roactual))/users)*100;

    %To calculate the Reverse Channel SIR for LTE-Advanced
    %CEU -- 60-SECTORING

    n = 4;      %Path loss exponent
    Rr=1:6;     %Rr is the ratio of R over r, where R=outer cell radius,
r=inner cell radius
    P=0.01:0.01:0.2;   %From LTE (Rel-8), the maximum UE transmit power
is 23dBm, that is, 200mW.

    Z1_rev=0;

    for Pto=0.01:0.01:0.2
        for Pta=0.01:0.01:0.2
            for Ptb=0.01:0.01:0.2
                for Ptoo=0.01:0.01:0.2
                    SIR_ceu1_rev = (Pto/( ((((3/2)*(sqrt(3)))^-
n)*Pta*p_A(load)) + ((((3/2)*(sqrt(3)))^-n)*Ptb*p_B(load)) + (((3+1/3)^-
n)*Ptoo*p_O2(load))))+Z1_rev;
                    Z1_rev=SIR_ceu1_rev;
                end
            end
        end
    end

    SIR_ceu1_rev_dB(load)= 10*log10(SIR_ceu1_rev);

SIR_ceu1_rev_dB_average(load)=10*log10(SIR_ceu1_rev*(1/length(P))^4);

end

%************************************************

SIR_ceu1_dB_average_without = 13.39*(ones(1,Nc));

SIR_ceu1_dB_average_without_120 = 11.69*(ones(1,Nc));


%***************************************************************

xaxis= 1:Nc;
```

```
display('Plotting');

figure;
grid on;
ax1 = gca;
get(ax1,'Position')
set(ax1,'XColor','k',...
    'YColor','b',...
    'YLim',[10,35],...
    'YTick',[10, 15, 20, 23, 25, 30,35]);
ylabel('Average SIR (dB)','fontsize',20)
a=line(xaxis, SIR_ceu1_rev_dB_average, 'Color', 'b', 'LineStyle', '-',
'Marker', 'sq', 'Parent', ax1);


ax2 = axes('Position',get(ax1,'Position'),...
           'XAxisLocation','bottom',...
           'YAxisLocation','left',...
           'Color','none',...
           'XColor','k',...
           'YColor','b',...
           'YLim',[10,35],...
           'YTick',[10, 15, 20, 23, 25, 30,35],...
           'XTick',[],'XTickLabel',[]);
b=line(xaxis,SIR_ceu1_dB_average_without, 'Color', 'b', 'LineStyle', '--
', 'Marker', '.', 'Parent', ax2);


ax3 = axes('Position',get(ax1,'Position'),...
           'XAxisLocation','bottom',...
           'YAxisLocation','left',...
           'Color','none',...
           'XColor','k',...
           'YColor','b',...
           'YLim',[10,35],...
           'YTick',[10, 15, 20, 23, 25, 30,35],...
           'XTick',[],'XTickLabel',[]);
c=line(xaxis,SIR_ceu1_dB_average_without_120, 'Color', 'b', 'LineStyle',
':', 'Marker', '.', 'Parent', ax3)

ax4 = axes('Position',get(ax1,'Position'),...
           'XAxisLocation','bottom',...
           'YAxisLocation','right',...
           'Color','none',...
           'XColor','k',...
           'YColor','r',...
           'YLim',[0,100],...
           'YTick',[0, 20, 40, 60, 80, 100],...
           'XTick',[],'XTickLabel',[]);
ylabel('Resource Utilization (%)','fontsize',20)
d=line(xaxis, utilization, 'Color', 'r', 'LineStyle', '-', 'Marker',
'o', 'Parent', ax4)
```

```
Leg = legend([a;b;c;d], {'SIR-60-LS','SIR-60','SIR-120','Resource
Utilization'},'fontsize',20);


xlabel('Number of users per Latin Square', 'fontsize',20)
%title('SIR Performance and Resource Utilization for Forward Channel,
with 20MHz Channel Bandwidth per sector','fontsize',20)
```

Reverse Channel, 60°-sectoring, CEU, Latin Square Scenario 2

```
clear all, close all;

%Forward Channel - CEU (60-sectoring)
%One RB per user

%Determine the number of users per sector (User input here)
%RB=6;             %For Channel BW of 1.4MHz  (input)
%RB=15;             %For Channel BW of 3MHz  (input)
%RB=25;             %For Channel BW of 5MHz  (input)
%RB=50;             %For Channel BW of 10MHz  (input)
%RB=75;             %For Channel BW of 15MHz  (input)
RB=100;             %For Channel BW of 20MHz  (input)

%End of user input

timeslots=20;       %No. of time slots per LTE frame
users=RB*timeslots;          %max no. of users per sector

%Determine the sizes of Latin Squares to accomodate the users per sector
PrimeNo=primes(100);
minN = ceil(sqrt(users));
maxN = ceil(sqrt(4*users));     %4 Base stations

j=0;
for j=1:length(PrimeNo)
    if (PrimeNo(j)>=minN) && (PrimeNo(j)<=maxN)
        N(j)= PrimeNo(j);
    end
end

N_loc = find(N~=0);
maxNprime = find(PrimeNo>maxN);
maxNprime = PrimeNo(maxNprime(1));

N=[N(N_loc) maxNprime];             %Prime value for the size of the
square
Nsq = N.*N;  %max no . of users allowable per sector

k=0;
```

```
for size = 1:length(N)
    mO = randperm(Nsq(size));
    mA = randperm(Nsq(size));
    mB = randperm(Nsq(size));
    mO2 = randperm(Nsq(size));

for k=1:50  %k number of runs for each latin square
    matchA=0;
    matchB=0;
    matchO2=0;
    i=0;
    for i=1:Nsq(size)

        if mO(i) <= users
            m_O(i)=1;
        else m_O(i)=0;
        end

        if mA(i) <= users
            m_A(i)=1;
        else m_A(i)=0;
        end

        if mB(i) <= users
            m_B(i)=1;
        else m_B(i)=0;
        end

        if mO2(i) <= users
            m_O2(i)=1;
        else m_O2(i)=0;
        end

        if (m_O(i)==1) &&(m_A(i)==1)
            matchA=matchA+1;
        end

        if (m_O(i)==1) &&(m_B(i)==1)
            matchB=matchB+1;
        end

        if (m_O(i)==1) &&(m_O2(i)==1)
            matchO2=matchO2+1;
        end

    end

    p_A(k) = matchA/Nsq(size);       %probability of overlaps
    p_B(k) = matchB/Nsq(size);       %probability of overlaps
    p_O2(k) = matchO2/Nsq(size);       %probability of overlaps

end
```

```
p_A_ave(size) = sum(p_A)/k;
p_B_ave(size) = sum(p_B)/k;
p_O2_ave(size) = sum(p_O2)/k;

n = 4;      %Path loss exponent
Rr=1:6;     %Rr is the ratio of R over r, where R=outer cell radius,
r=inner cell radius
P=0.01:0.01:0.2;   %From LTE (Rel-8), the maximum UE transmit power is
23dBm, that is, 200mW.

Z1_rev=0;

for Pto=0.01:0.01:0.2
    for Pta=0.01:0.01:0.2
        for Ptb=0.01:0.01:0.2
            for Ptoo=0.01:0.01:0.2
                SIR_ceu1_rev = (Pto/( ((((3/2)*(sqrt(3)))^-
n)*Pta*p_A_ave(size)) + ((((3/2)*(sqrt(3)))^-n)*Ptb*p_B_ave(size)) +
(((3+1/3)^-n)*Ptoo*p_O2_ave(size))))+Z1_rev;
                Z1_rev=SIR_ceu1_rev;
            end
        end
    end
end

SIR_ceu1_rev_dB(size)= 10*log10(SIR_ceu1_rev);
SIR_ceu1_rev_dB_average(size)=10*log10(SIR_ceu1_rev*(1/length(P))^4);

end

%************************************************************

SIR_ceu1_dB_average_without = 13.39*(ones(1,length(N)));

SIR_ceu1_dB_average_without_120 = 11.69*(ones(1,length(N)));
%************************************************************

%Calculate the resource utilization with Latin Square
k1=0;
for k1=1:length(N)
    utilization(k1) = (users./Nsq(k1))*100;
end

%************************************************************
display('Plotting');

figure;
grid on;
ax1 = gca;
get(ax1,'Position')
set(ax1,'XColor','k',...
```

```
    'YColor','b',...
    'YLim',[10,30],...
    'YTick',[10, 15, 20, 23, 25,30]);
ylabel('Average SIR (dB)','fontsize',20)
a = line(N, SIR_ceu1_rev_dB_average, 'Color', 'b', 'LineStyle', '-',
'Marker', 'sq', 'Parent', ax1);


ax2 = axes('Position',get(ax1,'Position'),...
           'XAxisLocation','bottom',...
           'YAxisLocation','left',...
           'Color','none',...
           'XColor','k',...
           'YColor','b',...
           'YLim',[10,30],...
           'YTick',[10, 15, 20, 23, 25,30],...
           'XTick',[],'XTickLabel',[]);
b = line(N,SIR_ceu1_dB_average_without, 'Color', 'b', 'LineStyle', '--',
'Marker', '.', 'Parent', ax2);


ax3 = axes('Position',get(ax1,'Position'),...
           'XAxisLocation','bottom',...
           'YAxisLocation','left',...
           'Color','none',...
           'XColor','k',...
           'YColor','b',...
           'YLim',[10,30],...
           'YTick',[10, 15, 20, 23, 25,30],...
           'XTick',[],'XTickLabel',[]);
c = line(N,SIR_ceu1_dB_average_without_120, 'Color', 'b', 'LineStyle',
':', 'Marker', '.', 'Parent', ax3)

ax4 = axes('Position',get(ax1,'Position'),...
           'XAxisLocation','bottom',...
           'YAxisLocation','right',...
           'Color','none',...
           'XColor','k',...
           'YColor','r',...
           'YLim',[0,100],...
           'YTick',[0, 20, 40, 60, 80, 100],...
           'XTick',[],'XTickLabel',[]);
ylabel('Resource Utilization (%)','fontsize',20)
d = line(N, utilization, 'Color', 'r', 'LineStyle', '-.', 'Marker', 'o',
'Parent', ax4)

Leg = legend([a;b;c;d], {'SIR-60-LS','SIR-60','SIR-120','Resource
Utilization'},'fontsize',16 );

xlabel('Size of Latin Square','fontsize',20)
%title('SIR Performance and Resource Utilization for Forward Channel,
with 5MHz Channel Bandwidth per sector','fontsize',20)
```

THIS PAGE INTENTIONALLY LEFT BLANK

LIST OF REFERENCES

[1] Sassan Ahmadi. (2006, December 7). "Introduction to mobile WiMAX Radio Access Technology: PHY and MAC Architecture" [Online]. Available: http://vivonets.ece.ucsb.edu/ahmadiUCSB_slides_Dec7.pdf

[2] Fan Xiangning et al., "An inter-cell interference coordination technique based on users' ratio and multi-level frequency allocations," *Proc. of International Conference on Wireless Communications, Networking and Mobile Computing,* pp.799–802, Sept. 2007.

[3] Zheng Xie and Bernhard Walke, "Frequency reuse techniques for attaining both coverage and high spectral efficiency in OFDMA cellular systems," *Proc. of Wireless Communications and Networking Conference*, pp.1–6, April 2010.

[4] M. Porjazoski, and B. Popovski, "Analysis of intercell interference coordination by fractional frequency reuse in LTE," *Proc. of International Conference on Software, Telecommunications and Computer Networks (SoftCOM)*, pp.160–164, Sept. 2010.

[5] M. Porjazoski, and B. Popovski, "Contribution to analysis of Intercell interference coordination in LTE: A fractional frequency reuse case," *Proc. of Mobile Congress*, pp.1–4, Oct. 2010.

[6] Yiwei Yu et al., "Performance analysis of soft frequency reuse for inter-cell interference coordination in LTE networks," *Proc. of International Symposium on Communications and Information Technologies (ISCIT),* pp.504–509, Oct. 2010.

[7] Freescale Semiconductor. (2008, October). *Long Term Evolution Protocol Overview Document Number: LTEPTCLOVWWP Rev 0* [Online]. Available: http://www.freescale.com/files/wireless_comm/doc/white_paper/LTEPTCLOVWWP.pdf

[8] Tri T. Ha, *Theory and Design of Digital Communication Systems.* Cambridge, United Kingdom: Cambridge University Press, 2011.

[9] David Tipper. "Fundamentals of cellular networks" [Online]. Available: http://www.sis.pitt.edu/~dtipper/2720/2720_Slides4.pdf

[10] *LTE; Evolved Universal Terrestrial Radio Access (E-UTRA); User Equipment (UE) radio transmission and reception*, 3GPP TS 36.101 version 10.6.0 Release 10, 2011.

[11] "Physical layer aspect for evolved Universal Terrestrial Radio Access (UTRA)," 3rd Generation Partnership Project, Valbonne, France, 3GPP TR 25.814, 2006.

[12] Christina Gessner and Andreas Roessler. (2009, April). *LTE technology and LTE test; a deskside chat* [Online]. Available: http://mobnet.epfl.ch/misc/Rohde_and_Schwarz_LTE_tutorial.pdf

[13] Eli Sofer and Yossi Segal. (2005, January). *Tutorial on Multi Access OFDM (OFDMA) Technology* [Online]. Available: http://www.scribd.com/doc/81322893/Tutorial-on-OFDMA

[14] IXIA. (2009, November). *SC-FDMA Single Carrier FDMA in LTE* [Online]. Available: http://www.ixiacom.com/pdfs/library/white_papers/SC-FDMA-INDD.pdf

[15] Jim Zyren. (2007, July). *Overview of the 3GPP Long Term Evolution Physical Layer* [Online]. Available: http://www.freescale.com/files/wireless_comm/doc/white_paper//3GPPEVOLUTIONWP.pdf

[16] Event Helix, (2009). *3GPP LTE Channels and MAC* [Online]. Available: http://www.eventhelix.com/lte/presentations/3GPP-LTE-MAC.pdf

[17] *LTE; Evolved Universal Terrestrial Radio Access (E-UTRA); Medium Access Control (MAC) protocol specification*, 3GPP TS 36.321 version 10.5.0 Release 10, 2012.

[18] Lichun Bao, "MALS: multiple access scheduling based on Latin squares," *Proc. of Military Communications Conference,* vol.1, pp. 315- 321, Nov. 2004.

[19] Erik Dahlman et al., *3G Evolution: HSPA and LTE for Mobile Broadband* (2^{nd} ed.). Massachusetts: Academic Press, 2008.

[20] Wenxin Liu et al., "An overload indicator & high interference indicator hybrid scheme for inter-cell interference coordination in LTE system," in *Proc. of 3rd IEEE International Conference on Broadband Network and Multimedia Technology*, pp.514–518, Oct. 2010.

[21] D. Tse and P. Viswanath, *Fundamentals of Wireless Communication*. Cambridge, United Kingdom: Cambridge University Press, 2005.

INITIAL DISTRIBUTION LIST

1. Defense Technical Information Center
   Ft. Belvoir, Virginia

2. Dudley Knox Library
   Naval Postgraduate School
   Monterey, California

3. Chairman, Code EC
   Department of Electrical and Computer Engineering
   Naval Postgraduate School
   Monterey, California

4. Tri T. Ha
   Naval Postgraduate School
   Monterey, California

5. Weilian, Su
   Naval Postgraduate School
   Monterey, California

6. Ric Romero
   Naval Postgraduate School
   Monterey, California

7. Tat Soon Yeo
   Temasek Defence Systems Institute (TDSI)
   National University of Singapore
   Singapore

8. Lai Poh Tan
   Temasek Defence Systems Institute (TDSI)
   National University of Singapore
   Singapore

9. Tiat Leng Teo
   Defence Science and Technology Agency (DSTA)
   Singapore

10. Kim Hong Tan
    Naval Postgraduate School
    Monterey, California